

# FEABAS - A USER-FRIENDLY SOFTWARE FOR PREDICTION OF BRIDGE APPROACH SETTLEMENT

(STUDY 2188, ORA 125-6074)

Submitted to  
Oklahoma Department of Transportation

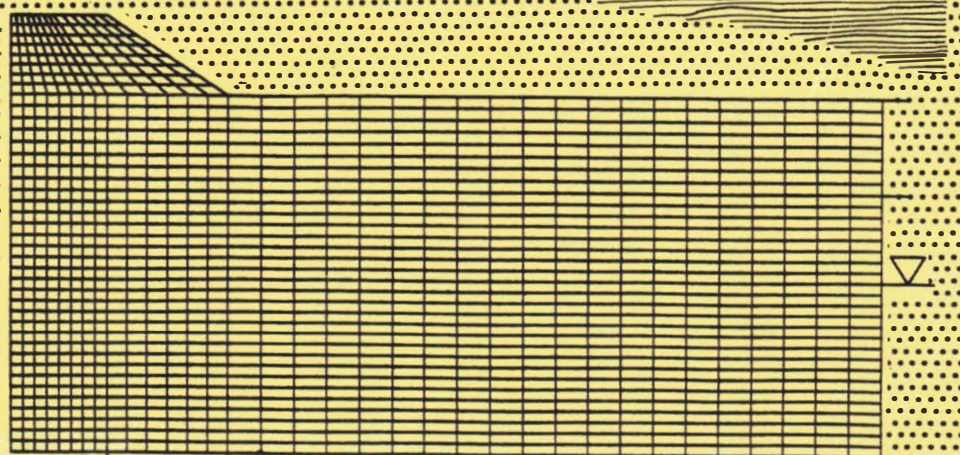
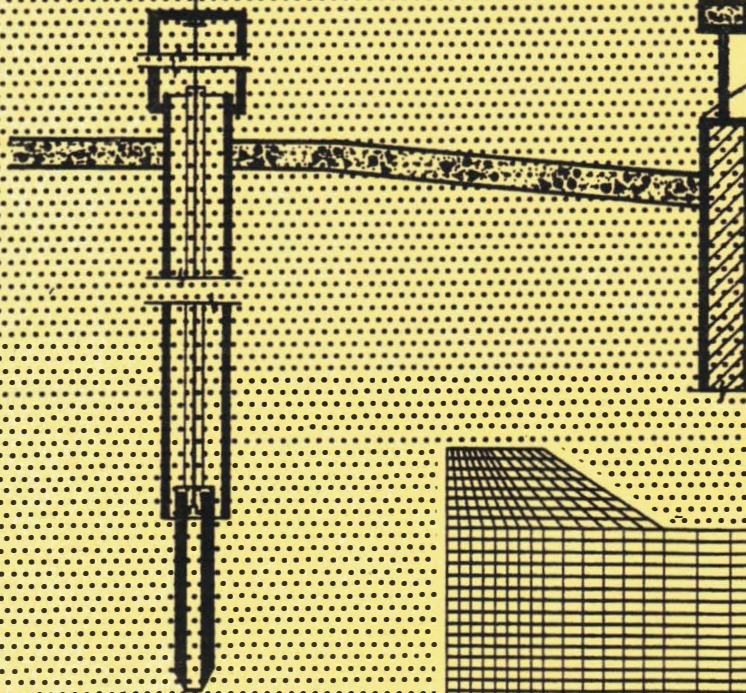
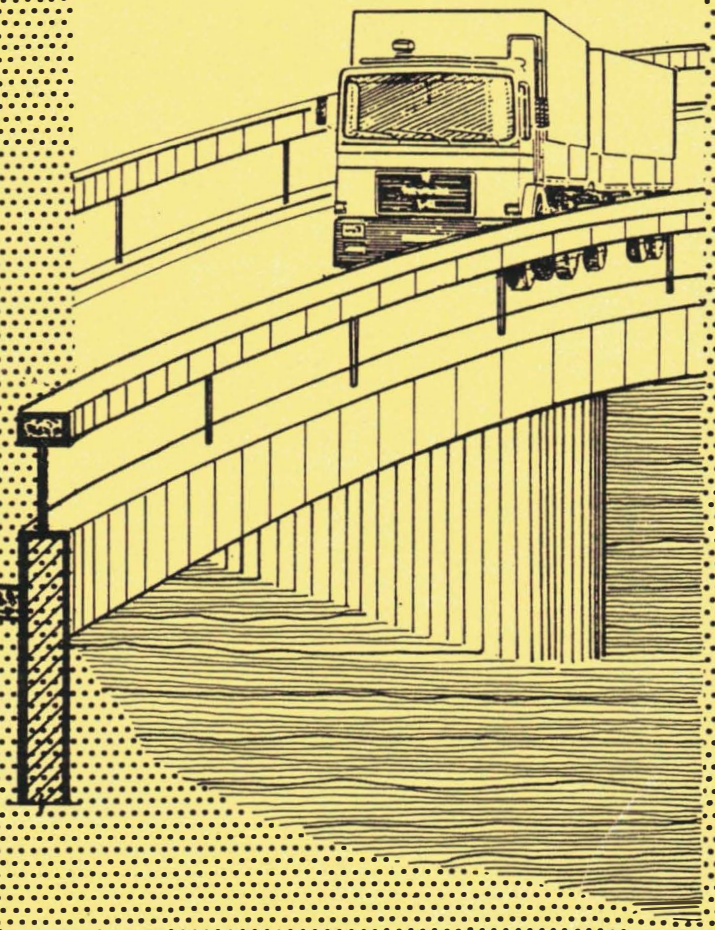
Submitted by  
Musharraf Zaman  
Joakim Laguros  
Hua Chen  
Motiar Rahman  
School of Civil Engineering and  
Environmental Science

from  
University of Oklahoma  
Office of Research Administration

May 1995



**DISPLAY COPY  
DO NOT REMOVE**



TG320  
.F43  
1995  
C.1

F



## TECHNICAL REPORT STANDARD TITLE PAGE

<b>1. REPORT NO.</b> FHWA/OK 95 (03)	<b>2. GOVERNMENT ACCESSION NO.</b>	<b>3. RECIPIENT'S CATALOG NO.</b>	
<b>4. TITLE AND SUBTITLE</b> FEABAS A User-Friendly Software for Prediction of Bridge Approach Settlement		<b>5. REPORT DATE</b> May 1995	
		<b>6. PERFORMING ORGANIZATION CODE</b>	
<b>7. AUTHOR(S)</b> Musharraf Zaman, Joakim G. Laguros, Hua Chen, and Motiar Rahman		<b>8. PERFORMING ORGANIZATION REPORT</b> ORA 125-6074	
		<b>10. WORK UNIT NO.</b>	
<b>9. PERFORMING ORGANIZATION AND ADDRESS</b> The University of Oklahoma Norman, Oklahoma 73019		<b>11. CONTRACT OR GRANT NO.</b> Item No. 2188	
		<b>13. TYPE OF REPORT AND PERIOD COVERED</b>	
<b>12. SPONSORING AGENCY NAME AND ADDRESS</b> Oklahoma Department of Transportation Research and Development Division 200 N.E. 21st Street Oklahoma City, Oklahoma 73105		<b>14. SPONSORING AGENCY CODE</b>	
		<b>15. SUPPLEMENTARY NOTES</b> Done in cooperation with FHWA	
<b>16. ABSTRACT</b>  <p>Bridge approach settlement is a major problem in highway design as well as maintenance. It creates an unsafe and uncomfortable riding surface. This report presents the details of a software that was developed at the University of Oklahoma, through a project funded jointly by the Oklahoma Department of Transportation (ODOT) and the Federal Highway Administration (FHWA). The objective of the software was to analyze the settlement characteristics of the problematic bridge approach sites in Oklahoma. To this end, a nonlinear Finite Element (FE) analysis procedure was developed for predicting the consolidation settlement of the foundation soil at a bridge approach due to the surcharge of embankment construction, as well as the settlement of the embankment itself due to the vehicular traffic loads.</p> <p>The software package, called <b>FEABAS</b>, is divided into a number of different modules: <i>Preprocessor</i>, <i>Data Converter</i>, <i>FE Main Program</i>, and <i>Postprocessor</i>. <b>FEABAS</b> works completely in the Windows operating environment in IBM compatible PC's. The interactive nature of the software makes it user-friendly; especially the graphical interface of the <i>preprocessor</i> enhances the data input operation. Existing data files can also be modified or edited using the <i>preprocessor</i>. The <i>preprocessor</i> is written in Actor 4.0, which is a complete development environment and programming language that make it easy to develop stand-alone applications for Microsoft Windows Version 3.0 or later. This report presents an overview of the steps involved in analyzing bridge approach settlement using the software package.</p> <p>The software package - <b>FEABAS</b> is a very useful tool for conducting parametric studies of a problematic bridge approach site to identify some of the important causative factors and their relative significance, that are expected to be helpful in finding appropriate remedial measures to the problem. The bridge approach settlement at a site in Oklahoma was predicted using <b>FEABAS</b> for illustration and application. The various capabilities of the software including graphical output are illustrated.</p>			
<b>17. KEY WORDS</b> Consolidation, Settlement, Bridge Approach, Finite Element, Cam-clay Model, Bump, Embankment, Traffic Landing, Foundation soil		<b>18. DISTRIBUTION STATEMENT</b>	
<b>19. SECURITY CLASSIF. (OF THIS REPORT)</b> None	<b>20. SECURITY CLASSIF. (OF THIS PAGE)</b> None	<b>21. NO. OF PAGES</b> 217	<b>22. PRICE</b>

*Final Report*

**FEABAS - A USER-FRIENDLY SOFTWARE**  
**FOR PREDICTION OF BRIDGE APPROACH SETTLEMENT**

(STUDY 2188, ORA 125-6074)

*Submitted to*

Mr. Lawrence J. Senkowski  
Assistant Research Division Engineer  
Oklahoma Department of Transportation  
200 N.E. 21st Street  
Oklahoma City, Oklahoma 73105

*Prepared by*

Musharraf Zaman, Professor  
Joakim G. Laguros, David Ross Boyd Professor Emeritus  
Hua Chen, Graduate Research Assistant  
Motiar Rahman, Graduate Research Assistant

School of Civil Engineering and Environmental Science  
The University of Oklahoma  
Norman, Oklahoma 73019  
(405) 325-5911

*From*

The University of Oklahoma  
Office of Research Administration  
1000 Asp Avenue, Room 314  
Norman, Oklahoma 73019

May 1995

\*\*\*\*\*

# **FEABAS**

## **FINITE ELEMENT ANALYSIS OF BRIDGE APPROACH SETTLEMENT**

**Copyright (C) 1995, Board of Regents, University of Oklahoma**

**All Rights Reserved**

\*\*\*\*\*

### **DISCLAIMER**

The **FEABAS** (Finite Element Analysis of Bridge Approach Settlement) was developed at the University of Oklahoma, Norman. The Project (Item 2188) was funded by the Oklahoma Department of Transportation (ODOT) in cooperation with the Federal Highway Administration (FHWA). The Preprocessor was developed using ACTOR 4.0 by Whitewater Group, 10 North Church Street, 4th Floor, West Chester, PA 19380. The Postprocessor uses the Graphic/Win software by Scientific Endeavor Corp., 508 North Kentucky Street, Kingston, TN 37763. The finite element main program is based on the work of Prof. Desai and his coworkers at the University of Arizona, Tucson. The user of **FEABAS** is totally responsible for the results, their interpretation and consequences.

The University of Oklahoma, ODOT, and FHWA make no representations or warranties of any kind with respect to the software, the accompanying written materials, and any accompanying hardware and expressly disclaim any all warranties, either expressed or implied, including, but not limited to, warranties of merchantability or fitness for a particular purpose and any/other implied warranties regarding the capabilities, utility, business or commercial application of same. In no event shall the University of Oklahoma, ODOT, FHWA, their agents or employees, be liable for any special, incidental, consequential or other damages whatsoever, (including, without limitation, damages for loss of bussiness information, or other pecuniary loss) arising out of the use of or inability to use this product, even if the University of Oklahoma, ODOT, FHWA have been advised of the possibility of such damages.



## **ACKNOWLEDGMENTS**

The authors would like to express their sincere appreciation to Mr. Dwight Hixon, Mr. Lawrence Senkowski, and Mr. Curt Hayes of the Research Division and to Dr. James Nevels, Jr. of the Materials Division, Oklahoma Department of Transportation (ODOT), for their assistance and advice on different phases of this study. The authors gratefully acknowledge the assistance of Professor C.S. Desai, University of Arizona, Tucson.

The financial support provided by the Federal Highway Administration (FHWA) in cooperation with ODOT is gratefully acknowledged.

Finally, the authors would like to thank Mr. A. Gopalasingam, Mr. Dinesh Bhat and Mr. Chandi Mohanty for their help.

## TABLE OF CONTENTS

	Page
LIST OF TABLES . . . . .	iii
LIST OF FIGURES . . . . .	iv
ABSTRACT . . . . .	vii
CHAPTER	
1. INTRODUCTION . . . . .	1
1.1 Background . . . . .	1
1.2 Consolidation Settlement Due to Foundation . . . . .	4
1.3 Settlement Due to Embankment . . . . .	6
1.4 Computer Program . . . . .	7
1.5 Report Content . . . . .	8
2. OVERVIEW OF FINITE ELEMENT ALGORITHM . . . . .	10
2.1 Introduction . . . . .	10
2.2 Preliminaries . . . . .	10
2.3 Scope and Limitations . . . . .	13
2.4 Nomenclature . . . . .	14
2.5 Finite Element Formulation . . . . .	16
2.6 Time Integration . . . . .	20
2.7 Type of Elements and Displacement Field . . . . .	22
2.8 Pressure Field . . . . .	28
2.9 Infinite Element Formulation . . . . .	29
2.9.1 Governing Equations for Plain Strain Analysis . . . . .	29
2.9.2 Analytical Solution for Vertical Distributed Load . . . . .	34
2.9.3 Far Field Behavior of Elastic Half Plane . . . . .	36
2.9.4 Displacements . . . . .	36
2.9.5 Pore Pressures . . . . .	37
2.9.6 Infinite Elements . . . . .	38
2.9.7 Saturated Porous Infinite Elements . . . . .	39
3. OVERVIEW OF THE COMPUTER PROGRAMS . . . . .	47
3.1 General . . . . .	47
3.2 Preprocessor . . . . .	51
3.2.1 Components of the Preprocessor's Window . . . . .	51
3.2.2 Running the Preprocessor - Create New Input Data File . . . . .	53
3.2.3 Running the Preprocessor - Edit an Existing Input Data File . . . . .	73
3.3 Data Convertor . . . . .	78
3.4 FE Main Program . . . . .	79
3.4.1 Description of the FE Main Program . . . . .	83
3.4.2 Input Quantities for the FE Main Program . . . . .	84
3.4.3 Running the FE Main Program . . . . .	85



3.5	The Postprocessor . . . . .	87
3.5.1	The Subroutines of the Postprocessor . . . . .	87
3.5.2	Running the Postprocessor . . . . .	88
4.	APPLICATION EXAMPLES, RESULTS AND COMPARISONS . . . . .	122
4.1	Site Description . . . . .	122
4.2	Soil Sampling . . . . .	123
4.3	Discussion of Laboratory Test Results . . . . .	124
4.4	Possible Causes for Approach Slab Settlement . . . . .	125
4.5	Analysis of Consolidation Settlement Using the FEM . . . . .	126
4.6	Interpretation of the FEM Results . . . . .	127
4.6.1	Foundation Analysis . . . . .	127
4.6.2	Embankment Analysis . . . . .	129
4.7	Verification of the Results . . . . .	130
5.	CONCLUSIONS AND RECOMMENDATIONS . . . . .	156
5.1	Conclusions . . . . .	156
5.2	Recommendations for Future Study . . . . .	158
	REFERENCES . . . . .	159
	APPENDIX	
I	SUMMARY OF DIFFERENT RESEARCH PHASES . . . . .	162
II	DETAILS OF THE CONSTITUTIVE MODEL . . . . .	173
III	NOTES ON INPUT FOR THE FE MAIN PROGRAM . . . . .	186
IV	NOTES ON THE OUTPUT DATA OF PREPROCESSOR . . . . .	201

## LIST OF TABLES

TABLE	Page
1.1	Different Phases Involved in the Overall Bridge Approach
	Settlement Project . . . . . 9
3.1	Input and Output of Different Programs . . . . . 89
3.2	Range of Variables Used in the Preprocessor . . . . . 90
3.3	Various Embankment Heights for the Preprocessor . . . . . 91
3.4	Various Water Table Depths for the Preprocessor . . . . . 91
4.1	General Site Description . . . . . 133
4.2	Soil Layers . . . . . 134
4.3	Strength Parameters from Triaxial Compression Tests . . . . . 135
4.4	Consolidation Test Results . . . . . 136
4.5	Input Soil Properties for the Example Problem . . . . . 137
III.1	Format and Order of the Input Variables for the FE Main Program . . . . 186
III.2	Identification of the Input Variables for the FE Main Program . . . . . 192



## LIST OF FIGURES

FIGURE		Page
2.1A	Approach Embankment and Foundation . . . . .	42
2.1B	FE Idealization . . . . .	43
2.1C	Elements Used . . . . .	43
2.2	Schematic Representation of Consolidation Mass . . . . .	44
2.3	Eight-Noded Isoparametric Quadrilateral Element . . . . .	44
2.4	Two-Dimensional Curved Isoparametric Element Mapped From the Rectangular Parent Element . . . . .	45
2.5	Two-Dimensional Four-Noded Isoparametric Element Mapped From the Rectangular Parent Element . . . . .	45
2.6	Elastic Half Plane Subjected to a Uniformly Distributed Vertical Load . . . . .	46
2.7	Singular Contraction of Infinite Element . . . . .	46
3.1	Different Components of the Software Package . . . . .	92
3.2	Main Components of the Preprocessor . . . . .	93
3.3	Various Components of A Window . . . . .	94
3.4	Bridge Approach Settlement Window . . . . .	94
3.5	Actor Window . . . . .	95
3.6	Actor Workspace Window . . . . .	95
3.7	Input Data File Type Window . . . . .	96
3.8	Unit System Window . . . . .	96
3.9	Coordinate Space Window . . . . .	96
3.10	Message Box Window . . . . .	97
3.11	Bridge Approach Settlement Analysis Main Window . . . . .	98
3.12	Site Data Option Window . . . . .	99
3.13	Control Parameters Window . . . . .	100
3.14	Idealized Soil Profile for East Cordell Bridge Site . . . . .	101
3.15A	Embankment Layer Information Window . . . . .	102
3.15B	Foundation Layer Information Window . . . . .	103
3.16	Embankment Layer No. Window . . . . .	104
3.17	Isotropic Property Window . . . . .	104
3.18A	Isotropic Material Window for Embankment Layer . . . . .	105
3.18B	Anisotropic Material Window for Embankment Layer . . . . .	106
3.18C	Isotropic Sand Window for Foundation Layer . . . . .	107
3.18D	Isotropic Clay Window for Foundation Layer . . . . .	108
3.18E	Anisotropic Sand Window for Foundation Layer . . . . .	109
3.18F	Anisotropic Clay Window for Foundation Layer . . . . .	110
3.19	Water Table Depth Window . . . . .	111
3.20	FE Mesh Option Window . . . . .	111
3.21	Three Parts in the X Direction for FE Mesh . . . . .	112

3.22A	Default Mesh at Visual Sub-window . . . . .	112
3.22B	Zoomed Custom Mesh . . . . .	113
3.23	Coordinate Space Window for Loading Option . . . . .	114
3.24A	Embankment Construction History . . . . .	114
3.24B	Load Data Window . . . . .	115
3.25	Embankment Loading Window . . . . .	116
3.26	Node Numbering and Element Numbering Adopted for a Typical Foundation Discretization . . . . .	117
3.27	Node Numbering and Element Numbering Adopted for a Typical Embankment Discretization . . . . .	118
3.28	Organization Structure of the FE Main Program . . . . .	119
3.29	Plot Title Window for Postprocessor . . . . .	120
3.30	Input Data File Window for Postprocessor . . . . .	120
3.31	GraphiC Window for Postprocessor . . . . .	121
4.1	Location of Captain Creek Bridge Site . . . . .	138
4.2	Bore Hole Locations . . . . .	139
4.3	Elevation Showing Bore Holes and Selected Samples . . . . .	139
4.4	Soil Profile for Borehole#1 at Captain Creek Bridge Site . . . . .	140
4.5	Soil Profile for Borehole#2 at Captain Creek Bridge Site . . . . .	141
4.6	SPT Values Obtained in the Field in Bore Hole 1 . . . . .	143
4.7	SPT Values Obtained in the Field in Bore Hole 2 . . . . .	143
4.8	e vs log (p) Curve for Sample 1U . . . . .	144
4.9	e vs log (p) Curve for Sample 2BB . . . . .	144
4.10	Determination of $C_v$ for Sample 1U . . . . .	145
4.11	Variation of $C_v$ with Applied Pressure for Sample 1U . . . . .	145
4.12	Stress-strain Variation from Triaxial Compression Test of Sample 1U . . . . .	146
4.13	Stress-strain Variation from Triaxial Compression Test of Sample 2BB . . . . .	146
4.14	Idealized Geometry of the Example Problem . . . . .	147
4.15	Default Mesh for the Example Problem . . . . .	148
4.16	Custom Mesh for the Example Problem . . . . .	148
4.17	Embankment Loading History . . . . .	149
4.18	Traffic Load Acting on the Embankment . . . . .	149
4.19	Foundation Surface Settlement . . . . .	150
4.20	Pore Pressure in Foundation . . . . .	150
4.21	Normal Stress Contours in Foundation at 250 Days . . . . .	151
4.22	Embankment Surface Settlement . . . . .	151
4.23	Settlement at Various Depths of Embankment . . . . .	152
4.24	Embankment Maximum Normal Stress Contours . . . . .	152
4.25	Idealized Site Condition for Analysis Using Terzaghi's Theory of 1-D Consolidation . . . . .	153
4.26	One Dimensional Idealization Using the Finite Element Method . . . . .	153



4.27	Comparison of Total Settlement of 22'-Clay Layer as Found by Different Methods . . . . .	154
4.28	Comparison of Degree of Consolidation as Found by Different Methods . . . . .	155
II.1	Modified Cam-Clay Model on the q-p Plane . . . . .	184
II.2	Strain Hardening Behavior . . . . .	184
II.3	Modified Cam-Clay Model . . . . .	185
II.4	Typical e-ln p Curve . . . . .	185
III.1	Example of Nodal Index - the Variable IX (1) Through IX (8) . .	198
III.2	First 26 Lines of the Data File Capdmf.dat Showing Items no.1 Through 7 in Whole and First Six Lines of Item no.8 . . . . .	199
III.3	Lines 577 to 585 from Input Data File Capdmf.dat Showing Last Four Lines of Item no.8 and First Five Lines of Item no.9 . . . . .	199
III.4	Lines 669 to 678 from the Data File Capdmf.dat Showing Last Two Lines of Items no.9 and First Eight Lines of Item no.10 . . .	200
III.5	Lines 729 to 744 from Input Data File Capdmf.dat Showing Last Two Lines of Item no.10 and Two Repetitions of Item no.9 .	200

## ABSTRACT

Bridge approach settlement is a major problem in highway design as well as maintenance. It creates an unsafe and uncomfortable riding surface. This report presents the details of a software that was developed at the University of Oklahoma, through a project funded jointly by the Oklahoma Department of Transportation (ODOT) and the Federal Highway Administration (FHWA). The objective of the software was to analyze the settlement characteristics of the problematic bridge approach sites in Oklahoma. To this end, a nonlinear Finite Element (FE) analysis procedure was developed for predicting the consolidation settlement of the foundation soil at a bridge approach due to the surcharge of embankment construction, as well as the settlement of the embankment itself due to the vehicular traffic loads.

The software package , called **FEABAS**, is divided into a number of different modules: *Preprocessor*, *Data Converter*, *FE Main Program*, and *Postprocessor*. **FEABAS** works completely in the Windows operating environment in IBM compatible PC's. The interactive nature of the software makes it user-friendly; especially the graphical interface of the *preprocessor* enhances the data input operation. Existing data files can also be modified or edited using the *preprocessor*. The *preprocessor* is written in Actor 4.0 , which is a complete development environment and programming language that make it easy to develop stand-alone applications for Microsoft Windows Version 3.0 or later. This report presents an overview of the steps involved in analyzing bridge

approach settlement using the software package.

The software package - **FEABAS** is a very useful tool for conducting parametric studies of a problematic bridge approach site to identify some of the important causative factors and their relative significance, that are expected to be helpful in finding appropriate remedial measures to the problem. The bridge approach settlement at a site in Oklahoma was predicted using **FEABAS** for illustration and application. The various capabilities of the software including graphical output are illustrated.

# CHAPTER 1

## INTRODUCTION

### 1.1 Background

Bridge approach settlement is one of the major problems facing the transportation agencies in the United States and in many other countries of the world. This problem results primarily from the differential settlement between a rigid bridge deck and the bridge approach embankment; it is referred to as 'bump' at the ends of a bridge. It not only leads to an uncomfortable and unsafe riding surface, but also can cause damage to the approach slab, requiring frequent maintenance. The approach settlement can be responsible for excessive impact load on the bridge structure by vehicular traffic thus causing damage to the bridge itself.

Although a number of researchers (e.g., Ardani, 1987; Gopalasingam, 1989; Hopkins, 1985; Laguros et al., 1986,1990 and 1991; Stewart, 1985; Tadros, 1989; Zaman et al., 1990) from transportation agencies and academic institutions attempted to study this problem, general and satisfactory solutions have not yet been found. The usual remedy for this problem is the frequent maintenance measures such as mudjacking (for concrete pavements), and patching (for both concrete and asphalt concrete approaches). Even though mudjacking provides a temporary solution, it often introduces cracks in the approach slab. The operation also impedes the normal flow of traffic, especially on

interstate highways and freeways, where the traffic volume and speeds are very high.

The bridge approach settlement problems are found to be quite extensive in Oklahoma. A large number of abutments and approach embankments placed on weak soils of former Oxbow lakes in Oklahoma have made such settlement problems particularly critical. Cognizant of the extensiveness of this problem in Oklahoma, the Oklahoma Department of Transportation (ODOT) commissioned the University of Oklahoma (OU) to undertake a systematic study of this problem to evaluate the causes of excessive approach settlement and recommend remedial measures. The ultimate goal of this research work is to provide ODOT with appropriate procedures and guidelines that can be used for the design, construction and maintenance of bridge approaches so as to effectively control the bridge approach settlement problems in the State.

To accomplish its intended goals, the study encompassed five different phases as outlined in Table 1.1.<sup>1</sup> An important part of the overall study was to conduct a two-level survey of selected bridge approaches in Oklahoma. The level-one survey included about 758 bridges and it involved field visits, review of information available at ODOT and collection of maintenance related data/information from various field divisions. All collected data were carefully analyzed using a statistical framework in an attempt to identify the important approach settlement causative factors (Laguros et al., 1990). In the level-two survey, field and laboratory tests were conducted for 29 sites to determine the

---

<sup>1</sup>Tables and Figures are presented at the end of a chapter.



site-specific causative factors and their relative contributions. A comprehensive analysis of level-one and level-two survey data/information revealed that bridge approach settlements are caused by various factors such as consolidation settlement of the approach foundations, settlement within the approach embankment due to traffic loads and dead loads, lateral movements of embankments, and embankment slope erosion (Laguros et al., 1991). One of the objectives of this study was to develop innovative approaches to assess these settlements using a numerical method. A novel finite element (FE) algorithm and a user-friendly computer program package, **FEABAS**, were developed to aid in the preparation of input data for bridge approach settlement assessment and in the interpretation of results.

The primary objectives of this phase of the bridge approach settlement study are two-fold:

- \* To enhance the user-friendliness of the finite element computer program for evaluation of consolidation settlement of approach foundation as well as inelastic settlement due to embankment dead load and traffic loading by developing pre- and post-processors.
- \* To combine the developed pre- and post-processors with the finite element program so as to obtain a complete software package ( **FEABAS** ) that can be used by the transportation agencies and academic institutes for approach settlement analyzes. To this end, a detailed user's manual (see Chapter 3) was

prepared.

## **1.2 Consolidation Settlement due to Foundation**

Settlement contributed by the approach foundation soil can be attributed by various factors. For predominantly clayey sites, this settlement is mainly due to consolidation of the compressible foundation soil. Elastic settlement or immediate settlements are usually of less significance since they take place during construction of the embankment and the roadway pavement. Consolidation settlement, on the other hand, is a time-dependent process that generally continues well beyond the construction period of the embankment. Both the rate of consolidation and the magnitude of consolidation settlement are important for an appropriate and cost effective design of the bridge approach pavement. Further, it is important to evaluate the consolidation settlement of approach foundations to quantitatively identify the relative contribution of consolidation settlement in assessing the overall approach settlement problem at a given site.

Several semi-empirical and numerical techniques can be used to predict the consolidation settlement of the approach foundation soil. Semi-empirical methods are usually based on statistical analysis of field observations and therefore may have limitations in predicting the bridge approaches settlements at specific sites (Hopkins, 1985; Schiffman, 1969). Furthermore, these methods are deficient in predicting the

time-dependent settlement history.

With rapid advances in computing capabilities, the Finite Element Method (FEM) has emerged as a very powerful tool for analyzing problems with complex geometry, boundary conditions, and nonlinear behavior. In this method, the approach foundation soil is divided into many small regions, called 'elements.' The consolidation behavior of each region which is due to construction of embankment or fluctuation of the water-table, is evaluated by using the Terzaghi's one-dimensional consolidation theory (Terzaghi et al., 1948) or by more advanced theories such as three-dimensional consolidation (Roscoe et al., 1963; Zienkiewicz, 1977). FEM is a very effective method in representing a layered foundation soil. Also, it can accurately represent the time-dependent nature of embankment loading and seasonal fluctuations of water-table depths. The FEM software package - **FEABAS** developed in this study is based on the Biot's theory of coupled three-dimensional consolidation (Biot, 1941) as proposed by Sandhu and Wilson (Sandhu et al., 1969). Plain strain idealization is assumed for simplicity. Eight noded quadrilateral elements are used for spatial discretization. Nodal displacements are considered to be unknowns at all the nodes. Pore pressure is considered to be the unknown at the corner nodes only. The nonlinear elastoplastic behavior of soil skeleton is represented by the modified Cam-Clay constitutive model proposed by Roscoe and Burland (Roscoe et al., 1968). Further details of the FEM algorithm are given in Chapter 2 (Sec. 2.1 through Sec. 2.9) and in Appendix II.

### **1.3 Settlement Due to Embankment**

The laboratory and field data from a large number of sites having severe approach settlement problems revealed that most of the approach embankments were not properly compacted at these sites (Laguros et al., 1991). Due to the difficulty in compacting the embankment material to the required degree in the vicinity of the bridge approach, considerable amount of settlement may occur due to the dead load of the embankment and the vehicular traffic. From this consideration, the approach embankment settlement may play an important role and it needs to be included in assessing the overall bridge approach settlement problems at a site.

In this study, the FEM algorithm for consolidation analysis was adopted to evaluate the approach embankment settlement. The approach foundation is treated as a continuum and stress-strain response is idealized by an elasto-plastic model. According to such a model, various foundation regions can either behave as an elastic material or as an inelastic material, depending upon the stress level. Response in elastic regions is evaluated by using the elastic properties (Young's modulus and Poisson's ratio), while response in plastic regions is evaluated in terms of failure parameters such as cohesion and angle of internal friction. Plastic zones become particularly important for portions of the embankment which are not properly compacted and where stresses are large due to extra heavy vehicular traffic or the dead load resulting from high embankments.

## 1.4 Computer Program

The FEM algorithm is implemented in a computer program, written in FORTRAN77 language. The computer code was originally developed by Dr. C.S. Desai, and his co-workers at the University of Arizona, Tucson, Arizona(Desai, 1987). The code was modified and extended substantially by Gopalasingam (1989) to incorporate the isoparametric quadrilateral and infinite elements. To make the computer program user-friendly, a *preprocessor* was developed to assist the user in preparing the required input data in an interactive environment. Graphical capabilities were incorporated for physical illustrations.

The output from the *preprocessor* is fed into a program called CONVERT.FOR, written in FORTRAN77, to obtain the input data for the *FE Main Program* in a compatible format. The input data are grouped separately for foundation and embankment analysis at this stage. The *FE Main Program* evaluates the settlements and excess pore pressures at specified points (called nodes) within the approach foundation and embankment domain. At the center of each element normal stresses, shear stresses and principal stresses are computed. A *postprocessor* was developed to plot the results from the *FE Main Program* in graphical form and to facilitate their interpretation. This user-friendly software package - **FEABAS** is expected to help ODOT analyze the bridge approach problems at specific sites and use these results in assessing the desired remedial measures. A flow chart showing the order of execution of various elements of **FEABAS**



is presented in Chapter 3 (Sec. 3.1)

## **1.5 Report Content**

An overall introduction of the ODOT Bridge Approach Settlement project, including objectives and goals, is presented in Chapter 1. Various phases of the research completed so far are summarized in Appendix I. Details of the finite element (FE) algorithm used for the analysis of consolidation settlement of the foundation due to construction of embankment, and embankment settlement due to its dead load and vehicular traffic loads are discussed in Chapter 2 (Sec. 2.1 through 2.9) and in Appendix II.

The **FEABAS** package consists of four different programs developed for the analysis of bridge approach settlement: *Preprocessor*, *Data Converter*, *FE Main Program*, and *Postprocessor*. In Chapter 3 a brief discussion of these programs is given. The User's Manual for the *FE Main Program* and the *Preprocessor* are presented in Appendix III and IV, respectively.

A sample bridge approach site is selected and analyzed using the **FEABAS**. The details of the site selected for the analysis and the results are presented in Chapter 4. The conclusions and recommendations are presented in Chapter 5.

Table 1.1 Different Phases Involved in the Overall Bridge Approach Settlement Project

Phase	Description
I	Literature review and survey of transportation agencies to investigate the extent of approach settlement problems in Oklahoma and other states.
II	Level-one survey of selected bridge approaches in Oklahoma for a qualitative assessment of causative factors.
III	Level-two survey of selected bridge approaches in Oklahoma for field testing and collecting samples for laboratory testing.
IV	Developing numerical and statistical models for prediction of approach settlement.
V	Developing guidelines for design, construction, and maintenance of bridge approaches.

## CHAPTER 2

### OVERVIEW OF THE FINITE ELEMENT ALGORITHM

#### 2.1 Introduction

Finite element method (FEM) is a numerical technique initially devised as a tool for structural analysis (Desai et al., 1984; Zienkiewicz, 1977). In the past three decades FEM has emerged as a versatile and efficient procedure/method for analyzing a wide range of geotechnical and geo-environmental engineering problems such as soil-structure interactions, slope stability, tunneling, geosynthetics, and contaminant transport. In the present study, FEM is used as a numerical tool for assessment of bridge approach settlements, particularly the settlements caused by the consolidation of the approach foundation soil, the self weight of the embankment and the vehicular traffic loading on the embankment. In this chapter an overview of the finite element formulation is presented; further details can be found elsewhere (Zaman et al., 1991).

#### 2.2 Preliminaries

Finite element (FE) analyses are usually based on a mathematical and spatial idealizations of the physical problem being analyzed. For example, the settlement analysis considered here, which involves contribution from both foundation soil and the embankment is three-dimensional (3-D) in nature. Since FE analysis of a 3-D system can be rather expensive in terms of computations and data preparation and therefore

uneconomical, simplified idealizations are normally introduced to treat the problem as either one-dimensional (1-D) or as two-dimensional (2-D). In the present study, a 2-D idealization, called the plane strain idealization, is adopted. In this idealization, the analysis is carried out for a section of unit thickness of approach embankment/foundation and perpendicular to the direction of traffic. An idealized section - also called the "idealized domain" - is shown in Fig. 2.1A. A sample problem is selected for demonstration. This section is taken close to the abutment where settlement problems are particularly critical. It may be noted that the actual domain (foundation soil) does not have the vertical boundaries considered in the "idealized section," or the "idealized domain." The reason is that a finite element analysis can only account for finite regions; thus, an infinite region is approximated by a finite one and the artificial boundaries are considered at a sufficient distance away from the region of interest so as to minimize the effects of artificial boundaries. In the present study, the boundary conditions are simulated in a very realistic manner by introducing a special feature in the FE mathematical formulation, called "infinite element."

In FE analysis the "idealized domain" or the "idealized section" is divided into small subregions called "elements." The idealized domain or the FE mesh is shown in Fig. 2.1B. Usually the accuracy of FE results increases with the number of elements used in the FE mesh. Generally, enough elements should be taken in analyzing a settlement problem so that the results obtained are reliable. However, it should also be

realized that the computational efforts and the computing time will increase significantly with increasing the number of elements. Selection of FE mesh is further discussed in sections 2.7 and 2.9. A typical FE mesh for the idealized foundation soil is presented in Fig. 2.1B.

The corner points of an element, called "nodes" or "nodal points" are shown in Fig. 2.1C. Both displacements (horizontal and vertical) and excess pore water pressure are considered to be the primary unknowns at these nodal points. In addition to corner nodes, the mid-point of each side of an element is treated as nodes. These nodes are called "mid-side nodes," where only displacements (horizontal and vertical) are treated as unknowns. Thus, a regular element has twenty unknowns (sixteen displacements and four pore pressures) or degrees-of-freedom. An infinite element, on the other hand, has only three nodes and eight degrees-of-freedom, as shown in Fig. 2.1C.

The finite element formulation presented in the following section is based on the governing differential equations that describe the coupled flow-deformation behavior of the idealized domain (i.e., idealized foundation soil and embankment). Biot's theory (Biot, 1941) of three-dimensional consolidation forms the basis of this mathematical formulation. Alternatively, it is possible to consider Terzaghi's consolidation theory (Terzaghi et al., 1948) in the formulation, but this theory does not have any mechanism to account for the coupling effects between flow (excess pore water dissipation) and deformation that are important in the consolidation process.



## 2.3 Scope and Limitations

1. Consolidation of the approach foundation is assumed to occur due to construction of embankment only. The in situ stresses are evaluated from the field test data, standard penetration test (SPT) values, cone penetration test (CPT) values in terms of field density, layer thickness, earth pressure coefficient at rest ( $K_0$ ) and water table depth.
2. Embankment loading is assumed to be a step-wise loading process in which each step of embankment construction is assumed to be completed within a specified time period, as illustrated graphically in Fig. 3.24A. The user can select the number of steps so as to simulate the actual construction scenario or may wish to consider various construction scenarios to identify the worst possible cases of approach settlement problem.
3. Nonlinear and inelastic behavior of approach foundation soil is represented by the Modified Cam-Clay model (Roscoe et al., 1963; and Schapery et al., 1962). According to this model the soil skeleton behaves as an elasto-plastic material. One of the strengths of this model is that it needs relatively fewer material constants (see Appendix II Section II-C for specifics) compared to other models. Furthermore, each material constant used in this model has physical meaning.
4. Stress-strain response of the embankment materials is represented by the elastic model (Hooke's law). If the embankment material is clay, then it can either be represented by the elastic model or the Cam-clay model.

5. The FE formulation is developed within the context of small strain theory. Geometric nonlinearity is not taken into account.
6. The soil below the water table is assumed to be completely saturated and that above the water table is assumed to be unsaturated.
7. The FE main program is based on the plane strain idealization. Though this idealization is appropriate for the foundation. It is merely a crude assumption for the embankment. However, it has been accepted here because it depicts the worst loading situation.

## 2.4 Nomenclature

$e$  = Dilation

$E^*$  = Displacement function

$E_c$  = Displacement function after Fourier transformation of infinite element governing differential equations.

$E_c$  = Displacement function after Laplace transformation of infinite element governing differential equations.

$G$  = Shear modulus

$i$  and  $j$  = Indices in tensor notation

$i,j$  = Differentiation with respect to  $j$

$[ J ]$  = Jacobian (transformation) matrix

$[K]$  = Global stiffness coefficient matrix

$k$  = Coefficient of permeability

$k_{ij}$  = Permeability tensor

$L_j(\eta)$  = Lagrangian polynomial for node  $j$  in an infinite element

$N_i$  = Shape functions

$\{ p_m \}$  = Nodal pore pressure vector

$q_i$  = Relative velocity of fluid

$\{ q_m \}$  = Nodal displacement vector

$\bar{Q}$  = Prescribed fluid flow normal to surface  $S_2$  (refer Fig. 2.2)

$\{ \bar{Q}_m \}$  = Prescribed nodal fluid flux vector

$\{ r \}$  = Vectors of displacement and pore pressure

$\{ r_p \}$  = Nodal pore pressure vector

$\{ r_q \}$  = Nodal displacement vector

$r_*$  = Real number greater than highest real part of singularities of the Laplace transform of infinite element governing differential equation

$\{ R \}$  = Global load vector

$S^*$  = Displacement function

$S_c$  = Displacement function after Fourier transformation of infinite element governing differential equation

$\overline{S}_c$  = Displacement function after Laplace transformation of infinite element  
governing differential equation

$\{ \overline{T}_i \}$  = Prescribed traction on surface  $S_1$  (refer Fig. 2.2)

$\{ \overline{T}_m \}$  = Prescribed nodal traction vector

$u_i$  = Displacements tensor

$x$  and  $y$  = Global coordinates

$\xi$  and  $\eta$  = Local coordinates

$\epsilon_{ij}$  = Strain tensor

$\rho$  = Mass density of soil

$\rho_w$  = Mass density of pore fluid

\* Represents convolution

## 2.5 Finite Element Formulation

The finite element formulation for a linearly elastic soil skeleton and incompressible pore fluid can be derived from the functional proposed by Sandhu and Wilson (Sandhu et al., 1969)

$$\begin{aligned}
\Omega(u, p) = & \int_v \left[ \frac{1}{2} \bar{\sigma}_{ij} * \varepsilon_{ij} - \rho F_i * u_i + p * u_{i,j} \right. \\
& \left. - \frac{1}{2} g * q_i * (p_{,i} + \rho_w F_i) \right] dV \\
& - \int_{s_1} (\bar{T}_i * u_i) dS + \int_{s_2} (g * \bar{Q} * p) dS
\end{aligned} \tag{2.1}$$

In the above expression the repetitive indices represent summation from 1 to 3 and a comma indicates differentiation with respect to x, y or z. The strain-displacement relations are given by

$$\varepsilon_{ij} = 1/2 (u_{i,j} + u_{j,i}) \tag{2.2}$$

Other terms of the functional  $\Omega(u, p)$  are defined in Section 2.4 (nomenclature). The functional in Eq. 2.1 can be rewritten in matrix form as

$$\begin{aligned}
\Omega(u, p) = & \int_v \left( \frac{1}{2} (\bar{\sigma})^T * \{\varepsilon\} - \int_v \{\rho F\}^T * \{u\} dV \right. \\
& \left. + \int_v p * \{\varepsilon\}_{vo1} dV - \frac{1}{2} \int_v g * \{q\}^T * (\{p_{,i}\} \right. \\
& \left. + \{\rho_w F\}) dV - \int_{s_1} \{\bar{T}\}^T * \{u\} ds + \int_{s_2} g * \bar{Q} * p ds \right)
\end{aligned} \tag{2.3}$$

Each of the terms in Eq. 2.3 can be expressed in terms of nodal displacements and nodal pore pressures as follows:

$$\{u\} = [N_u] \{q_m\} \tag{2.4a}$$

$$\{\bar{\sigma}\} = [\bar{C}] [B_e] \{q_m\} + \{\bar{\sigma}_o\} \tag{2.4b}$$



$$\{q\} = ([k] ([B_q] \{p_m\} + \{p_w F\})) \quad (2.4c)$$

$$\{p\} = [N_p] \{p_m\} \quad (2.4d)$$

$$\{\varepsilon_{vol}\} = [B_\Delta] \{q_m\} \quad (2.4e)$$

$$\{\bar{T}\} = [N_u] \{\bar{T}_m\} \quad (2.4f)$$

$$\{\varepsilon\} = [B_e] \{q_m\} \quad (2.4g)$$

$$\{p_{,i}\} = [B_q] \{p_m\} \quad (2.4h)$$

$$\{\bar{Q}\} = [N_p] \{\bar{Q}_m\} \quad (2.4i)$$

Substituting Eqs. 2.4a to 2.4i in the functional expression  $\Omega(u, p)$  in Eq. 2.3, the modified functional in terms of nodal displacements and nodal pore pressures is obtained in the following form:

$$\begin{aligned} \Omega(u, p) = & \sum_{m=1}^M \int_v \left( \frac{1}{2} \{q_m\}^T [B_e]^T [\bar{C}] [B_e] \{q_m\} + \{p_m\}^T [N_p]^T [B_\Delta] \{q_m\} \right. \\ & + \frac{1}{2} \{\bar{\sigma}_o\}^T [B_e] \{q_m\} - \{q_m\}^T [N_u]^T \{\rho F\} \\ & - \frac{1}{2} g \{p_m\}^T [B_q]^T [k] [B_q] \{p_m\} \\ & - g \{p_m\}^T [B_q]^T [k] \{\rho_w F\} - \frac{1}{2} g \{\rho_w F\}^T [k] \{\rho_w F\} \left. dV \right. \\ & \left. - \int_{s_1} \{q_m\}^T [N_u]^T [N_u] \{\bar{T}_m\} ds + \int_{s_2} g \{p_m\}^T [N_p]^T [N_p] \{\bar{Q}_m\} ds \right) \end{aligned} \quad (2.5)$$

The global stiffness equation can be obtained by summation of element stiffness equations. Thus, Eq. 2.5 becomes

$$\begin{aligned}
\Omega(u, p) = & \frac{1}{2} \{q\}^T [K_1] \{r_q\} + \{q\}^T [M_1] \cdot g + \{q\}^T [K_3] \{r_p\} \\
& - \{q\}^T [M_2] \cdot g - \frac{1}{2} g \cdot \{r_p\}^T [K_2] \cdot \{r_p\} - g \cdot \{r_p\}^T [M_3] \cdot g \\
& - \frac{1}{2} g \cdot [M_4] \cdot g - \{r_q\}^T \{P_1\} + g \cdot \{r_p\}^T \{P_2\}
\end{aligned} \tag{2.6}$$

where,

$$[K_1] = \sum_{m=1}^M \int_v [B_e]^T [C] [B_e] dV \tag{2.6a}$$

$$[K_2] = \sum_{m=1}^M \int_v [B_q]^T [K] [B_q] dV \tag{2.6b}$$

$$[K_3] = \sum_{m=1}^M \int_v [B_\Delta]^T [N_p] dV \tag{2.6c}$$

$$[M_1] = \sum_{m=1}^M \int_v [B_e]^T \{\bar{\sigma}_o\} dV \tag{2.6d}$$

$$[M_2] = \sum_{m=1}^M \int_v [N_u]^T \{\rho F\} dV \tag{2.6e}$$

$$[M_3] = \sum_{m=1}^M \int_v [B_q]^T [K] [\rho_w F] dV \tag{2.6f}$$

$$[M_4] = \sum_{m=1}^M \int_V \{\rho_w F\}^T [K] \{\rho_w F\} dV \quad (2.6g)$$

$$[P_1] = \sum_{m=1}^M \int_{S_1} [N_u]^T [N_u] \{\bar{T}_m\} dS \quad (2.6h)$$

$$[P_2] = \sum_{m=1}^M \int_{S_2} [N_p]^T [N_p] \{\bar{Q}_m\} dS \quad (2.6i)$$

Similarly, taking first variation of Eq. 2.6 with respect to  $\{r_q\}$  and setting the result to zero leads to

$$[K_1] \{r_q\} + [K_3] \{r_p\} = -\{M_1\} + \{M_2\} + \{P_1\} \quad (2.6j)$$

Similarly, taking first variation with respect to  $\{r_p\}$  of Eq. 2.6 and setting the result to zero leads to

$$[K_3]^T \{r_q\} - g^* [K_2] \{r_p\} = g^* \{M_3\} - g^* \{P_2\} \quad (2.6k)$$

## 2.6 Time Integration

It may be noted that the nodal displacement vector,  $\{r_q\}$ , and the nodal pore pressure vector,  $\{r_p\}$ , in Eqs. 2.5 and 2.6 are functions of time. The linear convolutions in Eq. 2.6k require an approximation to be made for the variation of  $\{r_p\}$  with time. Each term in the convoluted vector can be written as

$$g \cdot f(t) = \int_0^t f(\tau) g(t-\tau) d\tau = \int_0^t f(\tau) d\tau \quad (2.7)$$

In a discrete interval  $t_{n-1}$  to  $t_n$  with a time step of  $\Delta t$ , the integration can be approximated by

$$\int_{t_{n-1}}^{t_n} f(\tau) d\tau = \alpha \Delta t f(t_n) + (1-\alpha) \Delta t f(t_{n-1}) \quad (2.8)$$

The value of  $\alpha$  depends on the assumed variation of  $f(t)$  in the interval  $\Delta t$  considered.

A purely explicit scheme assumes  $\alpha = 0$ , while a purely implicit scheme assumes  $\alpha =$

1. Any scheme with  $\alpha$  greater than 0.5 is usually unconditionally stable as shown by

Booker and Small (Booker et al., 1975). Sandhu and Wilson (Sandhu et al., 1969)

suggested that a reasonable assumption is to vary  $f(t)$  linearly within the interval  $t_{n-1}$  and

$t_n$ . Thus,  $\alpha = 0.5$  can be used.

Substituting Eq. 2.7 in Eq. 2.6j gives a combined matrix equation of the form

$$\begin{aligned} & [K_3]^T \{r_q(t_n)\} - \alpha \Delta t [K_2] \{r_p(t_n)\} \\ & = [K_3]^T \{r_q(t_{n-1})\} - \Delta t (1-\alpha) [K_2] \{r_p(t_{n-1})\} \\ & + \alpha \Delta t \{M_3(t_n)\} + \Delta t (1-\alpha) \{M_3(t_{n-1})\} \\ & - \alpha \Delta t \{P_2(t_n)\} - \Delta t (1-\alpha) \{P_2(t_{n-1})\} \end{aligned} \quad (2.9)$$

Eq. 2.9 can be written in a more compact form as shown in Eq. 2.10

$$[K] \{r\} = \{R\} \quad (2.10)$$

or as in Eq. II.39 (Appendix II), in which

$$\{R_Q(t_n)\} = -\{M_1(t_n)\} - \{P_1(t_n)\} + \{M_2(t_n)\}$$

$$\begin{aligned}
\{R_p(t_n)\} &= [K_3]^T \{r_q(t_{n-1})\} - \Delta t (1 - \alpha) [K_2] \{r_p(t_{n-1})\} \\
&\quad + \alpha \Delta t \{M_3(t_n)\} + \Delta t (1 - \alpha) \{M_3(t_{n-1})\} \\
&\quad - \alpha \Delta t \{P_2(t_n)\} - \Delta t (1 - \alpha) \{P_2(t_{n-1})\}
\end{aligned} \tag{2.11}$$

All the terms in the coefficient matrix [K] in Eqs. 2.9 and 2.10 can be assumed as constant throughout the consolidation process so as to minimize computational costs or can be varied at selected time intervals within the entire time domain to obtain more accurate results.

## 2.7 Type of Elements and Displacement Field

Eight noded isoparametric quadrilateral elements with four corner nodes and four midside nodes are used in this study to discretize the near field. Fig. 2.3 represents an eight noded quadrilateral element used in the FE formulation with degrees-of-freedom marked at the corresponding nodes. In order to ensure the same degree of contraction and expansion for effective stresses as well as pore pressures, the nodal displacements are considered as primary unknowns at all the eight nodes while pore pressures are considered to be unknowns at the corner nodes only.

Curved isoparametric element mapped from quadrilateral element is shown in Fig. 2.4. The displacement functions (u, v) for the eight noded quadrilateral elements are given by

$$u(\xi, \eta) = C_1 + C_2\xi + C_3\eta + C_4\xi\eta + C_5\xi^2 + C_6\eta^2 + C_7\xi^2\eta + C_8\xi\eta^2 \quad (2.12a)$$

$$v(\xi, \eta) = C_1 + C_2\xi + C_3\eta + C_4\xi\eta + C_5\xi^2 + C_6\eta^2 + C_7\xi^2\eta + C_8\xi\eta^2 \quad (2.12b)$$

Substituting the expressions for nodal displacements from Eq. 2.13a and 2.13b into Eqs. 2.12a and 2.12b, the values of  $C_i$  can be obtained and  $u$  and  $v$  can be expressed as

$$u = \sum_{i=1}^8 N_i(\xi, \eta) u_i = [N_1, N_2, \dots, N_8] \begin{bmatrix} u_1 \\ u_2 \\ \cdot \\ u_8 \end{bmatrix} \quad (2.13a)$$

$$v = \sum_{i=1}^8 N_i(\xi, \eta) v_i = [N_1, N_2, \dots, N_8] \begin{bmatrix} v_1 \\ v_2 \\ \cdot \\ v_8 \end{bmatrix} \quad (2.13b)$$

where  $N_i$  ( $i=1, \dots, 8$ ) are the shape functions given by

$$N_1(\xi, \eta) = \frac{1}{4} (1-\xi) (1-\eta) (-\xi-\eta-1) \quad (2.14a)$$

$$N_2(\xi, \eta) = \frac{1}{4} (1+\xi) (1-\eta) (\xi-\eta-1) \quad (2.14b)$$

$$N_3(\xi, \eta) = \frac{1}{4} (1+\xi) (\xi+\eta-1) \quad (2.14c)$$

$$N_4(\xi, \eta) = \frac{1}{4} (1-\xi) (1+\eta) (-\xi+\eta-1) \quad (2.14d)$$

$$N_5(\xi, \eta) = \frac{1}{2} (1 - \xi^2) (1 - \eta) \quad (2.14e)$$

$$N_6(\xi, \eta) = \frac{1}{2} (1 + \xi) (1 - \eta^2) \quad (2.14f)$$

$$N_7(\xi, \eta) = \frac{1}{2} (1 - \xi^2) (1 + \eta) \quad (2.14g)$$

$$N_8(\xi, \eta) = \frac{1}{2} (1 - \xi) (1 - \eta^2) \quad (2.14h)$$

The nondimensional shape function is unity ( $N_i=1$ ) at node  $i$  and zero elsewhere.

The eight noded quadrilateral elements are defined by the global Cartesian coordinates

$(x,y)$  and the element is formulated in terms of the local curvilinear coordinates  $(\zeta,\eta)$ .

So, for the 8-noded quadrilateral element under consideration the displacement functions

can be written in a compact form as follows:

$$u = \sum_{i=1}^8 N_i u_i \quad (2.15a)$$

$$v = \sum_{i=1}^8 N_i v_i \quad (2.15b)$$

The coordinate transformation from the local coordinate system to the global

system is given by the expressions

$$x = \sum_{i=1}^8 N_i x_i \quad (2.16a)$$

$$y = \sum_{i=1}^8 N_i y_i \quad (2.16b)$$

The strain vector  $\{\epsilon\}$  can be expressed in terms of the nodal displacement vector  $\{q\}$  as

$$\{\epsilon\} = [B]\{q\} \quad (2.17)$$

In a more explicit form, Eq. 2.17 can be expressed as

$$\begin{Bmatrix} \epsilon_x \\ \epsilon_y \\ \gamma_{xy} \end{Bmatrix} = \begin{bmatrix} \frac{\partial N_i}{\partial x} & 0 \\ 0 & \frac{\partial N_i}{\partial y} \\ \frac{\partial N_i}{\partial y} & \frac{\partial N_i}{\partial x} \end{bmatrix} \begin{Bmatrix} u \\ v \end{Bmatrix} \quad (2.18)$$

Since the shape functions,  $N_i$ , are defined in terms of local coordinates,  $(\zeta, \eta)$ , the derivatives in Eq. 2.18 will have to be expressed with respect to local coordinates.

Using the chain rule of partial differentiation,

$$\begin{Bmatrix} \frac{\partial N_i}{\partial \xi} \\ \frac{\partial N_i}{\partial \eta} \end{Bmatrix} = \begin{bmatrix} \frac{\partial x}{\partial \xi} & \frac{\partial y}{\partial \xi} \\ \frac{\partial x}{\partial \eta} & \frac{\partial y}{\partial \eta} \end{bmatrix} \begin{Bmatrix} \frac{\partial N_i}{\partial x} \\ \frac{\partial N_i}{\partial y} \end{Bmatrix} = [J] \begin{Bmatrix} \frac{\partial N_i}{\partial x} \\ \frac{\partial N_i}{\partial y} \end{Bmatrix} \quad (2.19)$$

where,  $[J]$  is the transformation matrix that relates the local coordinates to the global coordinates and is given by,

$$[J] = \begin{bmatrix} \frac{\partial N_1}{\partial \xi} & \frac{\partial N_2}{\partial \xi} & \dots & \frac{\partial N_8}{\partial \xi} \\ \frac{\partial N_1}{\partial \eta} & \frac{\partial N_2}{\partial \eta} & \dots & \frac{\partial N_8}{\partial \eta} \end{bmatrix} \begin{bmatrix} x_1 & y_1 \\ x_2 & y_2 \\ \cdot & \cdot \\ \cdot & \cdot \\ x_8 & y_8 \end{bmatrix} \quad (2.20)$$



$$\begin{Bmatrix} \frac{\partial N_i}{\partial x} \\ \frac{\partial N_i}{\partial y} \end{Bmatrix} = [J]^{-1} \begin{Bmatrix} \frac{\partial N_i}{\partial \xi} \\ \frac{\partial N_i}{\partial \eta} \end{Bmatrix} \quad (2.21)$$

where,

$$\frac{\partial N_1}{\partial \xi} = \frac{1}{4} (1 - \eta) (2\xi + \eta) \quad (2.22a)$$

$$\frac{\partial N_2}{\partial \xi} = \frac{1}{4} (1 - \eta) (2\xi - \eta) \quad (2.22b)$$

$$\frac{\partial N_3}{\partial \xi} = \frac{1}{4} (1 + \eta) (2\xi + \eta) \quad (2.22c)$$

$$\frac{\partial N_4}{\partial \xi} = \frac{1}{4} (1 + \eta) (2\xi - \eta) \quad (2.22d)$$

$$\frac{\partial N_5}{\partial \xi} = -(1 - \eta) \xi \quad (2.22e)$$

$$\frac{\partial N_6}{\partial \xi} = (1 + \eta) (1 - \eta) \quad (2.22f)$$

$$\frac{\partial N_7}{\partial \xi} = -(1 + \eta) \xi \quad (2.22g)$$

$$\frac{\partial N_8}{\partial \xi} = -(1 + \eta) (1 - \eta) \quad (2.22h)$$

$$\frac{\partial N_1}{\partial \eta} = \frac{1}{4} (1 - \xi) (\xi + 2\eta) \quad (2.22i)$$

$$\frac{\partial N_2}{\partial \eta} = \frac{1}{4} (1 + \xi) (-\xi + 2\eta) \quad (2.22j)$$

$$\frac{\partial N_3}{\partial \eta} = \frac{1}{4} (1 + \xi) (\xi + 2\eta) \quad (2.22k)$$

$$\frac{\partial N_4}{\partial \eta} = \frac{1}{4} (1 - \xi) (-\xi + 2\eta) \quad (2.22l)$$

$$\frac{\partial N_5}{\partial \eta} = -(1 - \xi) (1 + \xi) \quad (2.22m)$$

$$\frac{\partial N_6}{\partial \eta} = -(1 + \xi) \eta \quad (2.22n)$$

$$\frac{\partial N_7}{\partial \eta} = -(1 - \xi) (1 + \xi) \quad (2.22o)$$

$$\frac{\partial N_8}{\partial \eta} = -(1 - \xi) \eta \quad (2.22p)$$

## 2.8 Pressure Field

For pressure field four noded quadrilateral elements are used. Fig. 2.5 shows a four noded quadrilateral pressure element as well as the mapped element from the parent element. Pore pressure at a particular node is given by the expression,

$$p(\xi, \eta) = c_1 + c_2\xi + c_3\eta + c_4\xi\eta \quad (2.23)$$

In a matrix form, this can be expressed as

$$p = \sum_{i=1}^4 N_i(\xi, \eta) p_i = [N_1 N_2, \dots, N_4] \begin{bmatrix} p_1 \\ p_2 \\ \cdot \\ \cdot \\ p_4 \end{bmatrix} \quad (2.24)$$

where,

$$\frac{\partial N_1}{\partial \xi} = -\frac{1}{4}(1 - \eta) \quad (2.25a)$$

$$\frac{\partial N_2}{\partial \xi} = -\frac{1}{4}(1 + \eta) \quad (2.25b)$$

$$\frac{\partial N_3}{\partial \xi} = \frac{1}{4}(1 + \eta) \quad (2.25c)$$

$$\frac{\partial N_4}{\partial \xi} = \frac{1}{4}(1 - \eta) \quad (2.25d)$$

$$\frac{\partial N_1}{\partial \eta} = -\frac{1}{4} (1 - \xi) \quad (2.25e)$$

$$\frac{\partial N_2}{\partial \eta} = \frac{1}{4} (1 - \xi) \quad (2.25f)$$

$$\frac{\partial N_3}{\partial \eta} = \frac{1}{4} (1 + \xi) \quad (2.25g)$$

$$\frac{\partial N_4}{\partial \eta} = -\frac{1}{4} (1 + \xi) \quad (2.25h)$$

## 2.9 Infinite Element Formulation

Soil medium is usually considered to be a semi-infinite mass or domain. Finite elements used in discretizing the near field (refer Fig. 2.1B) fail to represent the semi-infinite nature of soil mass. Therefore, the concept of infinite elements is used for analyzing the far field (refer Fig. 2.1C).

### 2.9.1 Governing Equations for Plain Strain Analysis

The governing differential equations (GDE) for a saturated medium in terms of displacements,  $u_i$ , and pore pressure,  $p_f$ , in Cartesian coordinate system are taken from the Biot's consolidation theory and are given by,

$$\nabla^2 u - (2\eta - 1) \frac{\partial e}{\partial x} - \frac{1}{G} \frac{\partial p_f}{\partial x} = 0 \quad (2.26a)$$

$$\nabla^2 v - (2\eta - 1) \frac{\partial e}{\partial y} - \frac{1}{G} \frac{\partial p_f}{\partial y} = 0 \quad (2.26b)$$

$$c \nabla^2 e = \frac{\partial e}{\partial t} \quad (2.26c)$$

where,

$$\eta = (1 - \nu) / (1 - 2\nu), \quad (2.26d)$$

$$c = 2G\eta k \quad (2.26e)$$

and

$$\nabla^2 = \frac{\partial^2}{\partial x^2} + \frac{\partial^2}{\partial y^2} \quad (2.26f)$$

The displacement functions  $E^*$  and  $S^*$ , as proposed by McNamee and Gibson (McNamee et al., 1960), are used to solve the above equations (Eqs. 2.26a to 2.26c).

These functions are related to the displacements as,

$$u = -\frac{\partial E^*}{\partial x} + y \frac{\partial S^*}{\partial x} \quad (2.27a)$$

$$v = -\frac{\partial E^*}{\partial y} + y \frac{\partial S^*}{\partial y} - s \quad (2.27b)$$

$$p_f = 2G \left( \frac{\partial S^*}{\partial y} - \eta \nabla^2 E^* \right) \quad (2.27c)$$

$$e = \nabla^2 E^* \quad (2.27d)$$

Substituting Eqs. 2.27a to 2.27d in the governing differential equations, (Eqs. 2.26a to 2.26c), it becomes evident that

$$c \nabla^4 E^* = \nabla^2 \frac{\partial E^*}{\partial t} \quad (2.28a)$$

and

$$\nabla^2 S^* = 0 \quad (2.28b)$$

The corresponding constitutive equations (linear elastic case) are given by

$$\frac{\sigma_{xx}}{2G} = \left( \frac{\partial^2}{\partial x^2} - \nabla^2 \right) E^* - \gamma \frac{\partial^2 S^*}{\partial x^2} + \frac{\partial S}{\partial y} \quad (2.29a)$$

$$\frac{\sigma_{yy}}{2G} = \left( \frac{\partial^2}{\partial y^2} - \nabla^2 \right) E^* - \gamma \frac{\partial^2 S^*}{\partial y^2} + \frac{\partial S}{\partial y} \quad (2.29b)$$

$$\frac{\sigma_{xy}}{2G} = \frac{\partial^2 E^*}{\partial x \partial y} - \gamma \frac{\partial^2 S^*}{\partial x \partial y} \quad (2.29c)$$

Using a non-dimensional approach, i.e., by choosing the variable 'a' in unit of

length and 'a<sup>2</sup>/c' in unit of time, Eqs. 2.28a and 2.28b become

$$\Delta^4 E^* = \Delta^2 \frac{\partial E^*}{\partial t} \quad (2.30a)$$

$$\Delta^2 S^* = 0 \quad (2.30a)$$

Considering the symmetry of loads about the Y-axis and applying the cosine

Fourier transformation gives,

$$E^*(x, y, t) = \frac{2}{\pi} \int_0^{\infty} \cos(x\xi) E_c(\xi, y, t) d\xi \quad (2.31a)$$

$$S^*(x, y, t) = \frac{2}{\pi} \int_0^{\infty} \cos(x\xi) S_c(s, y, t) d\xi \quad (2.31b)$$

Applying Laplace transformation with respect to variable time, t,

$$E_c(\xi, y, t) = \frac{1}{2\pi i} \int_{\gamma'-i\infty}^{\gamma'+i\infty} e^{pt} \bar{E}_c(\xi, y, p) dp \quad (2.32a)$$

$$S_c(\xi, y, t) = \frac{1}{2\pi i} \int_{\gamma'-i\infty}^{\gamma'+i\infty} e^{pt} \bar{S}_c(\xi, y, p) dp \quad (2.32b)$$

Likewise, Eqs. 2.31a and 2.31b can be transformed into

$$\left( \frac{d^2}{dy^2} - \xi^2 - p \right) \left( \frac{d^2}{dy^2} - \xi^2 \right) \bar{E}_c = 0 \quad (2.33a)$$

$$\left( \frac{d^2}{dy^2} - \xi^2 \right) \bar{S}_c = 0 \quad (2.33b)$$

The general solution for Eqs. 2.33a and 2.33b can be expressed in the form

$$\bar{E}_c = A_n e^{-\gamma\xi} + B_n e^{-\gamma y} + C_n e^{\gamma\xi} + D_n e^{\gamma y} \quad (2.34a)$$

$$\bar{S}_c = E_n e^{-\gamma\xi} + F_n e^{\gamma\xi} \quad (2.34b)$$

where,

$$\gamma^2 = \zeta^2 + p$$

It should be noted that  $A_n$  through  $F_n$  are unknowns which can be obtained by applying the appropriate boundary conditions and  $n=1$ . Using Eqs. 2.34, 2.27, and 2.29, displacements, pore pressures, and stresses can be written in the form

$$u = \frac{2}{\pi} \frac{1}{2\pi i} \int_0^{\infty} \int_{\gamma'-i\infty}^{\gamma'+i\infty} \xi \sin(\xi x) e^{pt} [ (A_n e^{-y\xi} + B_n e^{-y\gamma} + C_n e^{y\xi} + D_n e^{y\gamma}) - y(E_n e^{-y\xi} + F_n e^{y\xi}) ] dp d\xi \quad (2.35a)$$

$$v = \frac{2}{\pi} \frac{1}{2\pi i} \int_0^{\infty} \int_{\gamma'-i\infty}^{\gamma'+i\infty} \cos(\xi x) e^{pt} [ (A_n \xi e^{-y\xi} + B_n \gamma e^{-y\gamma} - C_n \xi e^{y\xi} - D_n \gamma e^{y\gamma}) - E_n (y\xi + 1) e^{-y\xi} + F_n (y\xi - 1) e^{y\xi} ] dp d\xi \quad (2.35b)$$

$$\frac{P_f}{2G} = \frac{2}{\pi} \frac{1}{2\pi i} \int_0^{\infty} \int_{\gamma'-i\infty}^{\gamma'+i\infty} \cos(\xi x) e^{pt} [ (-B_n \eta p e^{-y\gamma} - D_n \eta p e^{\gamma}) - E_n \xi e^{-y\xi} + F_n \xi e^{y\xi} ] dp d\xi \quad (2.35c)$$

$$\frac{\sigma_{xx}}{2G} = \frac{2}{\pi} \frac{1}{2\pi i} \int_0^{\infty} \int_{\gamma'-i\infty}^{\gamma'+i\infty} \cos(\xi x) e^{pt} [ (A_n \xi^2 e^{-y\xi} + B_n \gamma^2 e^{-y\gamma} - C_n \xi^2 e^{y\xi} - D_n \gamma^2 e^{y\gamma}) + E_n \xi (y\xi - 1) e^{-y\xi} + \xi (y\xi + 1) F_n e^{y\xi} ] dp d\xi \quad (2.35d)$$

$$\frac{\sigma_{yy}}{2G} = \frac{2}{\pi} \frac{1}{2\pi i} \int_0^{\infty} \int_{\gamma'-i\infty}^{\gamma'+i\infty} \cos(\xi x) e^{pt} [ \xi^2 (A_n e^{-y\xi} + B_n e^{-y\gamma} + C_n e^{y\xi} + D_n e^{y\gamma}) + E_n \xi (-y\xi - 1) e^{-y\xi} + \xi (-y\xi + 1) F_n e^{y\xi} ] dp d\xi \quad (2.35e)$$

$$\frac{\sigma_{xy}}{2G} = \frac{2}{\pi} \frac{1}{2\pi i} \int_0^{\infty} \int_{\gamma'-i\infty}^{\gamma'+i\infty} e^{pt} \{ -\xi [ -A_n \xi e^{-y\xi} + B_n \gamma + C_n \xi e^{y\xi} + D_n \gamma e^{y\gamma} ] + y \xi^2 (-E_n e^{-y\xi} + F_n e^{y\xi}) \} dp d\xi \quad (2.35f)$$

The inverse Laplace transform of Eqs. 2.35a through 2.35d is now carried out by using the approximate technique proposed by Schapery (Schapery et al., 1962).

Specifically, the Laplace inversion is approximated by,



$$E_c = (\overline{pE_c}(p))_{p=\frac{0.5}{t}} \quad (2.36a)$$

$$S_c = (\overline{pS_c}(p))_{p=\frac{0.5}{t}} \quad (2.36b)$$

These formulae guarantee exact initial time ( $t= 0^+$ ) and final time, ( $t= \infty$ ) values and

have been found to be applicable to many viscoelastic problems.

### 2.9.2 Analytical Solution for Vertical Distributed Load

For the uniformly distributed loading condition shown in Fig. 2.6, the boundary conditions can be expressed as follows:

$$\sigma_{xx} = 0, \text{ along } y = 0 \quad (2.37a)$$

$$P_f = 0, \text{ along } y = 0 \quad (2.37b)$$

$$\sigma_{yy} = 1 \text{ for } |x| < 1, \quad y=0 \quad (2.37c)$$

$$\sigma_{yy} = 0 \text{ for } |x| > 1, \quad y=0 \quad (2.37d)$$

Eqs. 2.37c and 2.37d can be expressed in a general form as,

$$\sigma_{yy} = \frac{1}{\Pi^2 i} \int_0^\infty \int_{\gamma'-i\infty}^{\gamma'+i\infty} \frac{\sin \xi \cos(x\xi) e^{p\xi}}{p\xi} dp d\xi = 1, \text{ for } |x| < 1, \quad (2.37e)$$

$$= 0, \text{ for } |x| > 1$$

Substituting the boundary conditions represented by Eqs. 2.37a through 2.37e

in Eqs. 2.35a through 2.35f, a system of three simultaneous equations with three

unknown are obtained and the solutions are as follows:

$$A_1 = -\frac{\gamma \sin \xi}{p \xi^2} \frac{1}{\xi^2 - \gamma \xi + \eta p} \quad (2.38a)$$

$$B_1 = \frac{\sin \xi}{p \xi} \frac{1}{\xi^2 - \gamma \xi + \eta p} \quad (2.38b)$$

$$E_1 = -\frac{\eta \sin \xi}{\xi^2} \frac{1}{\xi^2 - \gamma \xi + \eta p} \quad (2.38c)$$

Substituting these expressions in Eqs. 2.35a through 2.35f, the following expressions are obtained:

$$u = \frac{1}{\Pi^2 i} \int_0^\infty \int_{\gamma^* - i\infty}^{\gamma^* + i\infty} \sin \xi \sin(x\xi) \frac{e^{pt}}{\xi^2 - \gamma \xi + \eta p} \left( -\frac{\gamma}{p \xi} e^{-y\xi} + \frac{e^{-y\gamma}}{p} + \frac{y\eta}{\xi} e^{-y\xi} \right) dp d\xi \quad (2.39a)$$

$$v = \frac{1}{\Pi^2 i} \int_0^\infty \int_{\gamma^* - i\infty}^{\gamma^* + i\infty} \frac{\sin \xi \cos(x\xi) e^{pt}}{\xi (\xi^2 - \gamma \xi + \eta p)} \left( \frac{-\gamma e^{-y\xi}}{p} + \frac{\gamma e^{-y\gamma}}{p} + \frac{\eta(y\xi + 1)}{\xi e^{-y\xi}} \right) dp d\xi \quad (2.39b)$$

$$\frac{P_f}{2G} = \frac{1}{\Pi^2 i} \int_0^\infty \int_{\gamma^* - i\infty}^{\gamma^* + i\infty} \frac{\sin \xi \cos(x\xi) e^{pt}}{\xi (\xi^2 - \gamma \xi + \eta p)} \eta (-e^{y\gamma} + e^{-y\xi}) dp d\xi \quad (2.39c)$$

Using the Schapery's (Schapery, 1962) approximate inverse Laplace transform technique leads to

$$f(t) = [f(p)p]_{p=0.5/t} \quad (2.39d)$$

$$u = \frac{2}{\Pi} \int_0^\infty \frac{\sin \xi \sin(x\xi)}{\xi^2 - \gamma \xi + \eta p} \left( -\gamma \frac{e^{-y\xi}}{\xi} + e^{-y\gamma} + \frac{y\eta p}{\xi} e^{-y\xi} \right) d\xi \quad (2.39e)$$

$$v = \frac{2}{\Pi} \int_0^\infty \frac{\sin \xi \cos(x\xi)}{\xi (\xi^2 - \gamma \xi + \eta p)} \left( -\gamma e^{-y\xi} + \gamma e^{-y\gamma} + \frac{\eta p (2\xi = 1)}{\xi} e^{-y\gamma} \right) d\xi \quad (2.39f)$$

$$\frac{P_f}{2G} = \frac{2}{\pi} \int_0^{\infty} \frac{\sin \xi \cos(x\xi)}{\xi(\xi^2 - \gamma\xi + \eta p)} (-\eta p e^{-\gamma y} + \eta e^{-\gamma \xi}) d\xi \quad (2.39g)$$

### 2.9.3 Far Field Behavior of Elastic Half Plane

Displacement and pore pressure expressions consist of integral of the form,

$$\int_0^{\infty} f(\xi) \sin(x\xi) d\xi \quad (2.40a)$$

and

$$\int_0^{\infty} f(\xi) \cos(x\xi) d\xi \quad (2.40b)$$

Separating the real and imaginary parts of Eqs. 2.40a and 2.40b for convenience

$$\int_0^{\infty} f(\xi) \sin(x\xi) d\xi = \text{Im} \left( \int_0^{\infty} f(\xi) e^{ix\xi} d\xi \right) \quad (2.41a)$$

$$\int_0^{\infty} f(\xi) \cos(x\xi) d\xi = \text{Re} \left( \int_0^{\infty} f(\xi) e^{ix\xi} d\xi \right) \quad (2.41b)$$

Erdelyi's (Erdelyi, 1955) theorem of asymptotic expansion is used to evaluate the infinite integral in Eqs. 2.41a and 2.41b.

### 2.9.4 Displacements

From Eq. 2.39a, displacement  $u$  in  $x$ -direction can be expressed as,

$$u = \frac{2}{\pi} \int_0^{\infty} f(\xi) \sin(x\xi) d\xi \quad (2.42a)$$

where,

$$f(\xi) = \frac{\sin \xi}{\xi} \frac{(-\gamma e^{-\gamma \xi} + \xi e^{-\gamma \gamma} + \gamma \eta p e^{-\gamma \gamma})}{\xi^2 - \gamma \xi + \eta p}, \quad (2.42b)$$

$$\gamma^2 = \xi^2 + p^2 \text{ and } p = \frac{1}{2t} \quad (2.42c)$$

therefore,

$$f_{(0)} = \left( \frac{-1}{\eta} + \gamma \right) \neq 0 \quad (2.42d)$$

From Eq. 2.41a one can write

$$\begin{aligned} u &= \frac{2}{\pi} \left( \frac{-1}{\eta} + \gamma \right) \frac{1}{x} + \text{Order of } (x^{-2}) \\ &= C_1 x^{-1} + \text{Order of } (x^{-2}) \end{aligned} \quad (2.43)$$

By considering the highest term, i.e., the first term of the expansions (Eq. 2.43), a decaying function of the form  $1/x$  can be assumed to represent the far field displacement variation.

### 2.9.5 Pore Pressures

From Eq. 2.39c, the pore pressure ( $p_f$ ) can be written in the form

$$p_f = C_1 \operatorname{Re} \left( \int_0^\infty f(\xi) e^{ix\xi} d\xi \right) \quad (2.44a)$$

where,

$$f(\xi) = \sin \xi \left( \frac{-\eta p e^{-\gamma \xi} + \eta e^{-\gamma \xi}}{\xi^2 - \gamma \xi + \eta p} \right) \quad (2.44b)$$

Using Erdelyi's (Erdelyi,1955) theorem of asymptotic expansions  $p_f$  can be expressed as

$$p_f = C_1 (f'(0) x^{-2} + f'''(0) x^{-4} + \dots) \quad (2.45)$$

Since  $f'(0)$  is a non-zero quantity,

$$p_f = C_1 x^{-2} + \text{Order of } (x^{-4}) \quad (2.46)$$

By considering the highest term, i.e., the first term of the expansion, a decaying function of the form  $1/x^2$  can be chosen to represent the far field pore pressure variation.

### 2.9.6 Infinite Elements

As in the near field, the first step in the far field is to discretize the semi-infinite soil domain shown in Fig. 2.1A. Three noded horizontal elements having a constant thickness in the Y-direction and extending to infinity in the X-direction are used in the formulation. Rajapakse (Rajapakse et al., 1985) presented an infinite element algorithm called "finite elements by singular contraction" to model the elasto-static far field behavior of an infinite domain. The principal idea behind this approach is the contraction of an infinite element in the (X,Y) plane into a finite element in the (  $\zeta, \eta$  ) plane

by employing a singular function along  $\zeta = 1$  as shown in Fig. 2.7. This approach is adopted in the present study.

### 2.9.7 Saturated Porous Infinite Elements

The expressions for coordinate mapping for an infinite horizontal element are given by,

$$x = \sum_{j=1}^3 \frac{2}{(1-\xi)} L_j(\eta) x_j \quad (2.47a)$$

$$y = \sum_{j=1}^3 L_j(\eta) y_j \quad (2.47b)$$

Using a more explicit form, these equations can be written as

$$x = \sum_{j=1}^3 N_j^x x_j \quad (2.48a)$$

$$y = \sum_{j=1}^3 N_j^y y_j \quad (2.48b)$$

$$N_1^x = \frac{2}{(1-\xi)} \frac{\eta(\eta+1)}{2} \quad (2.48c)$$

$$N_2^x = -\frac{2}{(1-\xi)} (\eta-1)(\eta+1) \quad (2.48d)$$

$$N_3^x = \frac{2}{(1-\xi)} \frac{\eta(\eta-1)}{2} \quad (2.48e)$$

$$N_1^y = \frac{\eta(\eta+1)}{2} \quad (2.48f)$$

$$N_2^y = -(\eta-1)(\eta+1) \quad (2.48g)$$

$$N_3^y = \frac{\eta(\eta-1)}{2} \quad (2.48h)$$

In accordance with to the far field behavior presented in Section 2.9.6, the following shape functions are chosen:

Displacement shape functions:

$$N_j^u(\xi, \eta) = N_j^v(\xi, \eta) = \frac{(1-\xi)}{2} L_j(\eta) \quad (2.49)$$

Pore pressure shape functions:

$$N_j^p(\xi, \eta) = \frac{(1-\xi)^2}{4} L_j(\eta) \quad (2.50)$$

An explicit form of these shape functions is given by

$$u = \sum_{j=1}^3 N_j^u u_j \quad (2.51)$$

$$v = \sum_{j=1}^3 N_j^v v_j \quad (2.52)$$

and

$$p = \sum_{j=1}^3 N_j^p p_j \quad (2.53)$$

where

$$N_1^u = \frac{1-\xi}{2} \frac{\eta(\eta+1)}{2} \quad (2.54a)$$

$$N_2^u = -\frac{1-\xi}{2} (\eta-1)(\eta+1) \quad (2.54b)$$

$$N_3^u = \frac{1-\xi}{2} \frac{\eta(\eta-1)}{2} \quad (2.54c)$$

$$N_1^v = \frac{1-\xi}{2} \frac{\eta(\eta+1)}{2} \quad (2.54d)$$

$$N_2^v = -\left(\frac{1-\xi}{2}\right) (\eta-1)(\eta+1) \quad (2.54e)$$

$$N_3^v = \frac{1-\xi}{2} \frac{\eta(\eta-1)}{2} \quad (2.54f)$$

$$N_1^P = \frac{(1 - \xi)^2}{4} \frac{\eta(\eta + 1)}{2} \quad (2.54g)$$

$$N_3^P = \frac{(1 - \xi)^2}{4} \frac{\eta(\eta - 1)}{2} \quad (2.54h)$$

Using the shape functions given by Eqs. 2.54a through 2.54h, the global stiffness matrix is evaluated by the addition of the elemental stiffness matrices. The difference between the finite elements and the infinite elements is that the latter have only three shape functions for displacements and two shape functions for pore pressures as compared to the finite elements which have eight shape functions for displacements and four shape functions for pore pressures. Also, the-degrees of-freedom (DOF) for infinite elements is only 8 (6 displacements and 2 pore pressures) as compared to 20 (16 displacements and 4 pore pressures) in finite elements; consequently the infinite element has a smaller element stiffness matrix. The time integration scheme is the same for both types of elements (finite as well as infinite elements).



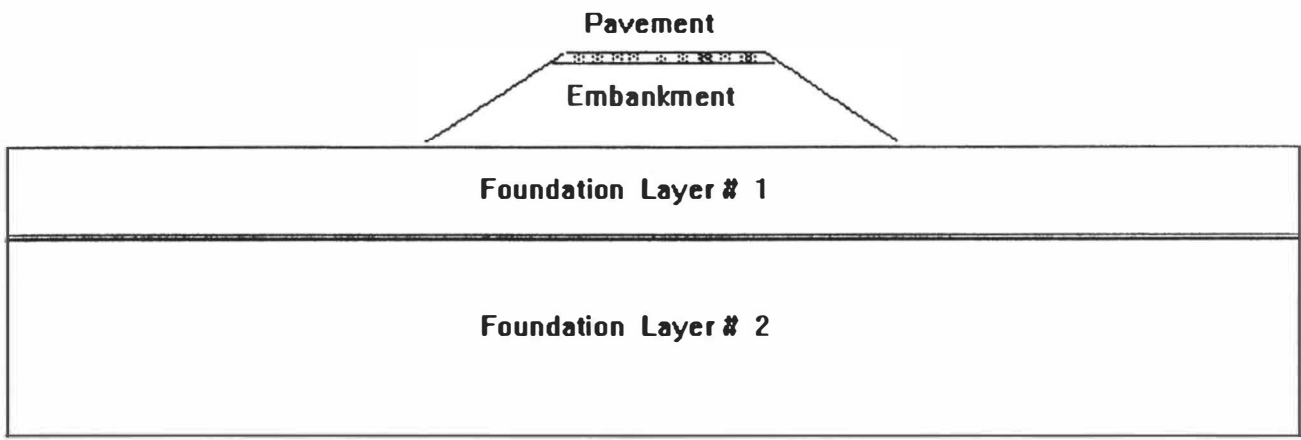


Fig. 2.1A Approach Embankment and Foundation

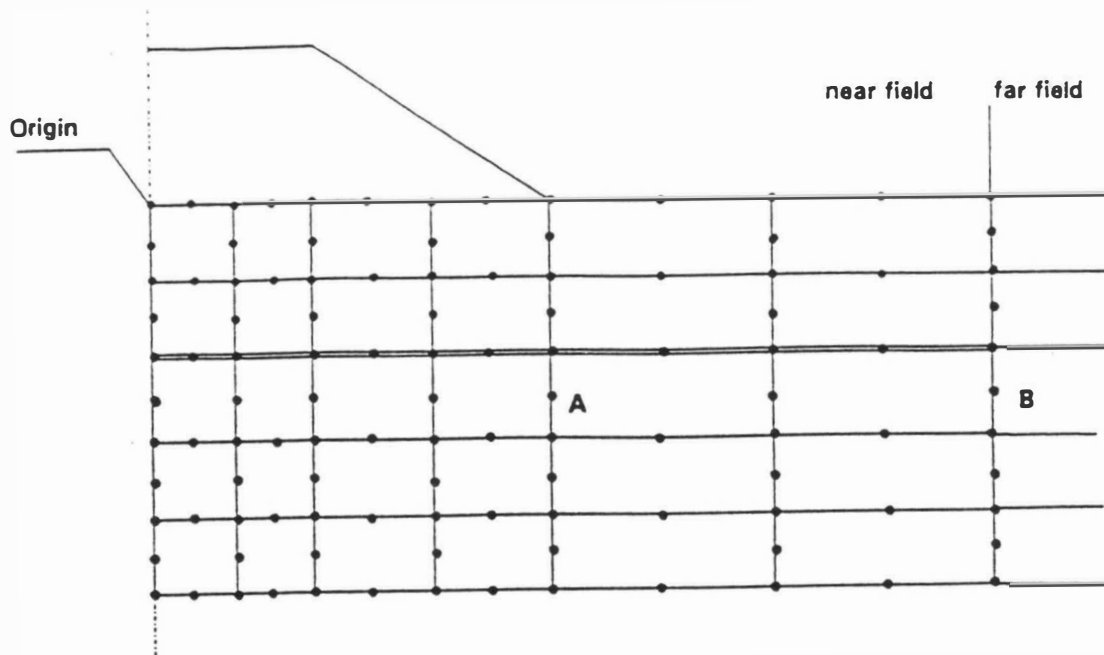


Fig. 2.1B FE Idealization

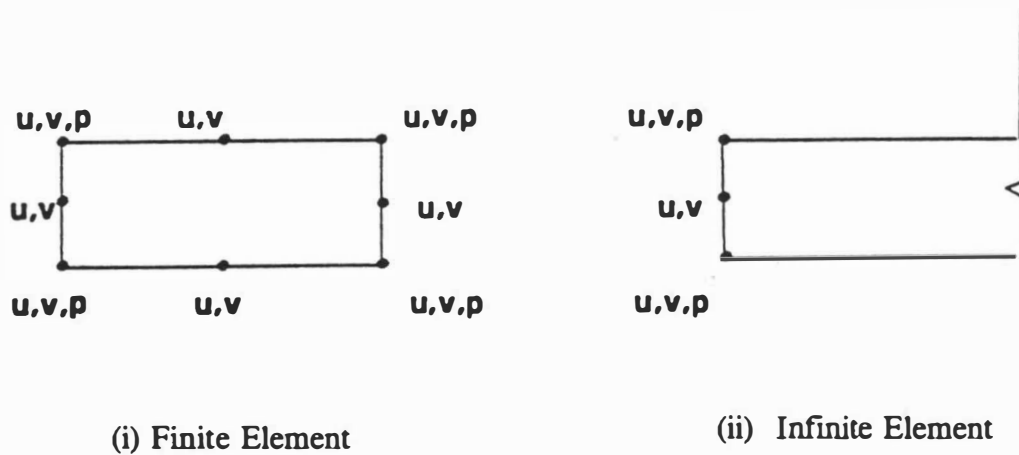
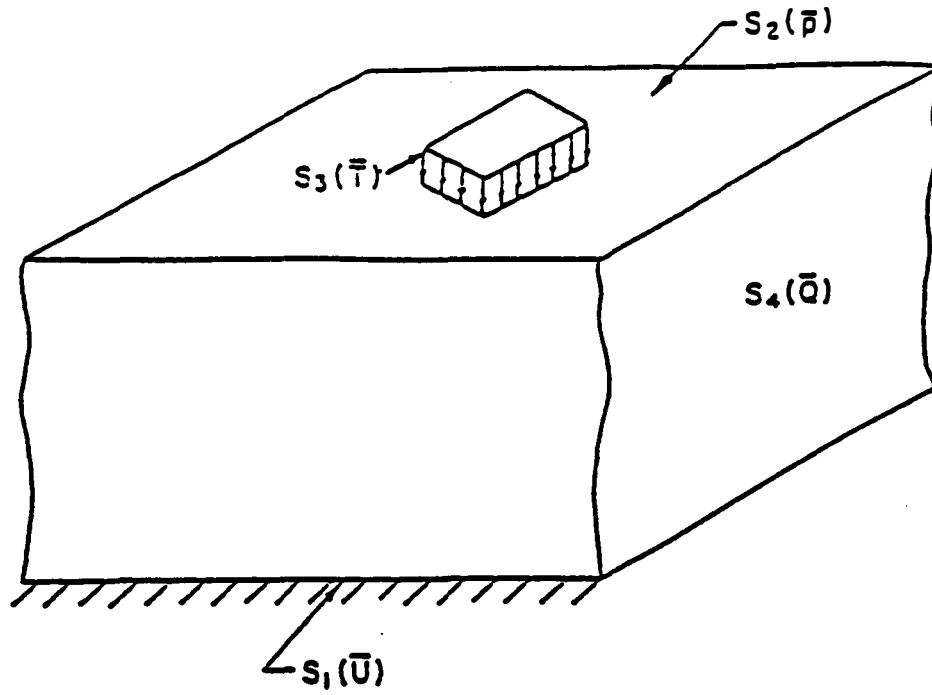
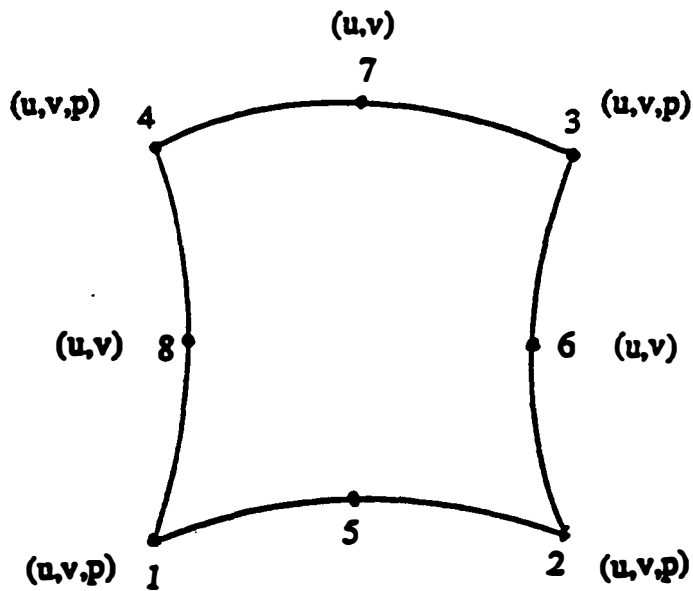


Fig. 2.1C Elements Used



**Fig. 2.2 Schematic Representation of Consolidation Mass**



**Fig. 2.3 Eight-Noded Isoparametric Quadrilateral Element**

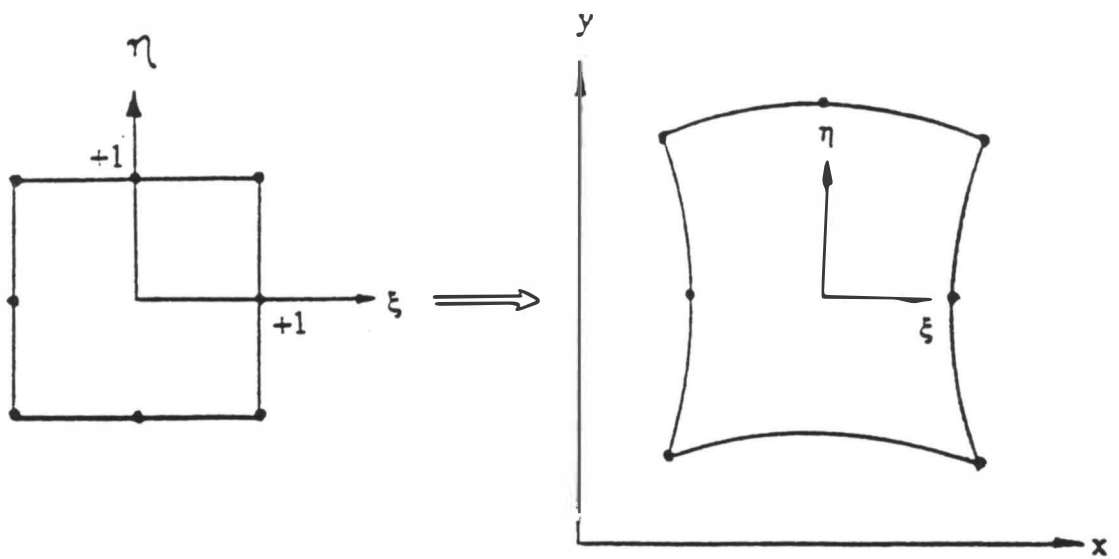


Fig. 2.4 Two-Dimensional Curved Isoparametric Element

Mapped From the Rectangular Parent Element

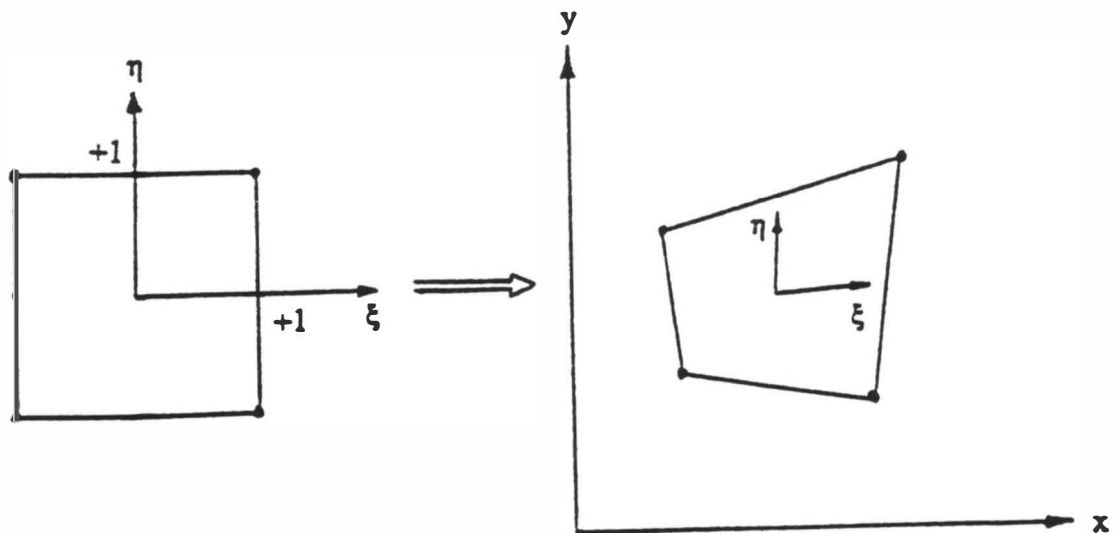


Fig. 2.5 Two-Dimensional Four-Noded Isoparametric Element

Mapped From the Rectangular Parent Element

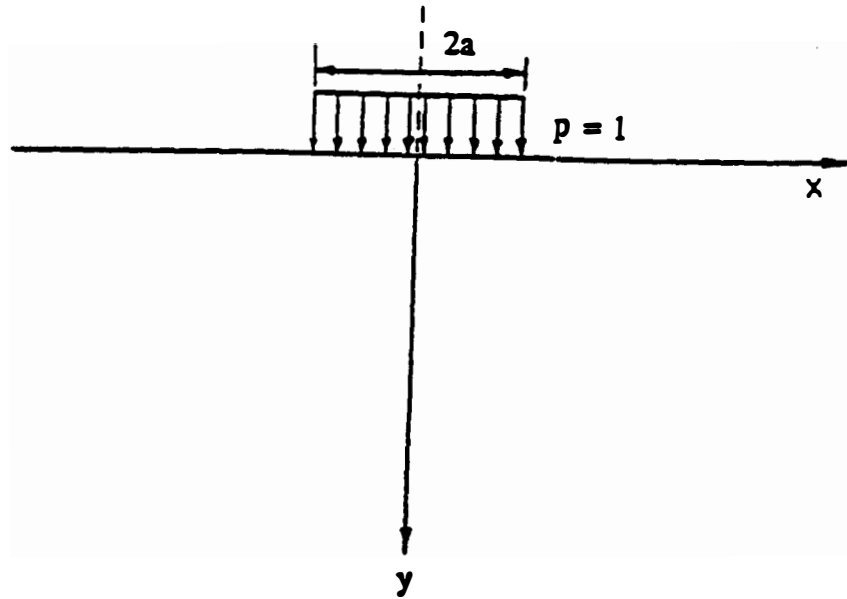


Fig. 2.6 Elastic Half Plane Subjected to a Uniformly Distributed Vertical Load

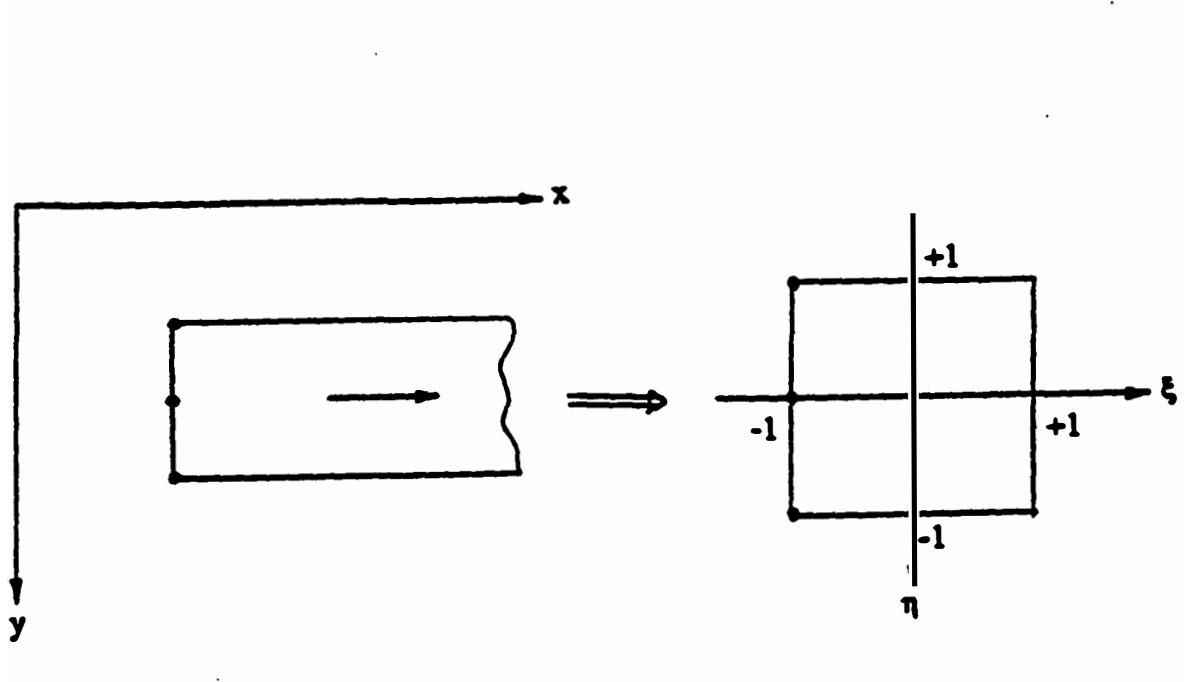


Fig. 2.7 Singular Contraction of Infinite Element

## CHAPTER 3

### OVERVIEW OF THE COMPUTER PROGRAMS

#### 3.1 General

The computer programs that constitute the whole software package for bridge approach settlement analysis are designed to run in an IBM personal computer or a compatible system. The systems requirements for the software package are listed below:

1. Computer: IBM personal computers or compatibles, with a 486 processor or higher.
2. Memory: The computer should have at least 4 mega bytes (MB) RAM, although 8 MB RAM is preferable.
3. Monitor: VGA, SVGA, or EGA-VGA color monitor.
4. Mouse: A mouse which is compatible with the computer system.
5. Hard disk capacity: The hard disk should have about 15 mega bytes (MB) of free space depending on the mesh size. This is in addition to the approximately 20 MB hard disk space occupied by the software itself. A hard disk with 175 MB or larger capacity is preferable.
6. Operating System: MS DOS version 5.0 or higher.
7. Operating environment: Microsoft Windows version 3.0 or higher.
8. Supporting software: (a) Actor version 4.0.

(b) Graphic C for Windows (GPCWin).

To install and use the bridge approach settlement analysis software package, any additional requirements of the operating system and the software mentioned above should also be met . The "Autoexec.Bat" file in the computer should declare the path for the GPCWin software. The user must review the "Disclaimer" and the "Copyright" file (see icon Fig. 3.4) before running the software package, **FEABAS**.

The entire software package consists of the following four basic programs:

- 1) *Preprocessor*;
- 2) *Data Converter*
- 3) *FE Main Program*;
- 4) *Postprocessor*

The *preprocessor* is an interactive module that facilitates preparation of input data, including editing of an existing data set. The *Data Converter* converts the user specified input data to a form suitable for the finite element program, *FE Main Program*. The *FE Main Program* evaluates the potential bridge approach settlement ( consolidation settlement and its rate ) at a site. The *postprocessor* processes and plots the results obtained from the *FE Main Program*.

Fig. 3.1 represents the different components of the software package developed in this study. After obtaining the geometric and the material properties of different soil layers encountered in embankment and foundation soil, the first step is to run the *preprocessor*. There are two types of output data files from the *preprocessor* - (i) The output data file named with an extension .inp ( such as site.inp) contains the original

data input by the user. This type of data file (\*.inp) can be easily reloaded and edited by reloading and editing this output data file (\*.inp). This can be easily accomplished by choosing appropriate options from the *preprocessor* menu. Due to this feature of the *preprocessor*, a parametric study can be conducted easily. Section 3.2.3 presents a typical example for performing a parametric study. (ii) The output data file named with an extension .dat (such as site.dat) is ready to be converted by the *Data Converter* and then used by the *FE Main Program*. If the user wants to edit this type of data file (\*.dat), refer to Appendix IV to know which data can be changed at this stage. The geometry of the soil domain cannot be altered arbitrarily in \*.dat data file. Because the initial dimensions (e.g., embankment height or foundation thickness) specified by the user are used by the *preprocessor* to set up the number of nodes, the nodal coordinates and the element connectivity. The problem geometry can be changed by reloading \*.inp data file at the *preprocessor* and inputting the new geometry. It is highly advisable to reload and edit \*.inp data file when the user wants to make some changes.

In order to avoid running the *preprocessor* separately for the analyses of embankment and foundation, the input data for embankment and foundation are given simultaneously. The data file (\*.dat) generated by the *preprocessor* cannot be directly used for the analysis of approach settlements for the following reasons:

- (i) The *preprocessor* output contains the information regarding both foundation and embankment, but the *FE Main Program* is capable of analyzing either foundation or embankment at a time.



- (ii) The *FE Main Program* requires that part of the data be input in a specified format. The output from the *preprocessor* is not in a compatible format for the *FE Main Program*.

After running the *preprocessor*, the next step for the analysis of a given site is to run the *Data Converter* program named, CONVERT.FOR, which was developed in FORTRAN77 language. The program takes the data from the *preprocessor* and separates it into two compatible data files, one for analyzing the foundation and the other for analyzing the embankment. Details of the *Data Converter program* are given in Section 3.3.

The third step involves running the *FE Main Program*. The salient features of the program are described in Section 3.4. The FE main program works in the Windows environment only. The name of the program is FEMWIN2.FOR. The program is capable of analyzing sites with a maximum of 1157 nodes and 18 different material types. The number of elements in the FE mesh should not be more than 378. The program needs to be run separately for the analysis of foundation and embankment. Output from the FE analysis of foundation contains the following information:

1. The overall results of the FEM analysis (saved as the "general output" file).
2. The summary of the FEM analysis (saved as the "condensed output" file).
3. Data for plotting settlement profile along the surface of approach foundation (i.e., surface settlement versus distance from centerline).

4. Data for plotting excess pore pressure distribution along the centerline of the cross section.
5. Data for plotting the maximum normal principal stress contours.

The output from the FE analysis of embankment contains following information:

1. The overall results of the FEM analysis (saved as the "general output" file).
2. The summary of the FEM analysis (saved as the "condensed output" file).
3. Data for plotting settlement profile along the surface of embankment (i.e., surface settlement versus distance from centerline).
4. Data for plotting settlement along the central plane of the cross section.
5. Data for plotting the maximum normal principal stress contours.

The fourth and the final step is to plot the results from the *FE Main Program* for the convenience of interpretation and discussion. Six different programs have been developed for plotting of settlements, pore-pressures, and stress contours.

## **3.2 Preprocessor**

The *preprocessor* is a window-based graphics-user-interface. It is a mouse as well as keyboard driven software. Its purpose is to provide a user friendly environment to enhance the data-input facility. The main components of this *preprocessor* are illustrated in Fig. 3.2.

### ***3.2.1 Components of the Preprocessor's Window***

The physical screen of the video monitor is partitioned into several windows.

Each window can consist of the following components.

1. Caption bar
2. Control-menu box
3. Minimize button
4. Maximize button
5. Menu bar
6. OK button
7. CANCEL button
8. Static fields
9. Edit fields

A window may consist of all the above components or their subset. Components 1 through 5 are shown in Fig. 3.3.

The **Caption bar** holds the title of the window.

The **Control-menu box** is located in the upper-left corner of the window. With Control-menu commands, one can resize, move, maximize, minimize, close, and switch to other windows.

The **Maximize** and **Minimize buttons** (chosen with the mouse) enlarge the active application window to fill the entire desktop (the video screen) or shrink the window to an icon. After a window is enlarged, the Maximize button changes to a Restore button. The Restore button can be used to return the window to its previous size.

The **Menu bar** lists the available menu.

The **OK button** is used for data validation. By pressing the OK button in a window (with the help of the mouse), the user validates all the data appearing in that window. They act as check points.

The **CANCEL button** provides an option to discard the data appearing in the current window. The CANCEL button is also pressed with the help of the mouse.

Contents of the **Static fields** cannot be changed. They are used to identify the various data fields.

The **Edit fields** are used to enter the data. When the cursor is in an Edit field, the user can change the contents of the Edit field. By using the *backspace* or the *delete* key, the user can delete the characters in the Edit field. If the user presses any other key, then that character is inserted into the Edit field. This process is called **editing**. Prior to editing, the cursor must reside in that Edit field. If the cursor is not in the desired edit field, it can be brought into the intended Edit field either by using the mouse, or with the help of the **arrow keys**. The user can move to the next Edit field by using the *Tab* key. Length of the data that can be typed in a field is limited by the length of the Edit field.

### ***3.2.2 Running the Preprocessor - Create New Input Data File***

Analysis of the East Cordell bridge site (Bridge# 75-10 x 0849) is used as an example for the *preprocessor*. The geometry of the embankment and the foundation along with the soil properties are all shown in Fig. 3.14.

The *preprocessor* appears as an icon in the *Bridge Approach Settlement* window

(Fig. 3.4). In order to start the execution of the *preprocessor*, the user needs to *double click* the **PREPROCESSOR** icon. The *preprocessor* activates the Actor Programming. At the Actor Window (Fig. 3.5) click the OK button. At Actor Workspace Window (Fig. 3.6), use mouse to highlight the last two lines and press the RETURN key. Then the *preprocessor* initiates its dialogue with the user.

### 1. Input Data File Type Window (Fig. 3.7)

The first window that appears on the screen asks the user to provide the type of the input data file. Specify '0' for creating a new data file and '1' for reloading an existing data file. For new data file option, the user needs to enter all information (such as geometry, material properties, and loading etc.) for this *preprocessor*. And for existing data file option, the user needs to specify the name of the existing data file (\*.inp). All the information for this *preprocessor* will be reloaded. The user can change the information based on the needs and then process and save it at new data files (\*.inp and \*.dat). This is a very useful option for parametric studies. The default data file name for reloading is **c:\demo\site.inp**. If this default file name is correct, then the user needs simply to click the OK button in the window. If the file name is to be changed, the user needs to edit the file name and then press the OK button. While giving the file name, the user needs to give the full pathname of the file. For example, if the input file named cap.inp is in the *sites* directory in D: drive, the user needs to specify the file as **d:\sites\cap.inp**. For this example, enter '0' to create a new data file.

## 2. Unit System Window (Fig. 3.8)

This window is a dialogue box which lists two unit systems. One of the units is the *Standard American System*, i.e., the Foot-Pound-Second system. The other unit is the *Scientific Units System*, i.e., Meter-Newton-Second system. Specify '0' for FPS unit and '1' for SI unit. The unit selected by the user from this window will be used in the *FE Main Program* in all the computations. For this example, enter '0' for FPS unit. Then press the OK button to go to the next window.

## 3. Coordinate Space Window (Fig. 3.9)

The *coordinate space* for graphics is defined in this window. The position of a point on the computer screen is defined in terms of *pixels*. In order to sketch a figure on the screen, the user specified coordinates (global coordinates) are converted to pixel units. In this window, the user should specify the maximum dimensions to be used along the X and Y axes. The sum of the embankment height and the thicknesses of all the foundation layers considered in the analysis must not exceed the specified maximum Y-coordinate value. The *half mesh width* must also be within the specified X-coordinate range. A value of  $3 * BW$  (bottom width of the embankment) (see Fig. 3.21) or more should be appropriate for maximum X-coordinate. Specify 0 (zero) for both minimum X-coordinate and Y-coordinate. This information helps the program to map the global coordinates (specified by the user) to the screen coordinates (pixels) in the parlance of graphics.

In this window (Fig. 3.9), there are four fields: minimum X-value, maximum

X-value, minimum Y-value, and maximum Y-value. When this window appears, the cursor is positioned on the first field, which is designated for the minimum value of the X-coordinate. After assigning each value, the user will move on to the next field by pressing the *Tab* key. The user must press the *Tab* key after entering each value. If the default values are provided and agreeable, then the user can simply *Tab* over those fields. Otherwise, the user can change those fields to the desired values.

After having entered values in all the four fields, the user needs to press the OK button in order to move on to the next window. If the user detects a mistake after the OK button has been pressed, then the value for the field that needs correction can be corrected after completion of a segment of the *preprocessor* program. This corrective measure can be taken only if the mistake is a minor one in the sense that it does not have many consequences or any fall out effect. If the mistake has fall out effects, then the user needs to start the execution of the *preprocessor* program all over again.

#### **4. Message box (Fig. 3.10)**

This is an overlapping window that is used to display *warning* messages when the value specified for a field does not lie within the expected range. The expected ranges and descriptions of the fields for which range checking is performed are provided in the Table 3.2. Whenever a value goes beyond the pre-defined limits, this window appears. The Caption bar of the window gives the field name whose value is beyond the limits. This window consists of a static field which displays the expected range of value for the field, and an OK button. The window will remain on the screen

until the user has pressed the OK button. When the user presses the OK button, the *Message box* disappears. If the value is erroneous, the user needs to select the corresponding options in the menu bar of the Bridge Approach Settlement Analysis Main Window (Fig. 3.11) and/or move the cursor to the corresponding field with the mouse to make the necessary changes. If the given value is the desired value, then the user may proceed after pressing the OK button.

## **5. Bridge Approach Settlement Analysis Main Window**

This window is the starting point for accepting data for the bridge approach settlement analysis. The main window which is captioned as “Bridge Approach Settlement Analysis Main Window.” It contains a *Menu bar* which is situated just below the Caption bar. **Site Data**, **FE Mesh**, **Loading**, **Process-Save**, and **Exit** options appear in this Menu bar (Fig. 3.11). The user needs to select one of the options in the Menu bar at a time and input corresponding information. A description of each option is given below:

### **1) Site Data Option**

This option consists of six items (Fig. 3.12).

#### **1. Control Parameters:**

When this item is selected, the Control Parameters Window will appear (Fig. 3.13). Elements of this window are listed below:

- a) Heading: Name or identification of the bridge approach site being analyzed
- b) Embankment Information:



- \* Height of the embankment
- \* Top half width of the embankment
- \* Bottom half width of the embankment
- \* Pore fluid density
- \* Number of embankment layers

Notes: Units for each field are displayed within parenthesis.

c) Number of foundation layers

- \* OK button
- \* DRAW button

When this window appears on the screen, the cursor is positioned on the first field of the Control parameters, which is the *Heading*. After entering the data in each field, the user needs to press the *Tab* key. Then the cursor automatically moves on to the next field. If any erroneous data has been entered by mistake in the process, the user can rectify that by moving the cursor to the corresponding Edit field and changing the data in that field. The warning message will appear when the "Number of embankment layers" or the " Number of foundation layers" being input by the user exceeds its limits (10) . Click the OK button at warning window and move the cursor to its corresponding field. Re-input the number and press the *Tab* key. After all the pertinent data have been entered correctly, the user can press the DRAW button to display the embankment geometry. Press the OK button to close this window. Note that the numerical values shown in various field of this window pertain to East Cordell

bridge site (Bridge # 75-10 x 0849).

## **2. Embankment Layer information:**

This window is used to specify information regarding the various embankment layers (Fig. 3.15A). The maximum number of layers is 10 for the current version of the *preprocessor*. This window consists of the following elements:

- a) Thickness of the layer
- b) Soil type of the layer

If soil type is *sand*, the user needs to input `0'. If the soil type is *clay*, the user should input `1'. For embankment layer #1, if it is pavement, the user needs to input `2' to indicate that it is a pavement layer. This is a rather broad classification of the soil. In reality, it could be a mixture of both sand, silt and clay or any other types of soil. The soil type can be determined from laboratory tests such as sieve analysis and hydrometer and Atterberg limits tests on the soils in question. Results from these tests can be used to classify the soil. Commonly used classification methods are the Textural Classification System, USDA Classification System, AASHTO Classification System, and the Unified Soil Classification system. As an example, when using the AASHTO Classification System, the soil can be classified as granular (*Sand*) if it has particles 35% or less passing through the No. 200 sieve; else it can be classified as *silt* or *clay* type material. Field test (SPT, CPT, etc.) data can also be used, in conjunction with laboratory tests, to determine the soil type. This window also has the following elements:

- c) Density of the soil in this layer
- d) OK button, and
- e) DRAW button.

The user should enter the data needed for the embankment layers. Press the *Tab* key after entering each data. If any data is wrong, the user can move the cursor to the corresponding field with the help of mouse or arrow key, and make the desired modifications. After all the data have been entered correctly, the user can press the DRAW button to draw a sketch of the embankment with dimensions (Fig. 3.15A). Press the OK button to close this window. If the total thickness of embankment layers does not match with the embankment height which was input at the Control Parameters Window, a warning message will appear. The user needs to click the OK button to close the warning window. Then re-select the " 2. **Embankment Layer Information:**" option to make the necessary changes in the thickness values or the " 1. **Control Parameters:** " option to change the embankment height. Fig. 3.15A depicts the process of entering data for the embankment layers for the selected example problem.

### 3. Foundation Layer information:

This window is used to specify information regarding the various foundation layers. (Fig. 3.15B). The maximum number of layers is 10 for this *preprocessor*. This window consists of the same elements as the Embankment Layer Information window.

- a) Thickness of the layer
- b) Soil type of the layer

- c) Density of the soil in this layer
- d) OK button
- e) DRAW button

The user needs to enter the data for all the foundation layers. Press the *Tab* key after entering each data. If any data is entered wrong, the user can move the cursor to the corresponding field with the help of the mouse or the arrow keys, and make the desired modifications. After all the data have been entered correctly, the user can press the DRAW button to draw a sketch of the foundation layers including dimensions. Press the OK button to close this window. Fig. 3.15B depicts the process of entering data for the foundation layers for the selected example problem.

#### **4. Embankment Material Properties:**

When the user selects this item, the embankment layer number window will be activated (Fig. 3.16). The user should specify the embankment layer number for which the material properties are to be input and click the OK button. Then the Isotropic property window (Fig. 3.17) will appear. In this window, the user needs to specify the isotropic property for this embankment layer followed by the selection of the OK button. Depending on the soil type, one of the following two cases will take place.

- a) Isotropic Material (Fig. 3.18A)

In this case the second sub-window appears as a blank window and the first sub-window captioned “Emb.layer#1:Isotropic ” appears with the following fields:

- \* Elastic modulus

- \* Angle of internal friction
- \* Cohesion
- \* Poisson's ratio
- \* Permeability coefficient

When these windows appear, the cursor is positioned on the "Elastic modulus" field. The *Tab* key will move the cursor to the next field in sequence. The user must press the *Tab* key after entering the data in each field. When the input data exceeds its normal range a warning message will appear. When this happens, the user needs to press the OK button to close the warning message window. If the input value is not desired, then the user needs to enter a new value. Otherwise, the user can continue to perform. After completing input data for a particular layer press the OK button to close the material window. The user needs to select the "4. **Embankment Material Properties**" item, assign another embankment layer number, and input desired material properties for this layer. These steps need to be repeated till the material properties for all the embankment layers have been entered. If any mistake is detected after the OK button has been pressed, it can be corrected by providing this soil layer number and editing the data at corresponding Edit fields.

b) Anisotropic Material (Fig. 3.18B)

In this case, everything is same as that of the "isotropic layer" except the "Emb.layer#1: Isotropic" sub-window is replaced by the "Emb.Layer#1: Anisotropic" sub-window. Fig. 3.18B shows the structure of the window. This window consists of

the following fields:

- \* Elastic modulus-X
- \* Poisson's ratio-X
- \* Permeability coefficient-X
- \* Angle of internal friction
- \* Cohesion
- \* Elastic modulus-Y
- \* Poisson's ratio-Y
- \* Permeability coefficient-Y

When these windows appear, the cursor is positioned on the "Elastic modulus-X" field. The *Tab* key will move the cursor to the next field in the sequence. The user must press the *Tab* key after entering the data in each field. When data for all the fields have been entered, the user needs to press the OK button in this window. That completes the material properties data for this layer. The program will proceed to accept data for the other layers when the user selects the "**4. Embankment Material Properties**" item again. The same steps needed to be followed as in case (a) Isotropic Material.

#### **5. Foundation Material Properties:**

When the user selects this item, the foundation layer number window will be activated. The user needs to input the foundation layer number for which the material properties are to be given and click the OK button. Then the Isotropic window appears.

In this window, the user should specify the isotropic property for that layer followed by the selection of the OK button. Depending on the soil type and the isotropic property, one of the following four cases will take place.

a) Isotropic Sand (Fig 3.18C)

In this case the second sub-window appears as a blank window and the first sub-window captioned "FND.layer#1:Isotropic " appears with the following fields:

- \* Elastic modulus
- \* Angle of internal friction
- \* Cohesion
- \* Poisson's ratio
- \* Permeability coefficient

For this example site, all the soil of foundation layers are isotropic clay. Fig. 3.18C only shows the structure of these windows. When these windows appear, the cursor is positioned on the "Elastic modulus" field. The *Tab* key will move the cursor to the next field in the sequence. The user must press the *Tab* key after entering the data in each field. When the user is done with entering data in all the fields, the OK button needs to be pressed to close this window. After completing input data for a particular layer, the user needs to select the " **5. Foundation Material Properties**" item, give another foundation layer number, and input the desired material properties for this layer. Those steps needs to be repeated till all the foundation layers have their material properties. If any mistake is detected after the OK button has been pressed, it

can be corrected by providing this soil layer number and editing the data at corresponding Edit fields.

b) Isotropic Clay (Fig. 3.18D)

In this case, the first sub-window is the same as above. The second sub-window captioned "Clay material properties" would contain the following additional fields:

- \* Crit. st. li. slope (Slope of the critical state line)
- \* Consolid. curve slope (Slope of the consolidation curve)
- \* Swelling curve slope (Slope of the swelling curve)
- \* Void ratio

As in the previous case, when these windows appear, the cursor is positioned on the "Elastic modulus" field. The *Tab* key will move the cursor to the next field in the sequence. When the user presses the *Tab* key after entering data in the "Permeability coefficient" field, the cursor will move to the "Clay material properties" sub-window and position itself in the Edit field for the "Crit. st. ln. slope." When the desired data have been entered in all the fields, the user needs to press the OK buttons in the "Clay material properties" sub-window and the "Properties for isotropic layers" window in that order. That will complete the data entry for this layer. The program will proceed to accept data for the other layers when the user selects the "5. Foundation Material Properties" item repeatedly.

c) Anisotropic Sand (Fig. 3.18E)

In this case, everything is same as that of the "Isotropic Sand" layer except the



“FND.layer#1: Isotropic” sub-window will be replaced by the "FND.Layer#1: Anisotropic” sub-window. This window consists of the following fields:

- \* Elastic modulus-X
- \* Poisson’s ratio-X
- \* Permeability coefficient-X
- \* Angle of internal friction
- \* Cohesion
- \* Elastic modulus-Y
- \* Poisson’s ratio-Y
- \* Permeability coefficient-Y

When these windows appear, the cursor is positioned on the “Elastic modulus-X” field. The same steps need to be followed as in case (a) Isotropic Sand.

d) Anisotropic Clay (Fig 3.18F)

This case is exactly the same as the “Isotropic Clay” layer except the “Properties for anisotropic layers” window will replace the “Properties for isotropic layers” window. As in the previous case, when these windows appear, the cursor is positioned on the “Elastic modulus-X” field. The *Tab* key will move the cursor to the next field in the sequence. When the user presses the *Tab* key after entering the data in the “Permeability coefficient-Y” field, the cursor will move to the “Clay material properties” sub-window and position itself in the Edit field for the “Crit. st. li. slope”. When data for all the fields have been entered, the user needs to press the OK buttons

in the “Clay material properties” sub-window and the “Properties for anisotropic layers” window in that order. That completes the data entry for this layer. The program will proceed to accept data for the other layers when the user selects the "5. **Foundation Material Properties**" item again. For this example, the foundation soil (for all layers) is isotropic clay, so Fig. 3.18F shows only the structure of these windows.

### **6. Water Table Depth**

The water table depth must be the same as that of the top surface of any of the foundation layers. If the water table depth does not coincide with one of the foundation layers, the user needs to make an additional layer at water table level. The detail steps are presented in Section 3.2.3, 3. Parametric Study - Water table depth. When the user selects the " 6. **Water Table Depth**" option, the Water Table Depth window (Fig. 3.19) appears and the acceptable values for this parameter are shown in the window. The user needs to select one of these values, press the *Tab* key, and click the OK button to close this window. If the input water table depth is not acceptable, a warning message will appear. If this happens, the user needs to click the OK button and select " 6. **Water Table Depth**" option again to input an acceptable value.

### **2) FE Mesh Option**

There are five items in this option (Fig. 3.20). These items are described below:

#### **1. Default Mesh**

For this selection the user does not need to furnish any more data. The user

needs to wait until the mesh is generated and all the internal calculations are done. The internal computation include generation of the nodal points, elements, and boundary conditions of the mesh. All these information are written into the output file (\*.dat).

Dimensions of the default mesh are given below:

#### X-direction

- \* Half mesh width is taken as the maximum X-value minus 10. The maximum X-value was input at Coordinate space window (Fig. 3.9).
- \* 3 divisions in the first part ("Part1" which is just below the top of the embankment, as shown in Fig. 3.21)
- \* 3 divisions in the second part ("Part2" which is below the slope portion of the embankment, as shown in Fig. 3.21)
- \* 3 divisions in the third part ("Part3" which is outside the embankment, as shown in Fig. 3.21)

#### Y-direction

- \* 3 divisions per layer

An example of the default mesh is shown in Fig. 3.22A.

## **2. Custom Mesh**

In this case, the user will have to supply values for all the above items in that order. For each item a small overlapping window will appear on the screen describing the item for which a value is being accepted. After giving each value, the user needs to press the *Tab* key and the OK button. The number of divisions should not be too

large or too small. For each layer, there should normally be 3 to 6 divisions. An example of the custom mesh is shown in Fig. 3.22B.

### **3. Draw Mesh**

Only after "1. **Default Mesh**" item or " 2. **Custom Mesh**" item has been selected, the user can select the "3. **Draw Mesh**" item. Then the foundation and embankment meshes defined by the user will be generated and displayed on the Visual sub-window (Fig. 3.22A).

### **4. Close Mesh Window**

The user needs to select this item to close the Mesh window which was created by " 3. **Draw Mesh**" option. Note that the mesh window must be closed before the user can execute the Loading option.

### **5. Zoom Mesh Window**

By selecting this option, the FE mesh can be enlarged and displayed on the full computer screen (Fig. 3.22B). This option only can be selected after " 3. **Draw Mesh**" has been selected. To close this window, the user needs to select "Close" option at its control menu box (Fig. 3.3).

### **3) Loading Option**

The user is expected to choose this option only after the mesh has been generated and the mesh window has been closed. In reality embankment construction is a time-related process. As the embankment construction proceeds, the stresses in the foundation soil increase resulting in elastoplastic and consolidation settlements of the

foundation soil. In this finite element analysis software, this process is simulated by providing the embankment loading data in a stepwise manner. For each step, the user needs to provide the time increment and the incremental height of the embankment that has been constructed during this time increment. The embankment construction history for the example site is depicted in Fig. 3.24A. While accepting the loading data, the *preprocessor* will plot the height completed in various intervals of time. For this reason, the user needs to define the coordinate space again. In this case, the user will have to specify the range (minimum and maximum values) for height and time (Fig. 3.23). The maximum values need to be at least 50 (because of the program design) in each direction (X and Y). After that three sub-windows will appear in the “Loading data” window. A brief description of each window is given below.

**a) Sequence information (Fig. 3.24B)**

This window includes two fields. The first field reads the number of time step sequences and the second one reads the time period to be used for the termination of the analysis (this is an estimate of the time required for completion of the primary consolidation settlement). The second field serves as a check for the *FE Main Program* from going into an infinite loop. If the time period for the *FE Main Program* exceeds this limit, the program will be terminated. For each time step sequence, the Time step information window is going to be used once.

**b) Time step information**

The caption of this window (Fig. 3.24B) indicates the time step number for

which the data are being read currently. It consists of the following fields:

\* Time interval:

It is the time interval between each analysis step.

\* Number of time steps:

It is the number of steps in the given time interval.

\* Number of steps between output:

The step interval at which the output needs to be generated.

\* Height completed in this time step:

This is the height of the embankment constructed at the end of the given time interval. This information is used for calculating the load on the approach foundation contributed by the embankment.

After entering the data in all the above fields, the user needs to press the OK button. Then, the user goes to the next time step. If it is the last time step, then the cursor will move to the second field "2. Time for term. of analysis " in the first window. Note that the sum of the height completed in each time step should be consistent with the embankment height which was given at the Control Parameters window (Fig. 3.13). No warning message is provided in this version of program when the inconsistency occurs. Fig. 3.24A and Fig. 3.24B depict the entire process of entering the loading data.

**c) Embankment Loading (Fig. 3.25)**

This is a graphics sub-window. It generates a plot of Height completed versus

Time required for construction of the embankment. When the user presses the OK button in the “Time step info” window, it generates a plot in this window.

When the user presses the OK button in the “Sequence Information” window, the “Time step info” window disappears and the “Sequence Information” window is replaced by the “Axle Load” window (Fig. 3.25). This window consists of two fields only. They are number of lanes and axle load. The limit of number of lanes is two. The user needs to specify the average axle load in those lanes so as to account for the traffic load in the analysis. The positions of the axle loads in the lanes and on the embankment are shown in the Fig. 3.21. After entering data in both of these fields, the user needs to press the OK button in this window to close it.

#### 4) Process-Save Option

There are two types output data file from the *preprocessor* (i) The name of the output data file with an extension .inp ( for example site.inp) which contains the original input data (such as geometry, material properties, and loading) regarding foundation and embankment. This type of data file (\*.inp) is used for editing the input file (for the *preprocessor*), if necessary. (ii) The name of output data file with an extension .dat (for example site.dat) is ready to be converted by the *Data Converter* and then used by the *FE Main Program*.

The first window that appears on the screen asks the user to provide the name of the data file (\*.inp) in which the input information will be stored. The default file name is c:\demo\site.inp. If the default file name is acceptable, then the user needs

simply to click the OK button in the window. If the file name needs to be changed, the user can edit the file name and then press the OK button. While giving the file name, the user needs to give the full pathname of the file. The second window that appears on the screen asks the user to give the name of the output data file (\*.dat). The default file name is c:\demo\site.dat. The user can select any other name by editing this field. The OK button needs to be clicked to start processing the input data and saving the output data.

#### 5) Exit Option

This option is to be selected when the user wants to exit the *preprocessor* program. This option is expected to be chosen when the user has completed all inputs for a given site. This option can also be specified when the user has made some major error and wants to start all over again.

After selecting the **Exit Option**, the Actor Window (Fig. 3.5) will appear. When this happens, the user needs to click the control menu box of this window and choose the "Exit Actor" option. The user is finally done with execution of the *preprocessor* and goes back to the *Bridge Approach Settlement* window (Fig. 3.4).

#### **3.2.3 Running the Preprocessor - Edit an Existing Input Data File**

In this option, the *preprocessor* reloads an existing input data file "Site.inp" (for this example) and makes appropriate changes as needed by the user. The new output data files from the *preprocessor* can overwrite the "Site.inp" and "Site.dat" data files or save them as different files using other names. This option is very useful for a



parametric study. A typical example for a parametric study is given below:

*1. Parametric study - Embankment Height*

The original embankment height is 22 ft. In order to investigate the effect of the embankment height to the bridge approach settlement, change the embankment height as 20 ft, 18 ft, 16 ft, 14 ft, 12 ft, and 10 ft. The steps involved in running the *preprocessor* for these cases are as follows.

Restart the *preprocessor* and type '1' at the Input Data File Type Window (Fig. 3.7). Specify the reload data file name as "Site.inp".

- \* Select the **Site Data** option from the Bridge Approach Settlement Analysis Main Window (Fig. 3.11).

Select **1. Control Parameters** option

Change the height of embankment from 22 ft to 20 ft. Then press the *Tab* key and click the *OK* button.

Select **2. Embankment Soil Layers Information** option

Change the thickness of Layer #2 from 21 ft to 19 ft. Press the *Tab* key and click the *OK* button.

- \* Select the **Loading** option from the Bridge Approach Settlement Analysis Main Window (Fig. 3.11).

At the time step 4, change the completed embankment height from 7 ft to 5 ft.

- \* Select the **Process-Save** option from the Bridge Approach Settlement Analysis Main Window (Fig. 3.11).

Save the revised input data file as Height1.inp file and the new output data file as Height1.dat file.

- \* Select the **Exit** option from the Bridge Approach Settlement Analysis Main Window (Fig. 3.11).

Exit the *preprocessor*.

Repeat the same steps for other embankment height cases. The corresponding changes are summarized in Table 3.3.

## 2. Parametric study - Elastic Modulus E

The original elastic modulus of soil in foundation layer #1 is 0.8064e5 psf. In order to investigate the influence of the elastic modulus E on the bridge approach settlement, the elastic modulus of soil in foundation layer #1 is changed to 0.4064e5 psf and 0.8064e6 psf, respectively. The steps used to run the *preprocessor* are as follows: Restart the *preprocessor* and specify '1' at the Input Data File Type Window (Fig. 3.7). Specify the reload data file name as "Site.inp." The user needs to change the elastic modulus of foundation layer #1 from 0.8064e5 psf to 0.4064e5 psf.

- \* Select the **Site Data** option from the Bridge Approach Settlement Analysis Main Window (Fig. 3.11).

Select **5. Foundation Material Properties** option

Specify layer No. 1 and change its elastic modulus from 0.8064e5 psf to 0.4064e5 psf. Press the *Tab* key and click the *OK* button.

- \* Select the **Process-Save** option from the Bridge Approach Settlement Analysis Main

Window (Fig. 3.11).

Save the revised input data file as Elast1.inp file and the new output data file as Elast1.dat file.

- \* Select the **Exit** option from the Bridge Approach Settlement Analysis Main Window (Fig. 3.11).

Exit the *preprocessor*.

The user needs to repeat those steps and change the elastic modulus from 0.8064e5 psf to 0.8064e6 psf. Save the output files as Elast2.inp, and Elast2.dat.

### 3. Parametric Study - Water Table Depth

The original water table for this example was considered at 20 ft below the ground surface. In order to investigate the settlement variation at similar bridge sites with different water table depths, the water table is assumed to be located at 0 ft, 20 ft, and 45 ft from the ground surface. For this example site, the actual foundation soil consists of three clay layers. Hence, depending upon the water table location, the number of clay layers undergoing consolidation is different. This causes difficulty in the comparison of settlement variations with different water table locations. To avoid this difficulty, the foundation soil for layer #1 and layer #2 are treated as sand, and only layer #3 is treated as clay which is allowed to consolidate. Thus, the results will show the variation of consolidation settlement of layer # 3 for different locations of ground water level.

The steps used to run the *preprocessor* are presented below. Restart the *preprocessor*

and specify '1' at the Input Data File Type Window (Fig. 3.7). Specify the reload data file name as "Site.inp."

- \* Select the **Site Data** option from the Bridge Approach Settlement Analysis Main Window (Fig. 3.11)

Select **3. Foundation Soil Layers Information** option

The user needs to specify '0' for the soil type option for layer #1 and layer #2.

Select **5. Foundation Material Properties** option

The soil properties shown at Table 3.4 are used for this portion of the parametric study.

Select **6. Water Table Depth** option

The user needs to input the water table depth as 0 ft, then press the *Tab* key and click the *OK* button.

- \* Select the **Process-Save** option from the Bridge Approach Settlement Analysis Main Window (Fig. 3.11)

Save the revised input data file as Water1.inp file and the new output data file as Water1.dat file.

- \* Select the **Exit** option from the Bridge Approach Settlement Analysis Main Window (Fig. 3.11)

Exit the *preprocessor*.

Repeat the same steps for other water table levels ( 20 ft and 45 ft). In case the changed water table depth does not coincide with one of the surface of the foundation layers,

then the user needs to increase the number of foundation layers from 3 to 4 , and introduce an additional layer at the depth where the water table is located.

The user needs to run the *Data Convertor* and the *FE Main Program* for each output data file (\*.dat). Then the user can analyze the FEM results and make the comparison.

### 3.3 Data Converter

The data converter converts the output data file (\*.dat) from the *preprocessor* to a form that is compatible with the *FE Main program* for analyzing the embankment and the foundation. The user needs to *double click* the **DATA CONVERTER** icon at the Bridge Approach Settlement window (Fig. 3.4) to start the data converter. Then the user needs to follow the following steps.

1. The user needs to enter '1' for generating the data files for foundation analysis only, '2' for generating the data files for embankment analysis only, and '0' for generating the data files for both foundation and embankment analysis. After the user input the appropriate selection, then press the *RETURN* key.
2. The user needs to specify '1' for using the default names for the input and output files, or '2' for using other names that the user will have to specify later on for those files. Enter the desired option. It may be noted that the default input file name is Site.dat, and the default output files are SiteF.dat (data for foundation analysis) and SiteE.dat (data for embankment analysis).

If '2' option is selected in the step above, the user needs to enter the names of the input data file and output file(s). Type in the proper file names and press the *RETURN* key. Note that the input for this program is the output of the *preprocessor* and the output of this program is the input for the *FE Main Program*.

3. In case the user already has a file with a name same as one of the output file names, enter '1' for overwriting (if required) the existing output files, or '2' for maintaining the existing output files and stop the *Data Converter*.

### **3.4 FE Main Program**

The finite element (FE) computer program developed in this study is based on the Biot theory of three-dimensional consolidation (Biot, 1941), as proposed by Sandhu and Wilson (Sandhu et al., 1969). Plain strain idealization is assumed as it is pertinent for the bridge approach settlement problem. The FE formulation assumes that the soil medium is fully saturated below the water table and considers the soil skeleton deformation coupled with the pore pressure effects. Above the water table and in case of embankment analysis, the pore pressure degrees-of-freedom are removed. The nonlinear elasto-plastic behavior of soil skeleton is represented by the modified Cam-clay constitutive model as proposed by Roscoe and Burland (Roscoe et al., 1968). The concept of infinite element is incorporated into the FE model to idealize the semi-infinite soil domain accurately. The details of the FE formulation adopted in this study

are discussed in Chapter 2.

In the analysis, the foundation soil medium is divided into two regions: the near field, and the far field (see Fig. 2.2B). The near field is discretized by the isoparametric quadrilateral elements with eight nodes, four corner nodes and four mid-side nodes. Nodal displacements are considered to be unknowns at all eight nodes, while pore pressures are considered to be unknowns at the corner nodes only. The far field beyond the near field is modelled by three noded horizontal infinite elements. Similar to the finite elements, in which nodal displacements are the primary unknowns at all three nodes, while pore pressure are the unknowns at the two corner nodes only. A brief discussion on the development of quadrilateral and infinite elements is presented in Chapter 2 (Sec. 2.7 and 2.9.6). For embankment analysis, the section is discretized by using eight noded isoparametric elements.

In order to demonstrate the node numbering and element numbering schemes adopted in the algorithm, typical foundation and embankment cross-sections are selected and are shown in Fig. 3.26 and Fig. 3.27, respectively. The foundation consists of three different types of soils and is discretized by 113 nodes and 35 elements. Of these 35 elements, the first 30 are finite elements while the remaining 5 are infinite elements. In other words, the first 30 elements are the near-field elements, the remaining 5 elements are the far-field elements. A typical embankment selected in this example is discretized by 51 nodes and 12 elements, all elements being finite elements only. In case of the custom mesh generation by the user, care must be taken to ascertain that the

number of nodes does not exceed the maximum capability of the software (i.e. 500 nodes).

The following details have to be obtained from the field and the laboratory investigations. Sources such as construction and maintenance records help in preparation of the input data for the FE analysis of a given site.

- \* The geometric configuration such as depth of foundation, top and bottom widths of the embankment, and the associated site specific properties of the foundation as well as embankment soils.
- \* Details of the design loading on foundation, i.e. the weight of the embankment construction completed at different time periods.
- \* Number of lanes and the maximum traffic load that might be acting on that lane.

***Geometric Configuration:*** From the construction records or from the boring log the desired information about the depth of the foundation, different soil layers encountered can be obtained. Findings from the laboratory tests will also be helpful in the selection of the thickness of each layer. Previous studies (Laguros et al., 1990, 1991; Gopalasingam, 1989; Zaman et al., 1991) performed with different mesh types revealed that twice the base width of the embankment provides very good results in terms of the settlements and excess pore pressure distributions. In the computer program developed, the width of the soil domain equal to 2.5 times the bottom width of embankment loading is considered for the purpose of FE analysis.

***Material Properties:*** The following soil properties for each layer have to be obtained



from laboratory and/or field tests or estimated before carrying out the analysis. Young's modulus (E), coefficient of permeability (k), unit weight( $\gamma$ ), slope of the critical state line (M), compression index ( $C_c$ ), swelling index( $C_s$ ), and initial void ratio ( $e_o$ ), required for defining the nonlinear soil behavior for each layer.

**Loading:** The loading on foundation due to embankment construction can be determined from the embankment height ( $H_e$ ) and the average unit weight of the embankment material. Since consolidation is a time-dependent process, the time taken for the construction of particular height of embankment is required for the calculation of the overburden on foundation. The construction records, if available, may be used for computing the embankment load on foundation at a particular time. In the absence of the construction records, empirical formulae relating the embankment height ( $H_e$  in ft) and the construction time ( $T_e$  in days) can be used.

The following relationship given by Hopkins (Hopkins, 1985) can be used to estimate the loading rate:

$$T_c = 10^{1.2376 \log_{10} H_e + 0.1122} \quad (3.1)$$

For embankment analysis the major loadings will be the self-weight of the embankment and the vehicular traffic load. Self weight can be computed from the dimensions of embankment and unit weight of the different embankment materials. Maximum vehicular traffic load that is anticipated on a highway can be obtained from Standard Specifications for Highway Bridges by the American Association of State

Highway Officials.

The idealized soil profile is discretized into a number of elements. As mentioned in Chapter 2 (Sec. 2.1), for foundation analysis, the near field of the soil domain is discretized by eight noded isoparametric quadrilateral elements, while the unbounded soil region, extending to a very large distance in the horizontal direction, is discretized by three noded horizontal infinite elements. For embankment analysis, the soil domain is discretized by eight noded isoparametric quadrilateral elements. The nodal points and the elements are numbered in a sequential manner (see Fig. 3.27) and input to the finite element program in accordance with the specified format.

#### ***3.4.1 Description of the FE Main Program***

The computer code used in this study was originally developed by Dr. C. S. Desai, and his co-workers at the University of Arizona, Tucson, Arizona (Desai, 1987). The code was modified and extended substantially by Gopalasingam (1989) to incorporate the isoparametric quadrilateral and infinite elements. In this study, a complete software package was developed by adding a user-friendly *preprocessor* and *postprocessor* with the *FE Main program*. Fig. 3.28 shows the organizational structure of the *FE Main program*. The program is divided into the following major parts:

- (i) The first operation performed by the program is to read the basic control parameter information.
- (ii) The second operation is to process the input data, which is performed by a subroutine called INPT. This will set up the FE mesh, generate bandwidth, if

required, set up the equation labels, count the number of cycles for printing the output, read new load conditions, and alter the size of time step.

- (iii) In the third step the subroutine ELEMEN is called. Several other subroutines are called by the subroutine ELEMEN (i.e., SHAPE, SHAPEF, B, BF, INVER2, MULT, and ADD) to generate several matrices by direct stiffness addition of element contributions. For infinite elements, the subroutine IELEMEN is called instead of the subroutine ELEMEN.
- (iv) In the fourth step the output from both ELEMEN and IELEMEN is transferred to the subroutine SOLVE to form the system matrix and the system load vectors. The subroutine MODIFY is used to modify the system equations to account for the prescribed boundary conditions.
- (v) In the fifth and final step, the subroutine SYSSOL is used to solve the set of equations at each time step by using the Gaussian elimination method. The subroutine STRESS is used for the stress calculations.

### ***3.4.2 Input Quantities for the FE Main Program***

The *FE Main Program* is capable of analyzing the foundation and embankment at a given site, provided the input is in a consistent set of units. Correspondingly, the output produced by the program conforms to the same set of units. Therefore, if the user decides to use pound (lb) and foot (ft) as the input unit, all dimensions must be in feet, loads in pounds, unit-weights in pcf, stresses in psf and so on. The material properties should also conform to these units. The output units will then be in pounds

and feet, so that displacements will be in feet, pore pressures and stresses will be in pounds per square feet. The *preprocessor* has been developed for two types of unit: the FPS (Feet, Pound, Second), and the SI (Meter, Newton, Second) systems, as they are most commonly used. The following data has to be furnished for the *FE Main Program* as input:

- \* The geometric configurations and material properties.
- \* The details of the loading such as the self weight of the soil which may be due to embankment, approach pavements, etc.
- \* Arbitrary rate of loading which can be specified as step loading and variable time steps for specific time-periods of consolidation.
- \* Vehicular traffic loading details for the analysis of embankment.

Preparation of geometric configuration data manually is a time consuming process and prone to errors. The *preprocessor* developed in this study relieves the burden of generation of nodal data and boundary conditions data manually by generating the geometric configuration data with a minimum amount of input.

Appendix III provides further details of the input data for the *FE Main Program*.

### **3.4.3 Running the FE Main Program**

*Double click* the **FEM ANALYSIS** icon from the Bridge Approach Settlement window (Fig. 3.4) to start the program.

1. The user needs to specify '1' for foundation analysis and '2' for embankment analysis. Input the appropriate option and press *RETURN*.

2. The user needs to enter '1' for using default names for the input and output files or '2' for using other names for those files. The default files for this program are listed below:

	<u>Foundation Analysis</u>	<u>Embankment Analysis</u>
Input file:	SiteF.Dat	SiteE.Dat
General output file:	SiteF.Out	SiteE.Out
Condensed output file:	SiteFCd.Out	SiteECd.Out
Plot file #1:	SiteFS.Out (Surface Settlement)	SiteES.Out (Surface Settlement)
Plot file #2:	SiteFP.Out (Pore Pressure)	SiteEP.Out (Central Settlement)
Plot file #3:	SiteFCr.Out (Stress Contours)	SiteECr.Out (Stress Contours)

If the user selects option '2' at the step above, the program requires that you enter the names for the different input and output files at this stage.

3. In case the user already has a file with a name same as one of the output file names, the program needs to know whether the user want to overwrite the existing file or stop the program. The user needs to enter '1' for overwriting the existing output files, or '2' for keeping the existing output files and stopping the program.

### 3.5 The Post-Processor

When executed, the *FE Main Program* yields detailed analysis results for both foundation and embankment. The outputs are generally in the form of tables which are not very easy to comprehend and to draw inferences. In order to overcome this difficulty, a *postprocessor* was developed in this study. The *postprocessor* helps in presenting the results from the *FE Main Program* in the form of graphical plots which are much easier to understand and convenient to interpret.

The *postprocessor* makes use of a graphic software package, called Graphic/Win developed by the Scientific Endeavors Corporation, TN. This *postprocessor* contains six subroutines which can be called for plotting various results. These programs are written in "C" language.

#### 3.5.1 The Subroutines of the Postprocessor

The following are different subroutines for plotting the results:

##### **a. Foundation Analysis:**

- (i) FSETTLE.C - for plotting the surface settlement versus horizontal distance.
- (ii) FPORE.C - for plotting the excess pore pressure versus depth.
- (iii) CONTOUR.C - for plotting the maximum normal principal stress contours in the cross section.

##### **b. Embankment Analysis:**

- (i) ESETTLE.C - for plotting the surface settlement versus horizontal distance.
- (ii) EDEPTH.C - for plotting the settlement versus depth along the central section.

- (iii) CONTOUR1.C - for plotting the maximum normal principal stress contours in the cross section.

### **3.5.2 Running the Postprocessor**

Efforts were made to make the *postprocessor* programs user-friendly. The methods for using the six *postprocessor* subroutines ( Fsettle, FPoreore, FContour, Esettle, Edepth, and EContour) are basically the same. Double-click the appropriate icon from the Bridge Approach Settlement window (Fig. 3.4) to start the *postprocessor*. The first window displays the title of the plot on the screen (Fig. 3.29). Then, click the *OK* button to go to the next window. Then the user needs to enter '0' for default files or enter '1' otherwise (Fig. 3.30). If '1' is selected, the user needs to input the file name with the complete pathname in the next window. The GraphiC Window shows the relevant plot. The user can obtain a hardcopy of the plot by selecting the "print" option at "File" selection on the menu bar of this window (Fig. 3.31). Then at the "File" selection, choose the "Exit" option to exit the *postprocessor*.

Table 3.1 Input and Output of Different Programs

Input	Program	Output
To be given or reload *.inp data file	Preprocessor	<ol style="list-style-type: none"> <li>1. *.inp data file - contains the original inputs specified by the user</li> <li>2. *.dat data file- contains all the information for foundation and embankment settlement analysis</li> </ol>
Output - *.dat file from Preprocessor	<p>Data Converter</p> <p>Foundation Analysis</p> <p>Embankment Analysis</p>	<ol style="list-style-type: none"> <li>1. Data file for foundation analysis</li> <li>2. Data file for embankment analysis</li> </ol> <ol style="list-style-type: none"> <li>1. General output file</li> <li>2. Condensed output file</li> <li>3. Surface settlements</li> <li>4. Excess pore pressure</li> <li>5. Max. normal principal stresses</li> </ol> <ol style="list-style-type: none"> <li>1. General output file</li> <li>2. Condensed output file</li> <li>3. Surface settlements</li> <li>4. Settlement along the central plane</li> <li>5. Max. normal principal stresses</li> </ol>
Output from FE Main program	<p>Postprocessor</p> <p>Foundation Analysis</p> <p>FSETTLE.C FPORE.C CONTOUR.C</p> <p>Embankment Analysis</p> <p>ESETTLE.C EDEPTH.C CONTOUR1.C</p>	<p>Plots</p> <ol style="list-style-type: none"> <li>1. Surface settlement plot</li> <li>2. Excess pore pressure plot</li> <li>3. Max. normal principal stress contours</li> </ol> <ol style="list-style-type: none"> <li>1. Surface settlement plot</li> <li>2. Settlement along the central plane</li> <li>3. Max. normal principal stress contours</li> </ol>



Table 3.2 Range of Variables Used in The Preprocessor

Variable	FPS System		SI System	
	Lower Limit	Upper Limit	Lower Limit	Upper Limit
Embankment Height	0 ft.	100 ft.	0 M	30 M
Density a. Sand b. Clay	85 pcf 75 pcf	150 pcf 150 pcf	14000 N/M <sup>3</sup> 12500 N/M <sup>3</sup>	25000 N/M <sup>3</sup> 25000 N/M <sup>3</sup>
Void Ratio a. Sand b. Clay	0.4 0.3	1.0 3.2	0.4 0.3	1.0 3.2
Emb. Top Width	10 ft.	100 ft.	4 M	40 M
Young's Modulus, E, a. Sand b. Clay c. Pavement	158000 psf 39000 psf 5e7 psf	4e6 psf 4e5 psf 6e7 psf	8e6 Pa 2e6 Pa 2.4e9 Pa	2e8 Pa 2e7 Pa 2.9e9 Pa
Poisson's Ratio	0.001	0.499	0.001	0.499
Permeability Coeff. a. Sand b. Clay	2.88 ft/day 1e-7 ft/day	2800 ft/day 2.88e-3 ft/day	0.75 M/day 3e-6 M/day	900 M/day 9e-2 M/day
Angle of Int. Fric. a. Sand b. Clay	27 Degrees 0 Degrees	48 Degrees 30 Degrees	27 Degree 0 Degree	48 Degree 30 Degrees
Cohesion c, a. Sand b. Clay	0 psf 0 psf	0 psf 5000 psf	0 Pa 0 Pa	0 Pa 2.5e5 Pa
Slope of Consolidation Curve	0.01 1/psf	0.5 1/psf	0.01 1/Pa	0.5 1/Pa
Slope of Swelling Curve	0.001 1/psf	0.1 /psf	0.001 1/Pa	0.1 /Pa

Table 3.3 Various Embankment Heights For the Preprocessor

Embank. Height (ft)	Embank. Layer #2 Height	Completed Ht. at Time Step 3	Completed Ht. at Time Step 4	Save the Output Files as
22	21	5	7	Site.inp; Site.dat
20	19	5	5	Height1.inp; Height1.dat
18	17	5	3	Height2.inp; Height2.dat
16	15	5	1	Height3.inp; Height3.dat
14	13	4	0	Height4.inp; Height4.dat
12	11	2	0	Height5.inp; Height5.dat
10	9	0	0	Height6.inp; Height6.dat

Table 3.4 Various Water Table Depths For The Preprocessor

WT. Depth	Material Properties of layer #1	Material Properties of layer #2	Material Properties of layer #3
0 ft	Thickness: 20 ft Soil Type: 0 Density: 113 pcf E : 180640 psf $\Phi$ : 30 <sup>0</sup> c : 0 psf $\nu$ : 0.4 k : 20 ft/day	Thickness: 25 ft Soil Type: 0 Density: 115 pcf E : 187200 psf $\Phi$ : 30 <sup>0</sup> c : 0 psf $\nu$ : 0.4 k : 30 ft/day	Thickness: 15 ft Soil Type: 1 Density: 117 pcf E : 112320 psf $\Phi$ : 10 <sup>0</sup> c : 100 psf $\nu$ : 0.4 k : 2.2e-4 ft/day
20 ft	same as above except Density: 108 pcf E : 280640	same as above	same as above
45 ft	same as above except Density: 108 pcf E : 280640	same as above except Density: 108 pcf E : 287200	same as above

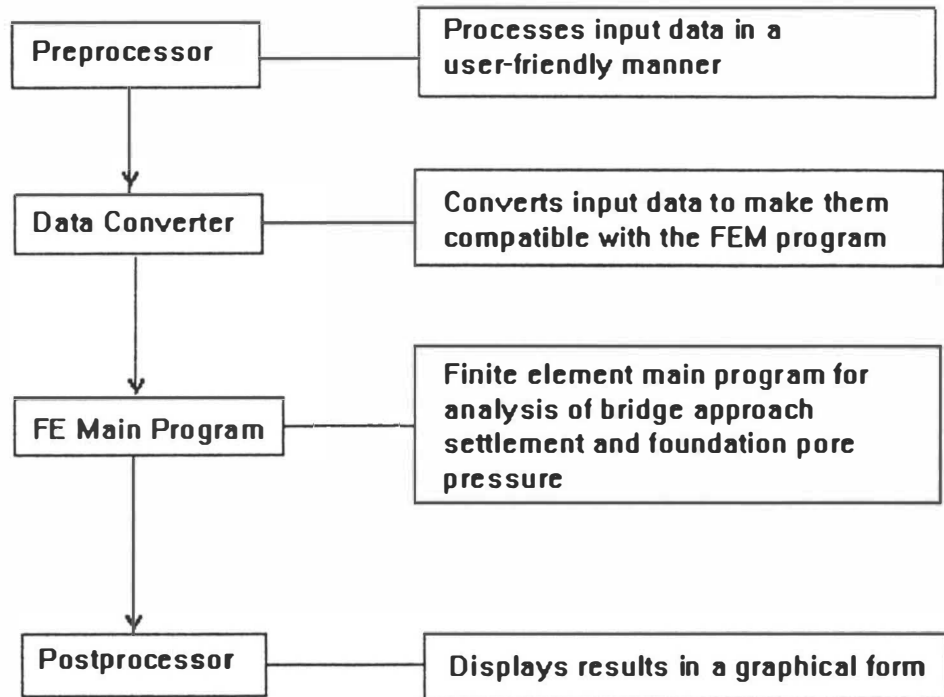


Fig. 3.1 Different Components of the Software Package

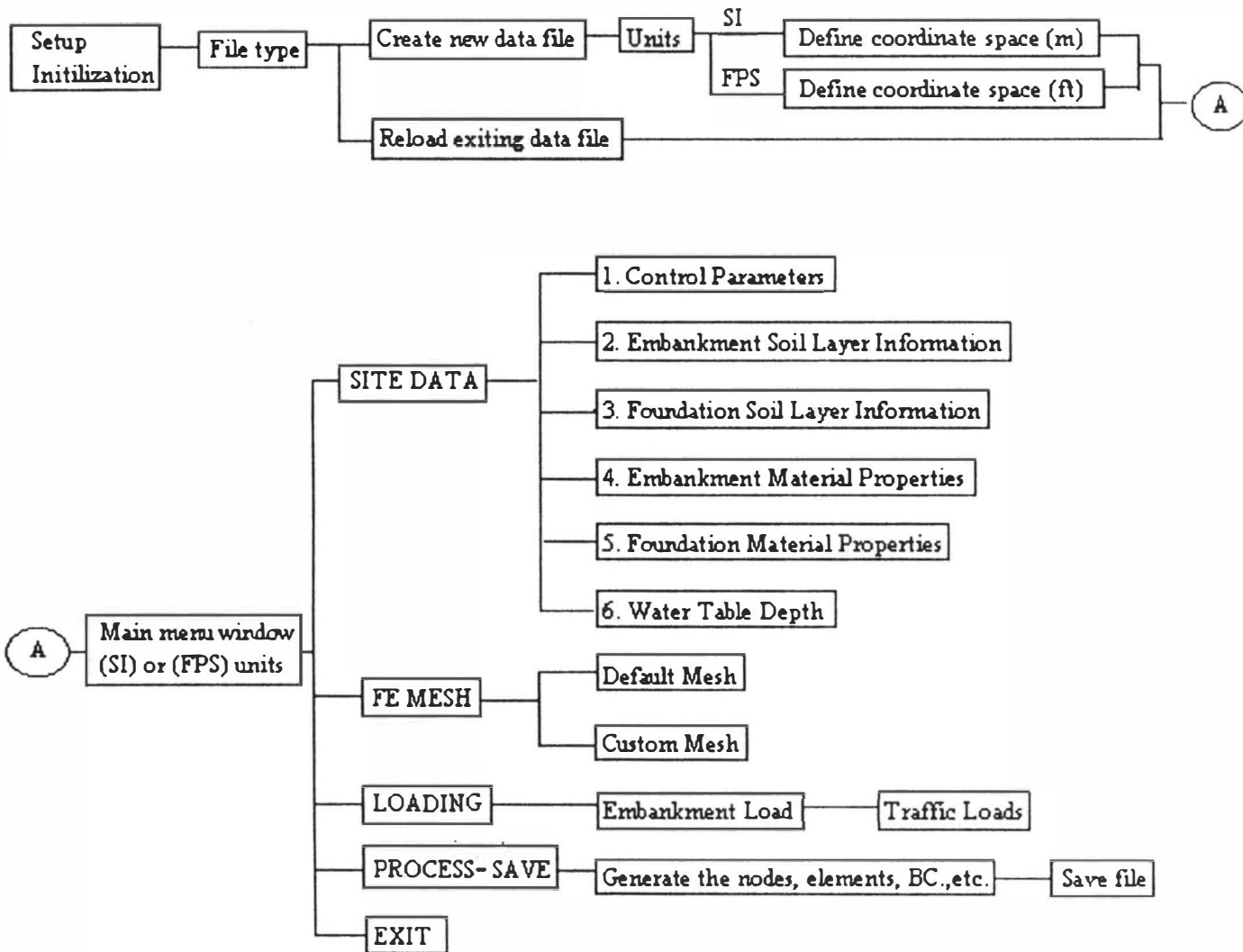


Fig. 3.2 Main Components of The Preprocessor

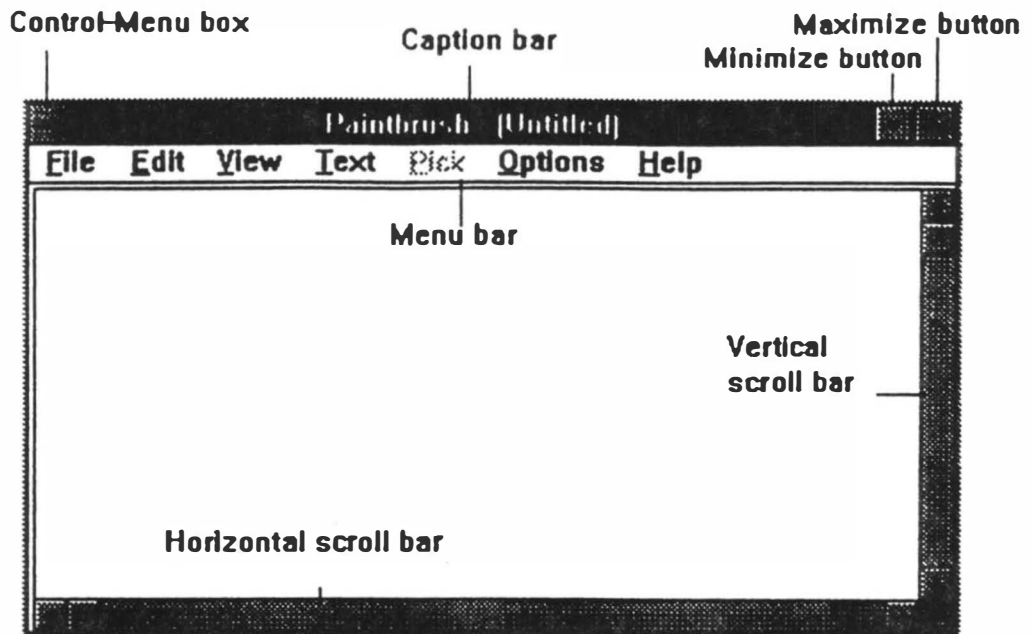


Fig. 3.3 Various Components of A Window

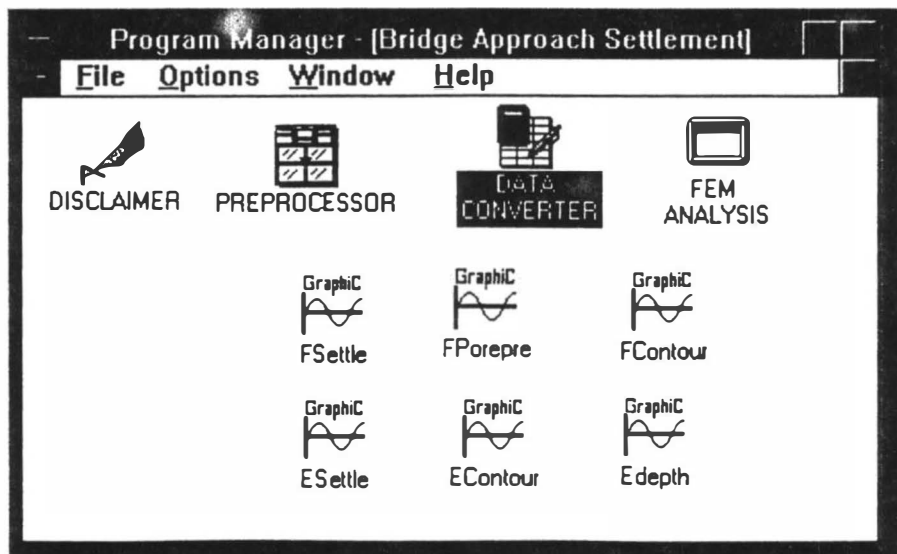


Fig. 3.4 Bridge Approach Settlement Window

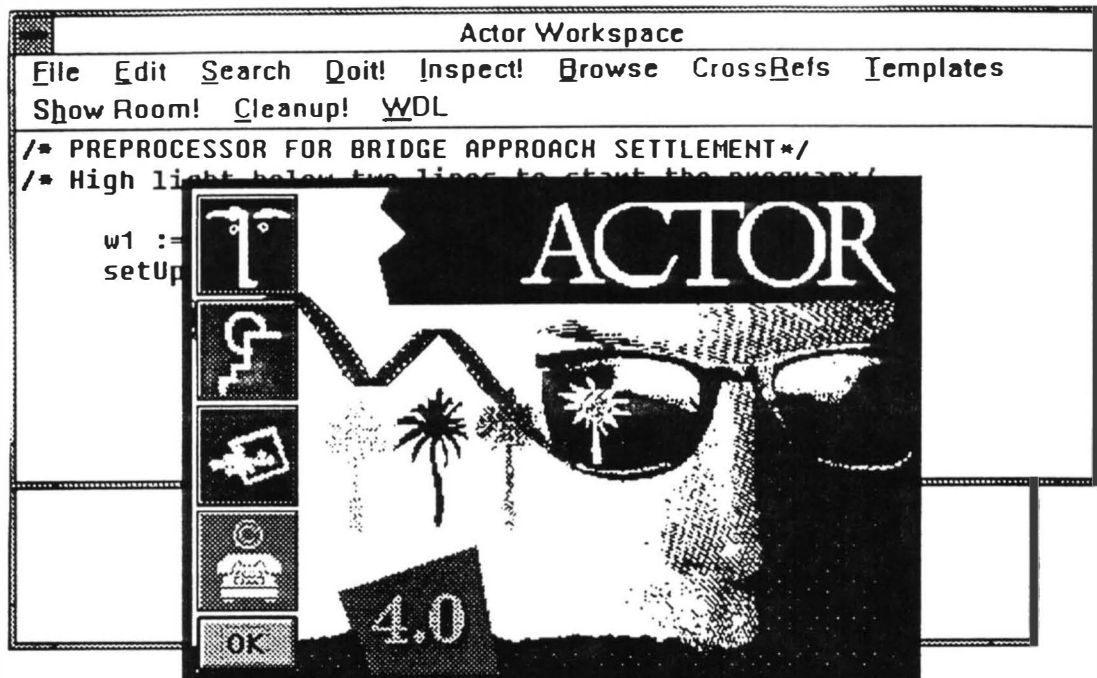


Fig. 3.5 Actor Window

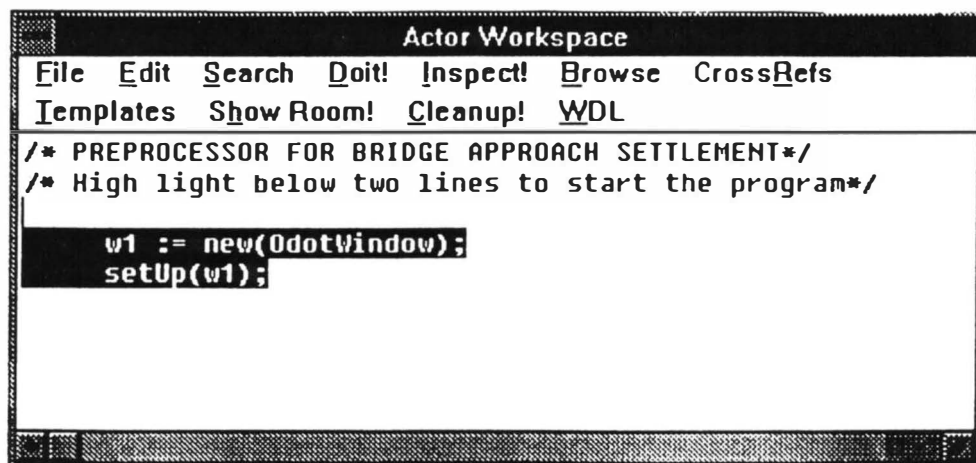


Fig. 3.6 Actor Workspace Window

Input Data File Type	
Give 0 for New File; Give 1 for Existing File	
<input type="text" value="1"/>	
<input type="button" value="OK"/>	<input type="button" value="Cancel"/>

Fig. 3.7 Input Data File Type Window

Specify Unit System	
Give 0 for FPS; Give 1 for SI	
<input type="text" value="0"/>	
<input type="button" value="OK"/>	<input type="button" value="Cancel"/>

Fig. 3.8 Unit System Window

Define coordinate space (ft)	
<u>Minimum:</u>	<u>Maximum:</u>
<u>X</u> -coordinate:	<u>X</u> -coordinate:
<input type="text" value="0"/>	<input type="text" value="170"/>
<u>Y</u> -coordinate:	<u>Y</u> -coordinate:
<input type="text" value="0"/>	<input type="text" value="100"/>
<input type="button" value="OK"/>	

Fig. 3.9 Coordinate Space Window

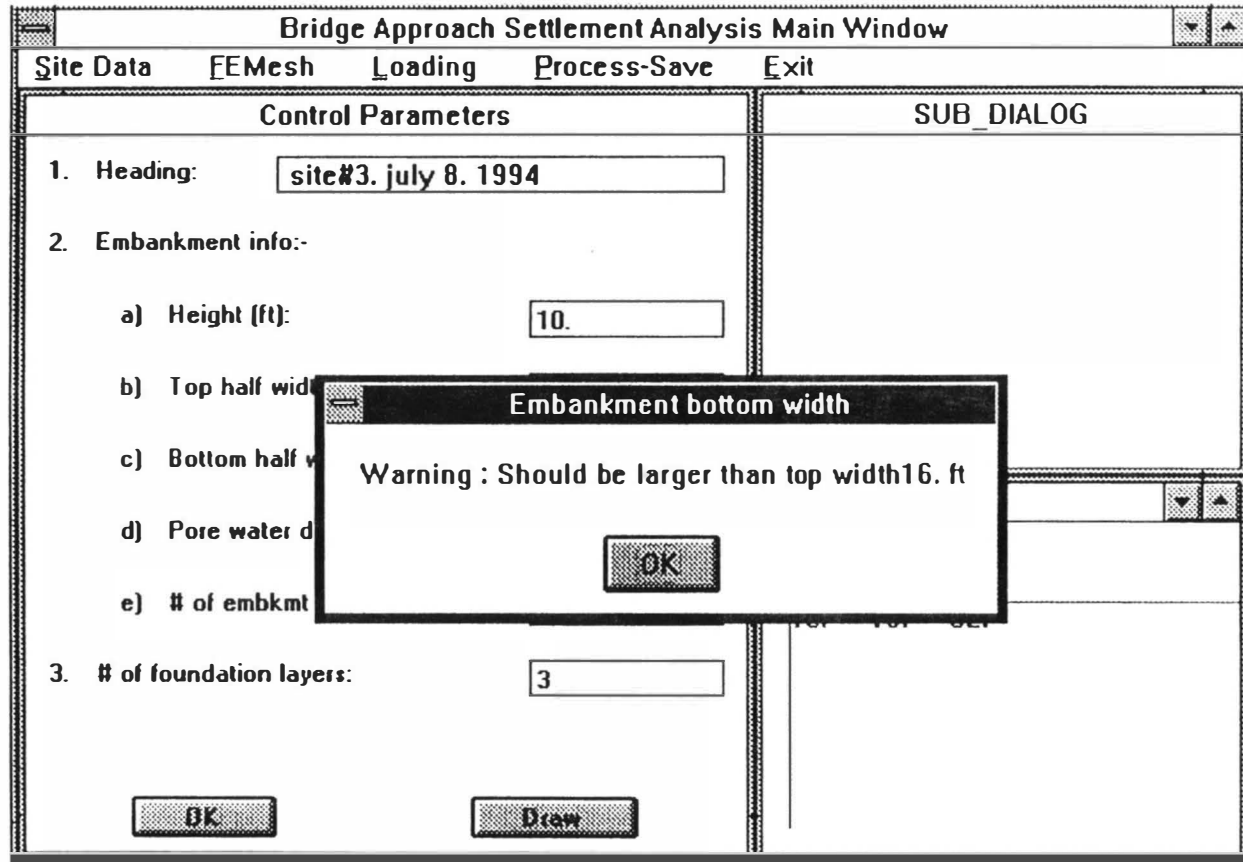


Fig. 3.10 Message Box Window



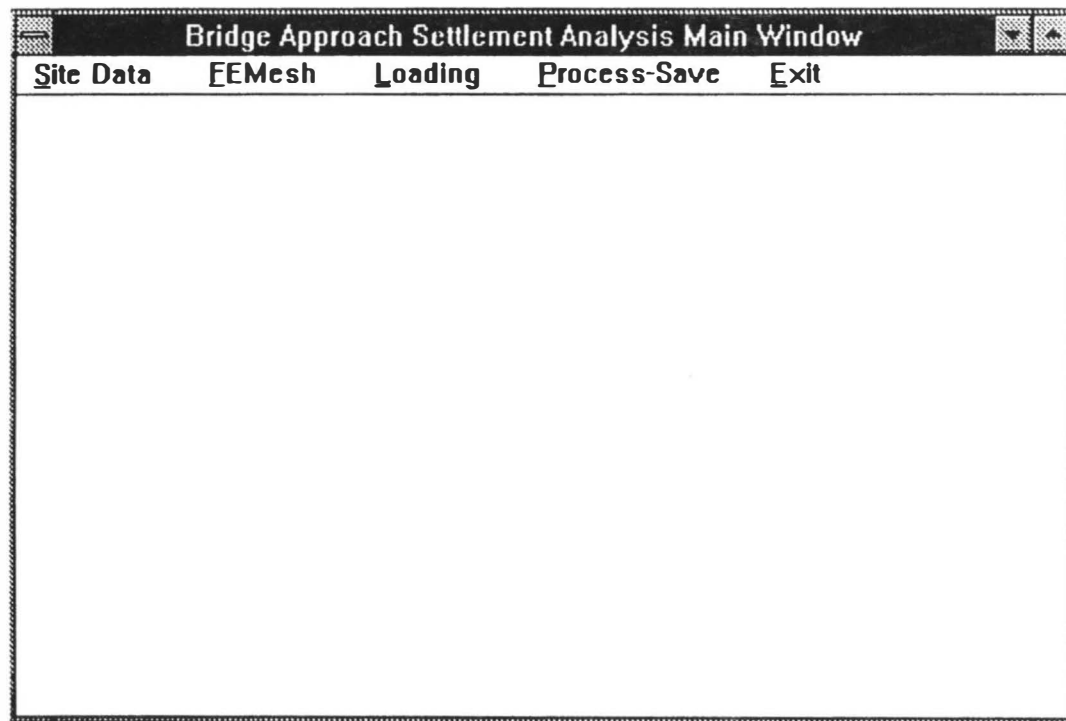


Fig. 3.11 Bridge Approach Settlement Analysis Main Window

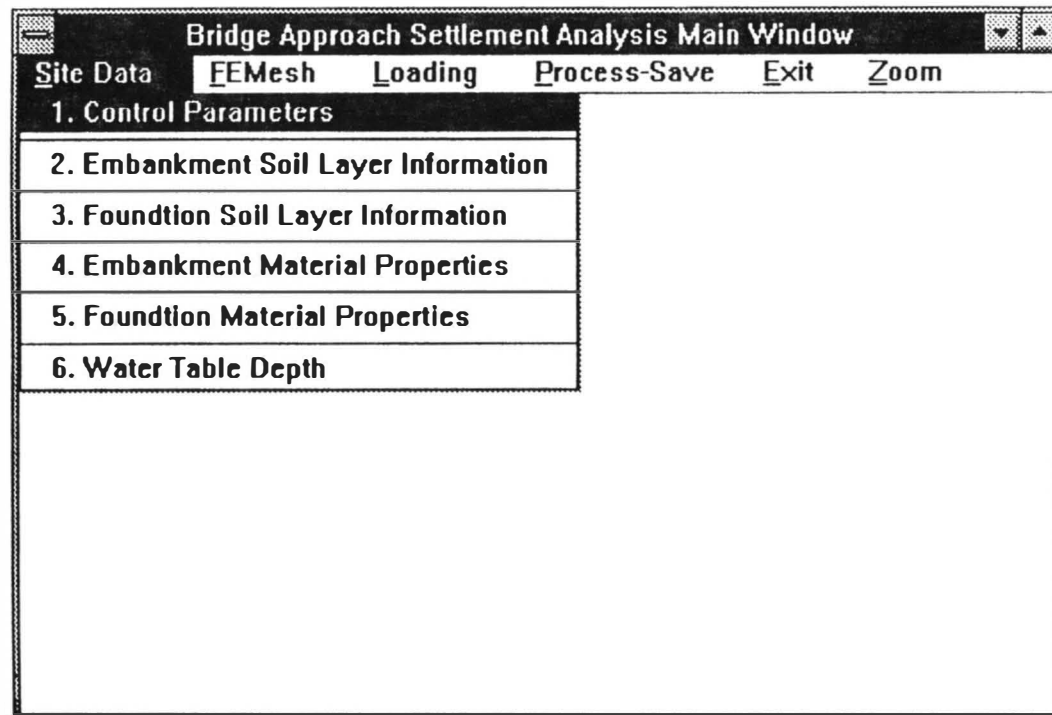


Fig. 3.12 Site Data Option Window

**Bridge Approach Settlement Analysis Main Window**

Site Data FEMesh Loading Process-Save Exit

**Control Parameters**

1. Heading:

2. Embankment info:-

a) Height (ft):

b) Top half width (ft):

c) Bottom half width (ft):

d) Pore water density (pcf):

e) # of embkmt layers:

3. # of foundation layers:

**SUB\_DIALOG**

**Visual**

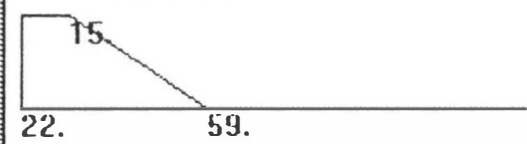


Fig. 3.13 Control Parameters Window

Emb.layer#1  
 $E = 5.0e6$  psf  
 $\phi = 30^\circ$   
 $c = 0$  psf  
 $\nu = 0.3$   
 $k = 3$  ft/day

Emb.layer#2  
 $E = 1.44e5$  psf  
 $\phi = 0^\circ$   
 $c = 50$  psf  
 $\nu = 0.4$   
 $k = 1.9e-4$  ft/day

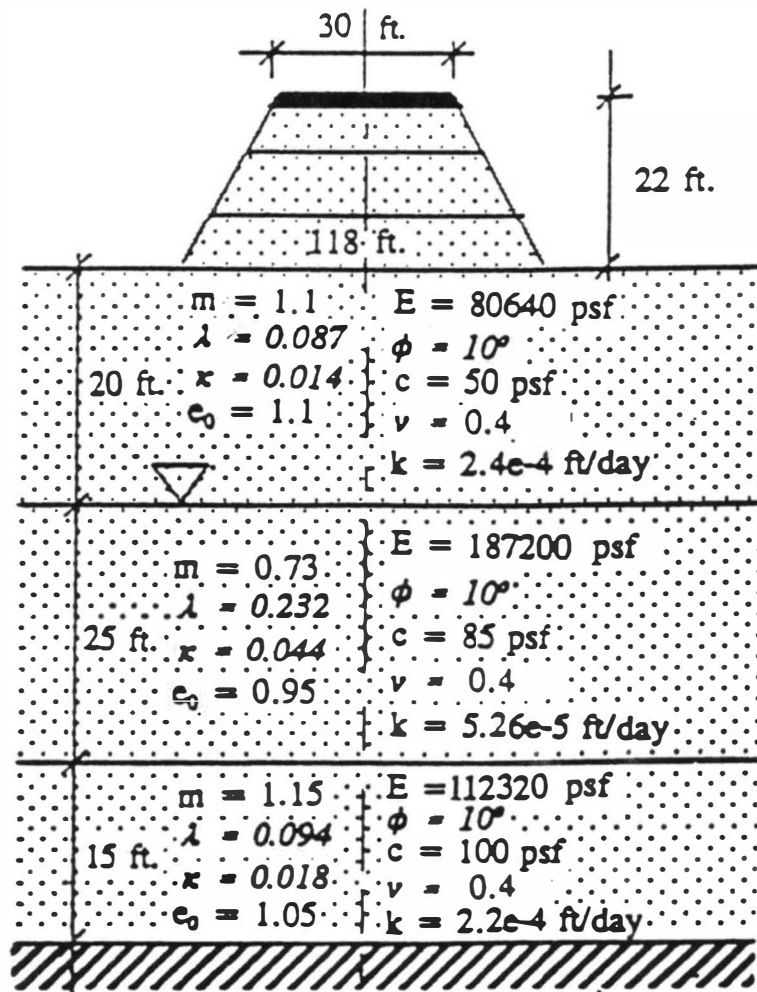


Fig. 3.14 Idealized Soil Profile for East Cordell Bridge Site

**Bridge Approach Settlement Analysis Main Window**

Site Data   FEMesh   Loading   Process-Save   Exit

**Embankment Layer information**

For layer # 1	For layer # 2	For layer # 3
a) Thickness (ft): <input type="text" value="1."/>	a) Thickness (ft): <input type="text" value="21."/>	a) Thickness (ft): <input type="text" value="0."/>
b) Soil type: s=0/c=1/p=2 <input type="text" value="2"/>	b) Soil type: (S=0/C=1) <input type="text" value="1"/>	b) Soil type: (S=0/C=1) <input type="text" value="nil"/>
c) Density (pcf): <input type="text" value="140."/>	c) Density (pcf): <input type="text" value="112.7"/>	c) Density (pcf): <input type="text" value="0."/>
For layer # 4	For layer # 5	
a) Thickness (ft): <input type="text" value="0."/>	a) Thickness (ft): <input type="text" value="0."/>	
b) Soil type: (S=0/C=1) <input type="text" value="nil"/>	b) Soil type: (S=0/C=1) <input type="text" value="nil"/>	
c) Density (pcf): <input type="text" value="0."/>	c) Density (pcf): <input type="text" value="0."/>	

**Visual**

1.15  
22. 21. 59.

Fig. 3.15A Embankment Layer Information Window

**Bridge Approach Settlement Analysis Main Window**

Site Data   FEMesh   Loading   Process-Save   Exit

---

**Foundation Layer information**

<p><b>For layer # 1</b></p> <p>a) Thickness (ft): <input style="width: 60px;" type="text" value="20."/></p> <p>b) Soil type: (S=0/C=1) <input style="width: 60px;" type="text" value="1"/></p> <p>c) Density (pcf): <input style="width: 60px;" type="text" value="113."/></p>	<p><b>For layer # 2</b></p> <p>a) Thickness (ft): <input style="width: 60px;" type="text" value="25."/></p> <p>b) Soil type: (S=0/C=1) <input style="width: 60px;" type="text" value="1"/></p> <p>c) Density (pcf): <input style="width: 60px;" type="text" value="115."/></p>	<p><b>For layer # 3</b></p> <p>a) Thickness (ft): <input style="width: 60px;" type="text" value="15."/></p> <p>b) Soil type: (S=0/C=1) <input style="width: 60px;" type="text" value="1"/></p> <p>c) Density (pcf): <input style="width: 60px;" type="text" value="117."/></p>
<p><b>For layer # 4</b></p> <p>a) Thickness (ft): <input style="width: 60px;" type="text" value="0."/></p> <p>b) Soil type: (S=0/C=1) <input style="width: 60px;" type="text" value="nil"/></p> <p>c) Density (pcf): <input style="width: 60px;" type="text" value="0."/></p>	<p><b>For layer # 5</b></p> <p>a) Thickness (ft): <input style="width: 60px;" type="text" value="0."/></p> <p>b) Soil type: (S=0/C=1) <input style="width: 60px;" type="text" value="nil"/></p> <p>c) Density (pcf): <input style="width: 60px;" type="text" value="0."/></p>	

**Visual**

Fig. 3.15B Foundation Layer Information Window

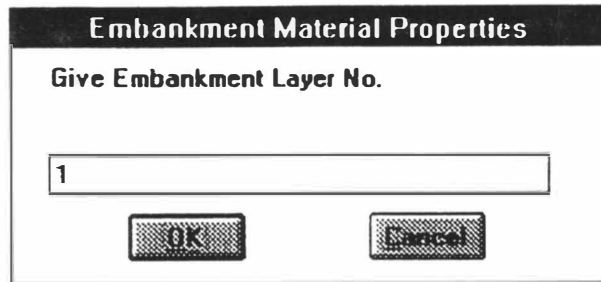


Fig. 3.16 Embankment Layer No. Window

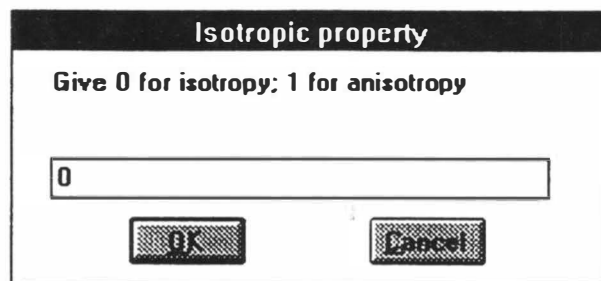


Fig. 3.17 Isotropic Property Window

The image shows a software window titled "Bridge Approach Settlement Analysis Main Window". It has a menu bar with "Site Data", "FEMesh", "Loading", "Process-Save", and "Exit". The main area is split into two panes. The left pane is titled "Emb.layer#1: Isotropic" and contains a list of five material properties, each with a corresponding input field:

Property	Value
1. Elastic modulus (psf):	5.0e6
2. Angle of int. fric (deg):	30
3. Cohesion (psf):	0
4. Poisson's ratio:	0.3
5. Permeability coeff. (ft/day):	3.0

At the bottom of the left pane are two buttons: "OK" and "CANCEL". The right pane is titled "SUB\_DIALOG" and is currently empty.

Fig. 3.18A Isotropic Material Window for Embankment Layer



**Bridge Approach Settlement Analysis Main Window**

Site Data FEMesh Loading Process-Save Exit

Emb.layer#3: anisotropic

1. Elastic modulus-X (psf):

2. Poisson's ratio-X

3. Permeability coeff.-X (ft/day):

4. Angle of int. fric. (deg):

5. Cohesion:

6. Elastic modulus-Y (psf):

7. Poisson's ratio-Y

8. Permeability coeff.-Y (ft/day):

OK CANCEL

SUB\_DIALOG

Fig. 3.18B Anisotropic Material Window for Embankment Layer

The image shows a software window titled "Bridge Approach Settlement Analysis Main Window". The window has a menu bar with the following items: "Site Data", "FEMesh", "Loading", "Process-Save", and "Exit". The main area is divided into two panes. The left pane is titled "FND.layer#1: Isotropic" and contains a list of five parameters, each with an associated input field:

1. Elastic modulus (psf):
2. Angle of int. fric (deg):
3. Cohesion (psf):
4. Poisson's ratio:
5. Permeability coeff. (ft/day):

At the bottom of the left pane, there are two buttons: "OK" and "CANCEL". The right pane is titled "SUB\_DIALOG" and is currently empty.

Fig. 3.18C Isotropic Sand Window for Foundation Layer

**Bridge Approach Settlement Analysis Main Window**

Site Data FEMesh Loading Process-Save Exit

**FND.layer#1: Isotropic**

1. Elastic modulus (psf):	<input type="text" value="80640."/>
2. Angle of int. fric (deg):	<input type="text" value="10."/>
3. Cohesion (psf):	<input type="text" value="50."/>
4. Poisson's ratio:	<input type="text" value="0.4"/>
5. Permeability coeff. (ft/day):	<input type="text" value="2.4e-4"/>

**Clay material properties**

1. Crit. st. In. slope	<input type="text" value="1.1"/>
2. Compression Index	<input type="text" value="0.087"/>
3. Swelling Index	<input type="text" value="0.014"/>
4. Void ratio	<input type="text" value="1.1"/>

Fig. 3.18D Isotropic Clay Window for Foundation Layer

**Bridge Approach Settlement Analysis Main Window**

Site Data FEMesh Loading Process-Save Exit

**FND.layer#4: Anisotropic**

1. Elastic modulus-X (psf):

2. Poisson's ratio-X

3. Permeability coeff.-X (ft/day):

4. Angle of int. fric. (deg):

5. Cohesion:

6. Elastic modulus-Y (psf):

7. Poisson's ratio-Y

8. Permeability coeff.-Y (ft/day):

OK CANCEL

**SUB\_DIALOG**

Fig. 3.18E Anisotropic Sand Window for Foundation Layer

**Bridge Approach Settlement Analysis Main Window**

Site Data FEMesh Loading Process-Save Exit

FND.layer#4: Anisotropic		Clay material properties	
1. Elastic modulus-X (psf):	<input type="text"/>	1. Crit. st. ln. slope	<input type="text"/>
2. Poisson's ratio-X	<input type="text"/>	2. Compression Index	<input type="text"/>
3. Permeability coeff.-X (ft/day):	<input type="text"/>	3. Swelling Index	<input type="text"/>
4. Angle of int. fric. (deg):	<input type="text"/>	4. Void ratio	<input type="text"/>
5. Cohesion:	<input type="text"/>	<input type="button" value="OK"/>	<input type="button" value="CANCEL"/>
6. Elastic modulus-Y (psf):	<input type="text"/>		
7. Poisson's ratio-Y	<input type="text"/>		
8. Permeability coeff.-Y (ft/day):	<input type="text"/>		
<input type="button" value="OK"/>	<input type="button" value="CANCEL"/>		

Fig. 3.18F Anisotropic Clay Window for Foundation Layer

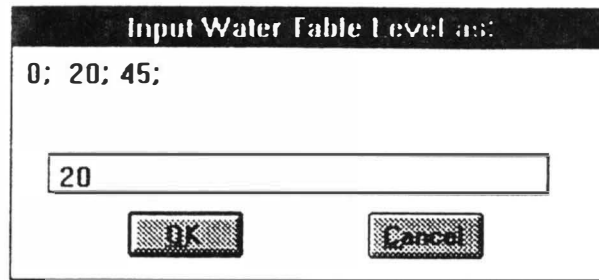


Fig. 3.19 Water Table Depth Window

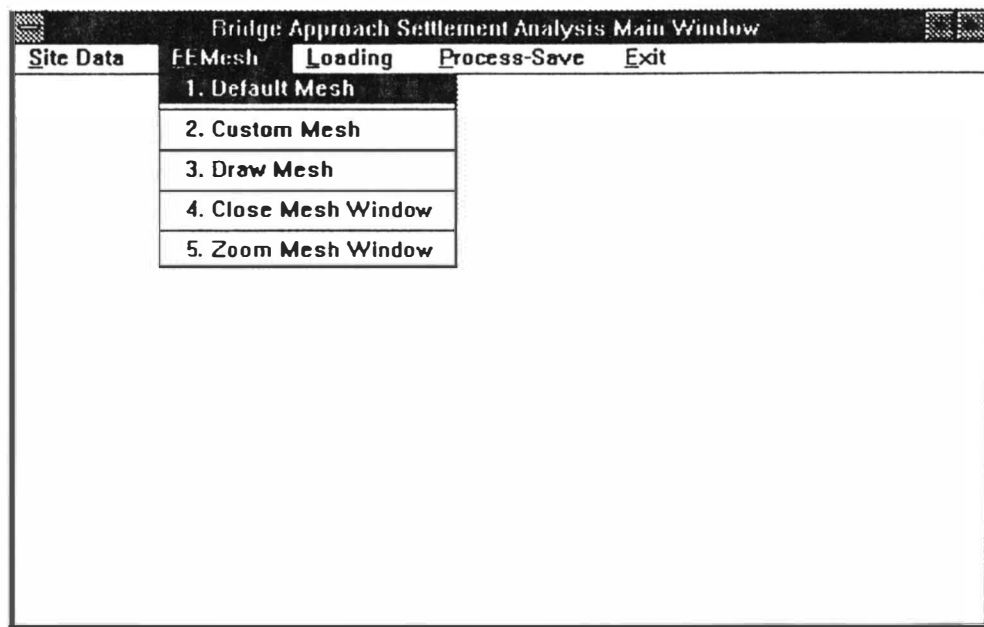


Fig. 3.20 FE Mesh Option Window

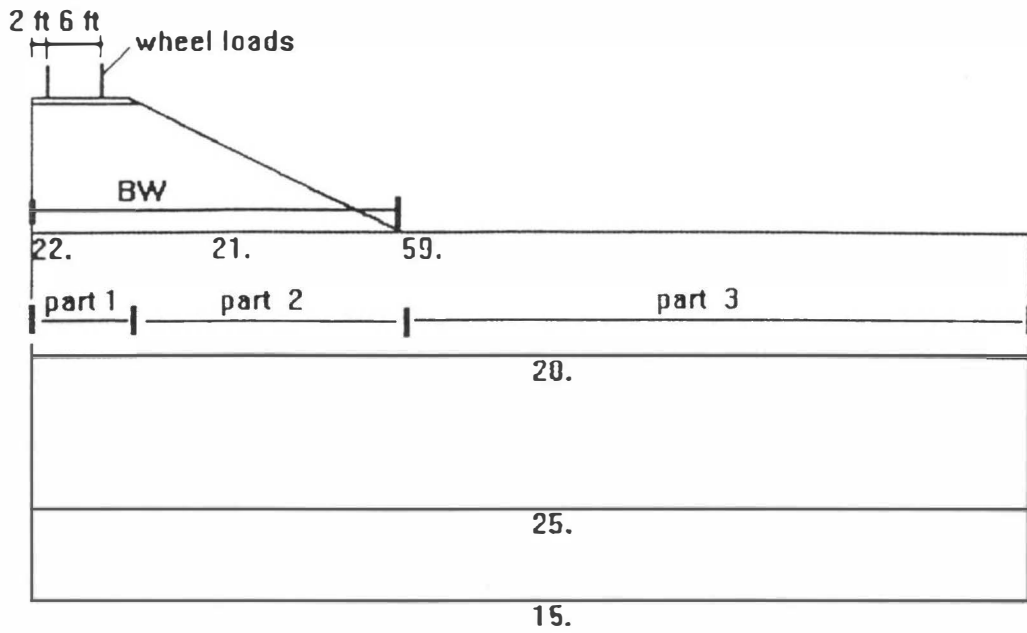


Fig. 3.21 Three Parts In the X Direction for FE Mesh

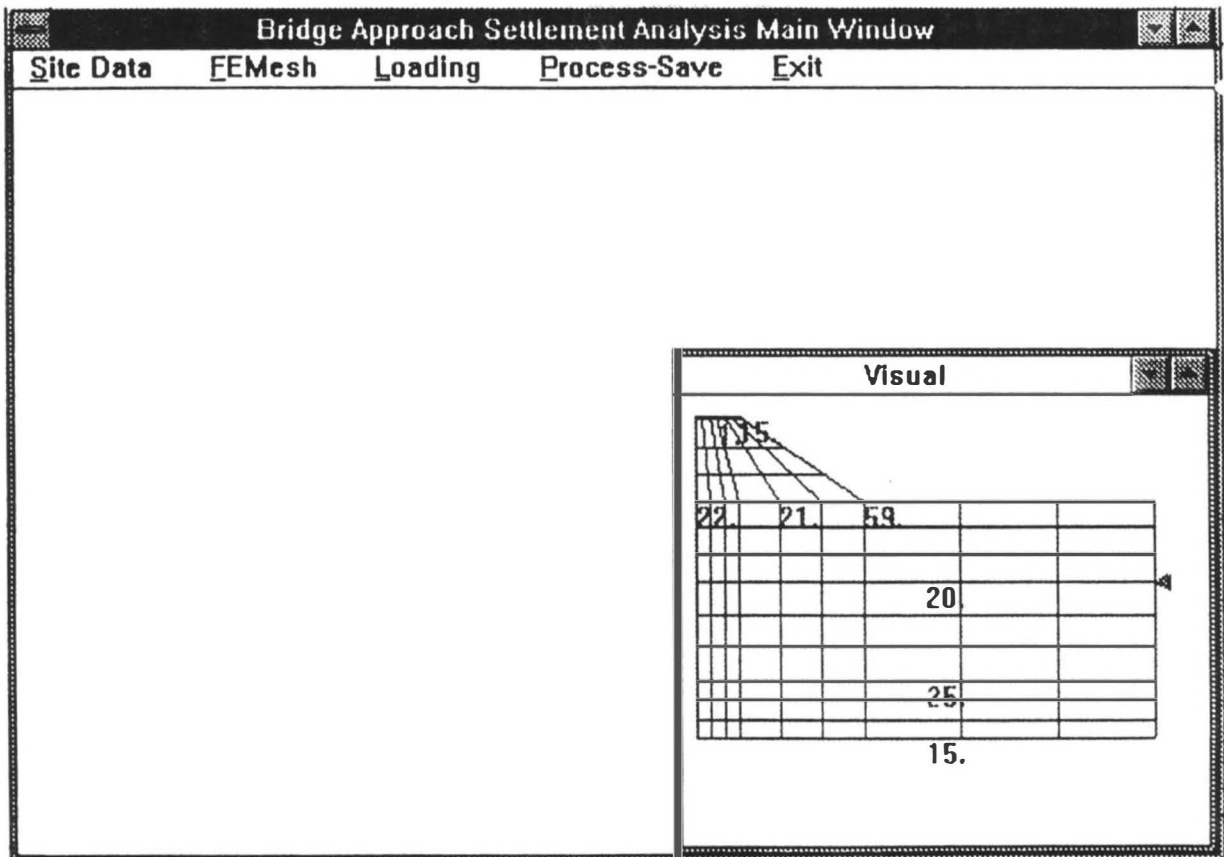


Fig. 3.22A Default Mesh at Visual Sub-window

rotated image

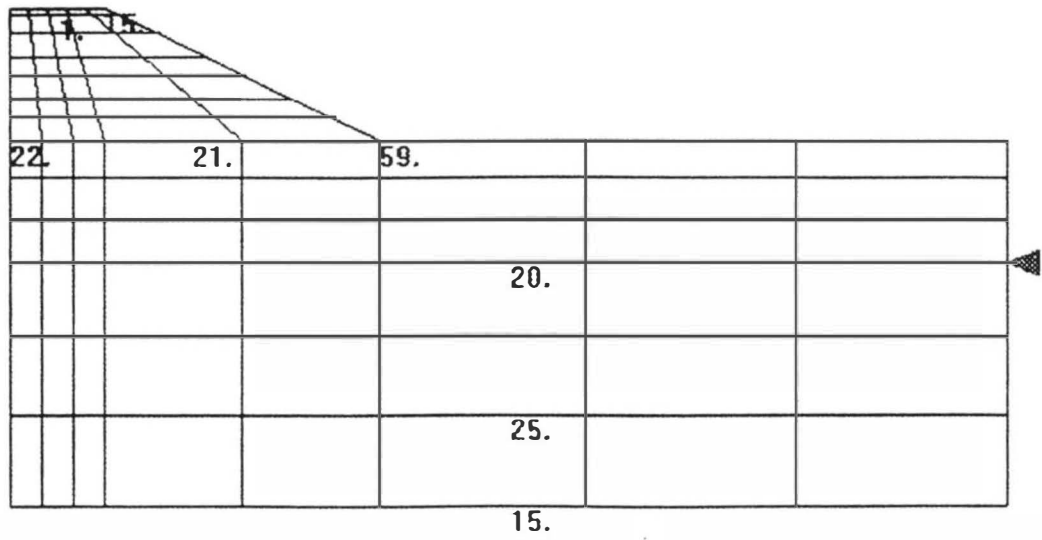


Fig. 3.22B Zoomed Custom Mesh



Define coordinate space	
Minimum:	Maximum:
Time step (days)	Time step (days)
<input type="text" value="0"/>	<input type="text" value="300"/>
Emb. Height (ft)	Emb. Height (ft)
<input type="text" value="0"/>	<input type="text" value="50"/>
<input type="button" value="OK"/>	

Fig. 3.23 Coordinate Space Window for Loading Option

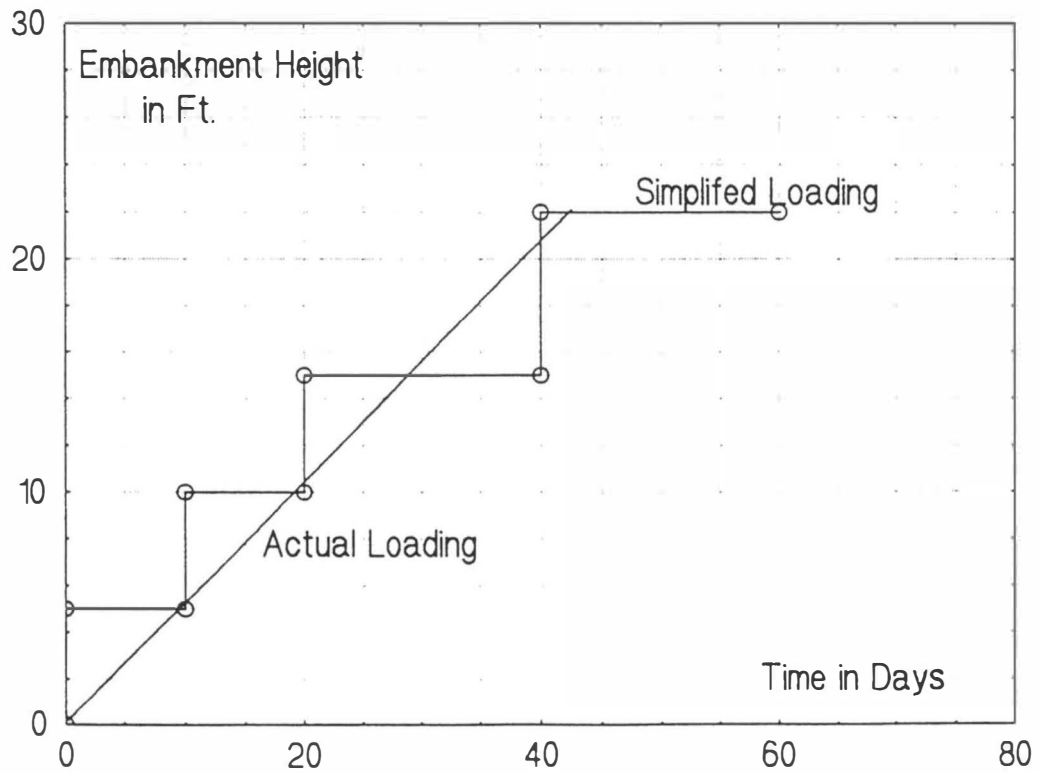


Fig. 3.24A Embankment Construction History

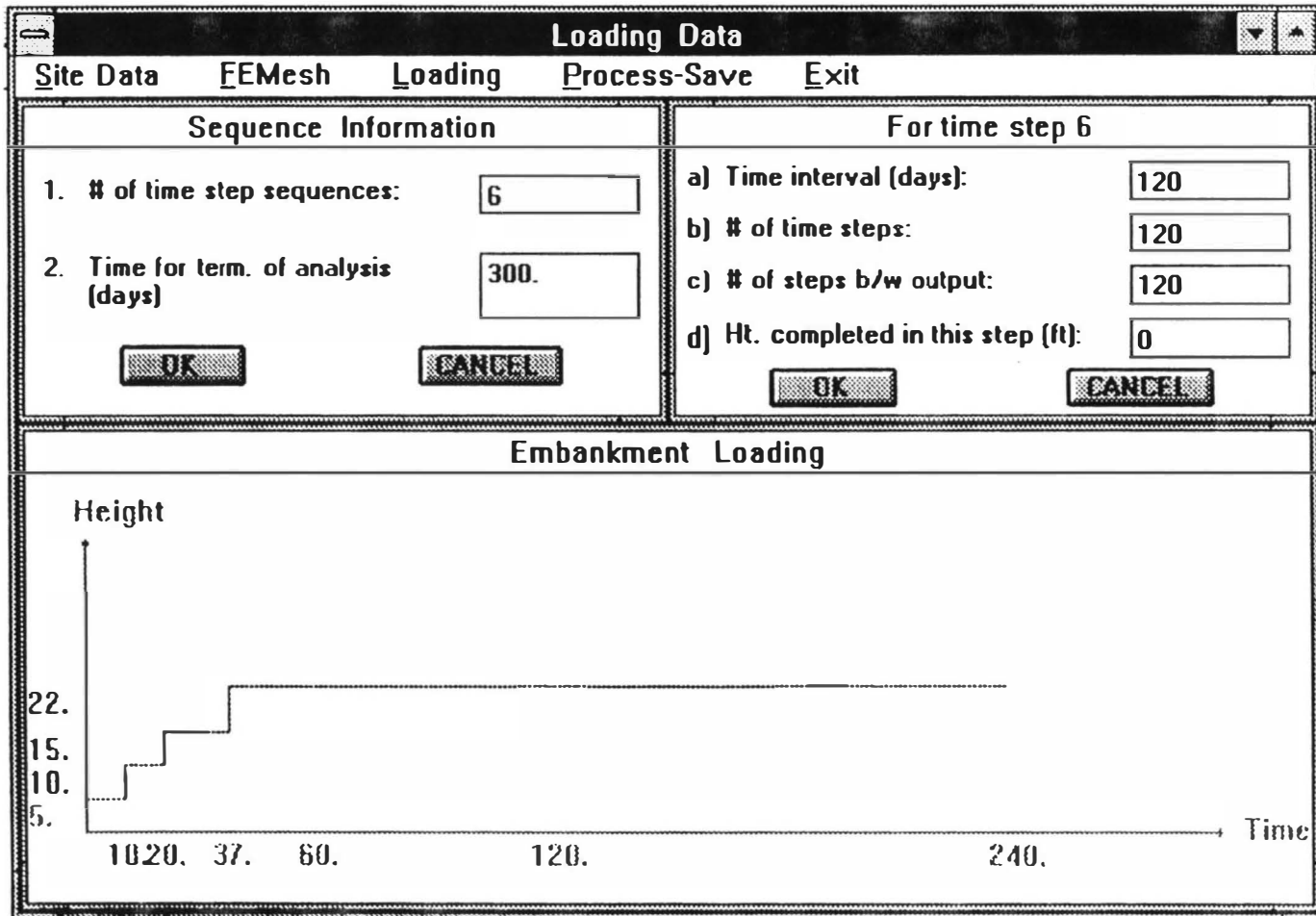


Fig. 3.24B Load Data Window

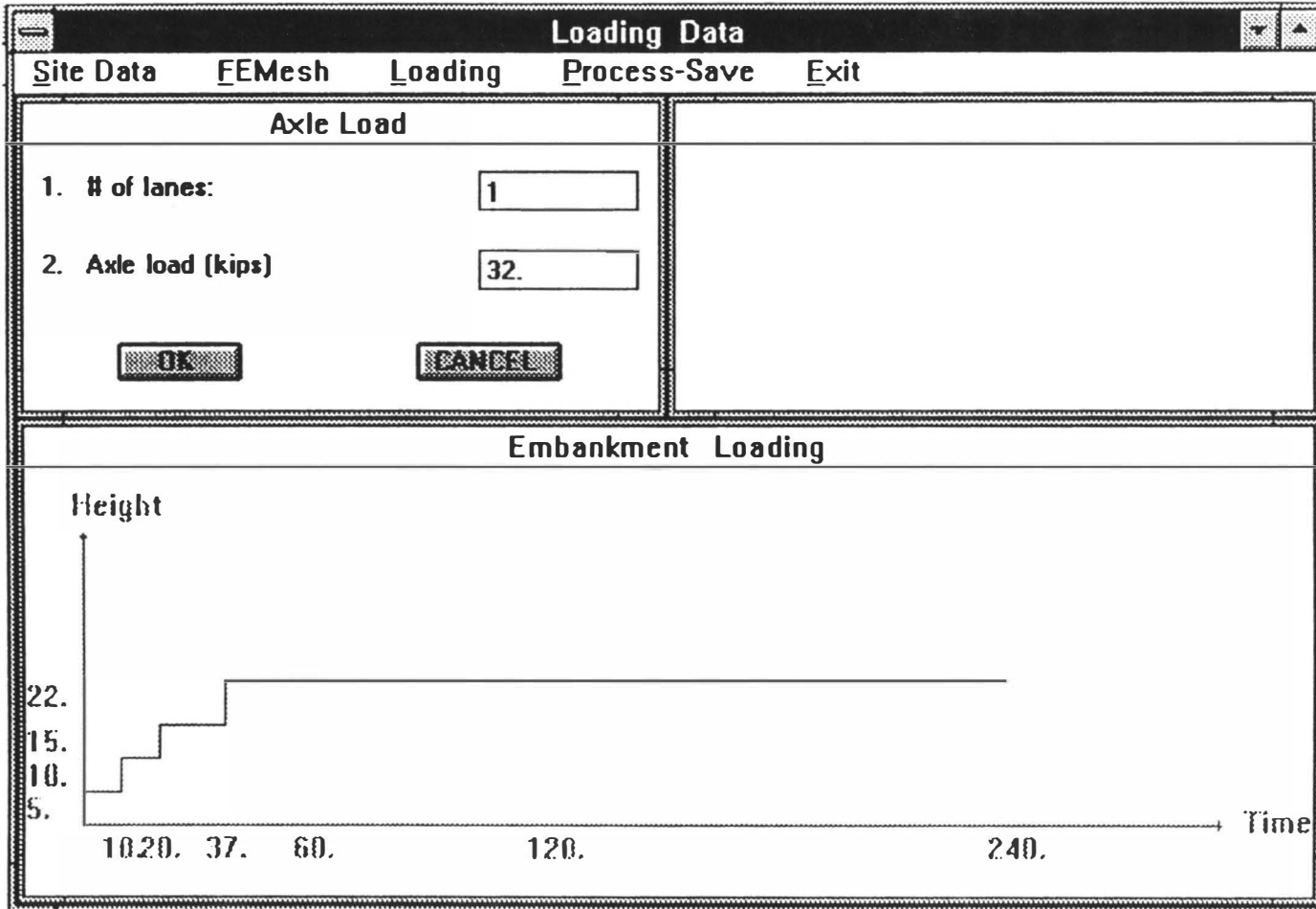


Fig. 3.25 Embankment Loading Window

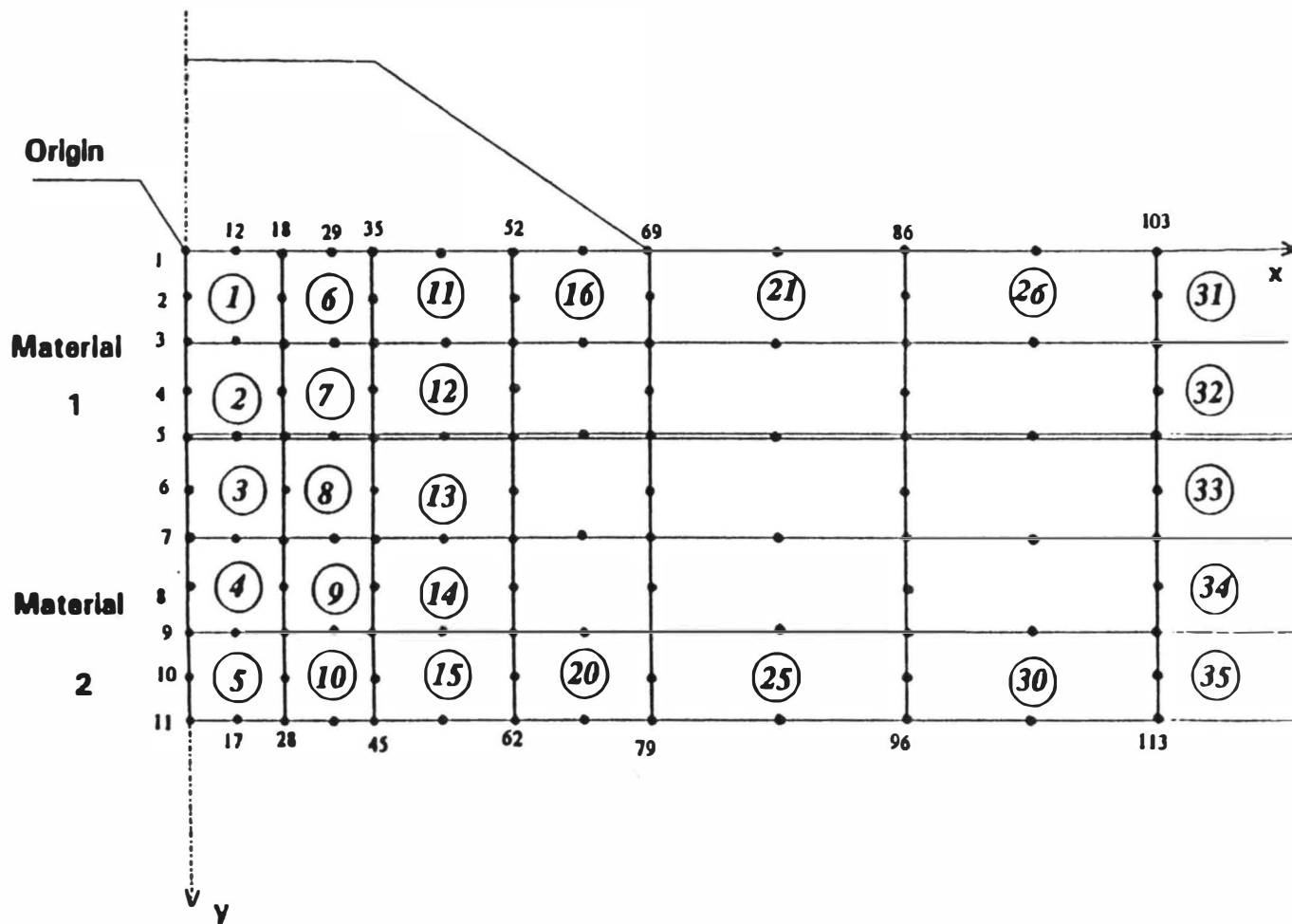


Fig. 3.26 Node Numbering and Element Numbering Adopted for a Typical Foundation Discretization

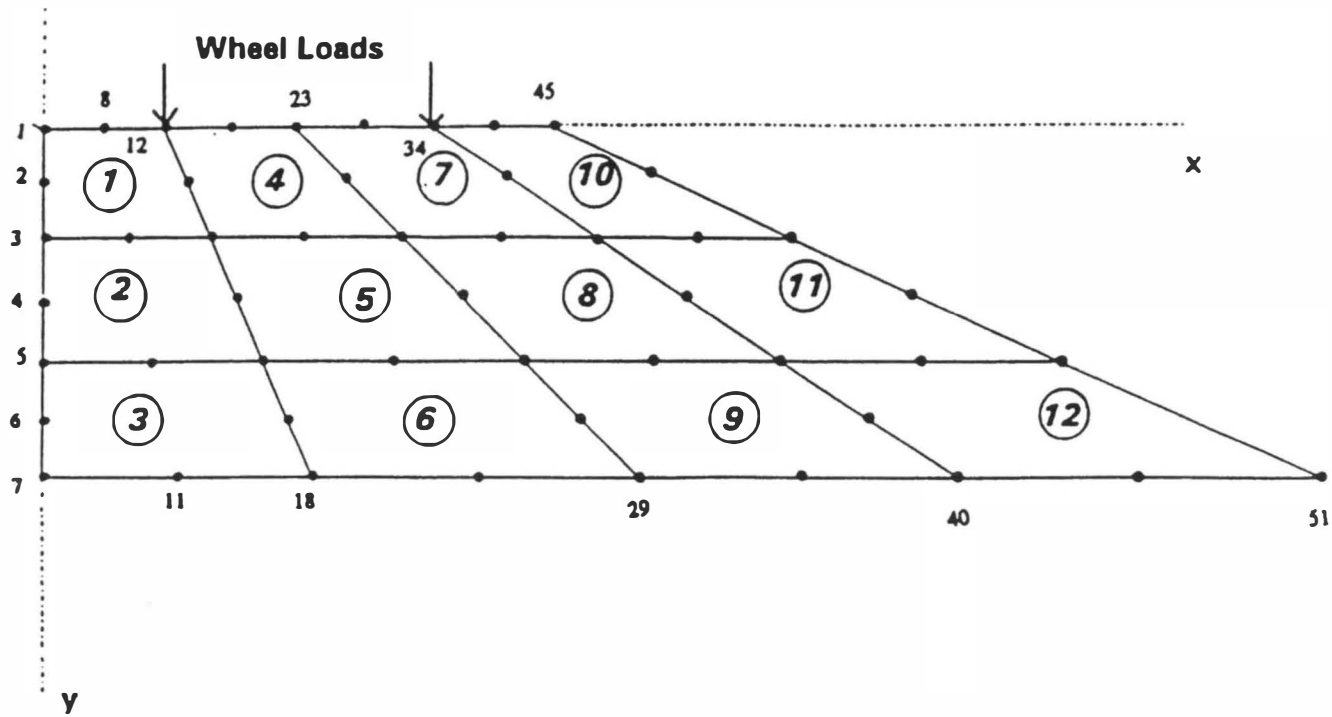


Fig. 3.27 Node Numbering and Element Numbering

Adopted for a Typical Embankment Discretization

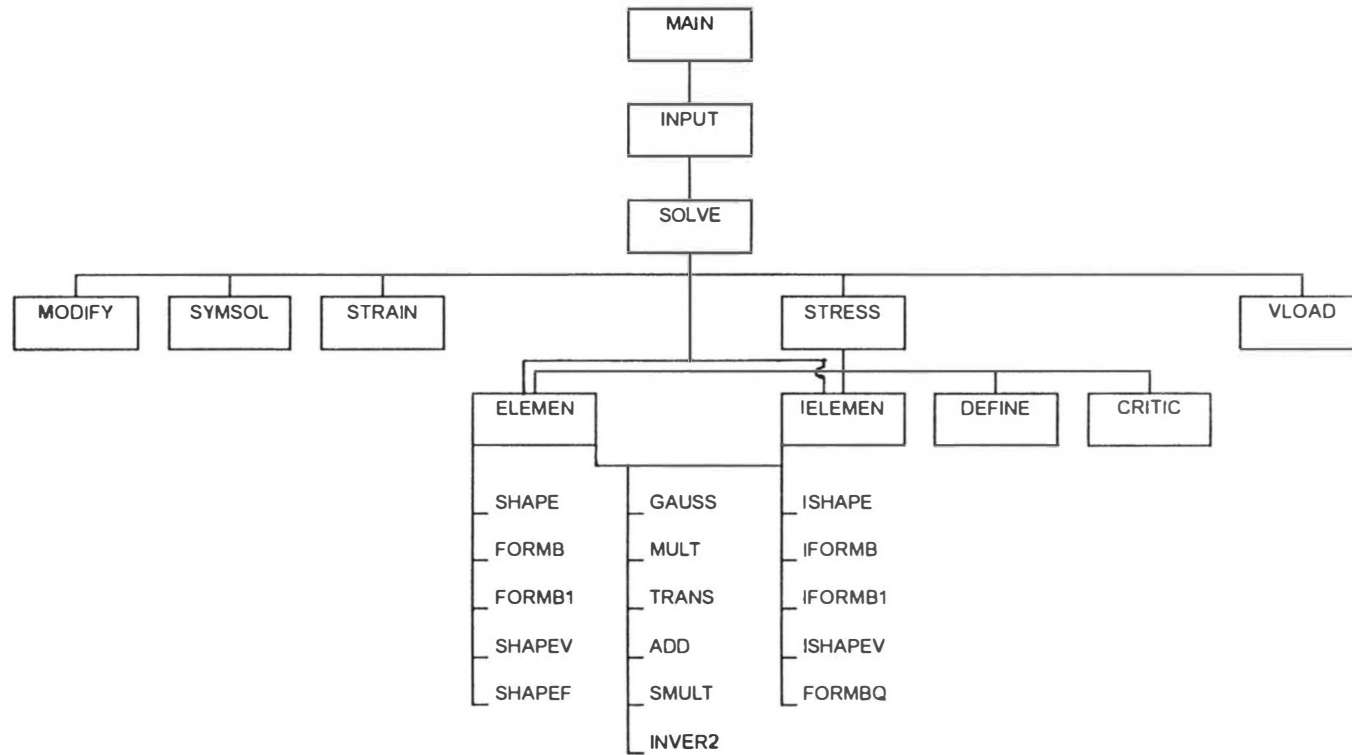


Fig. 3.28 Organization Structure of the FE Main Program

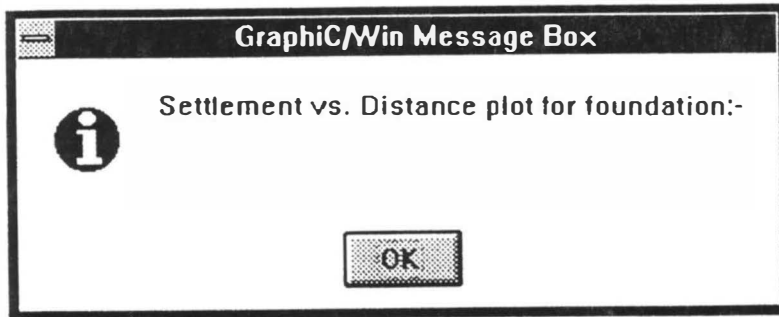


Fig. 3.29 Plot Title Window for Postprocessor

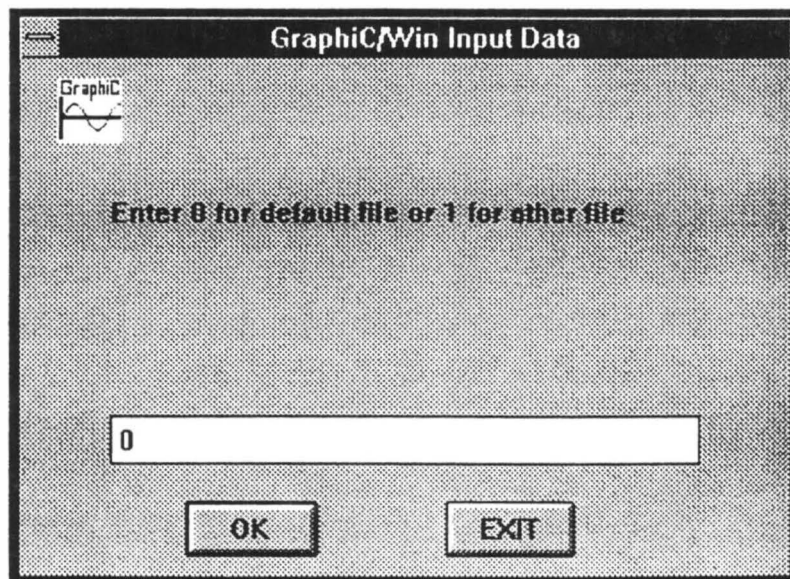


Fig. 3.30 Input Data File Window for Postprocessor

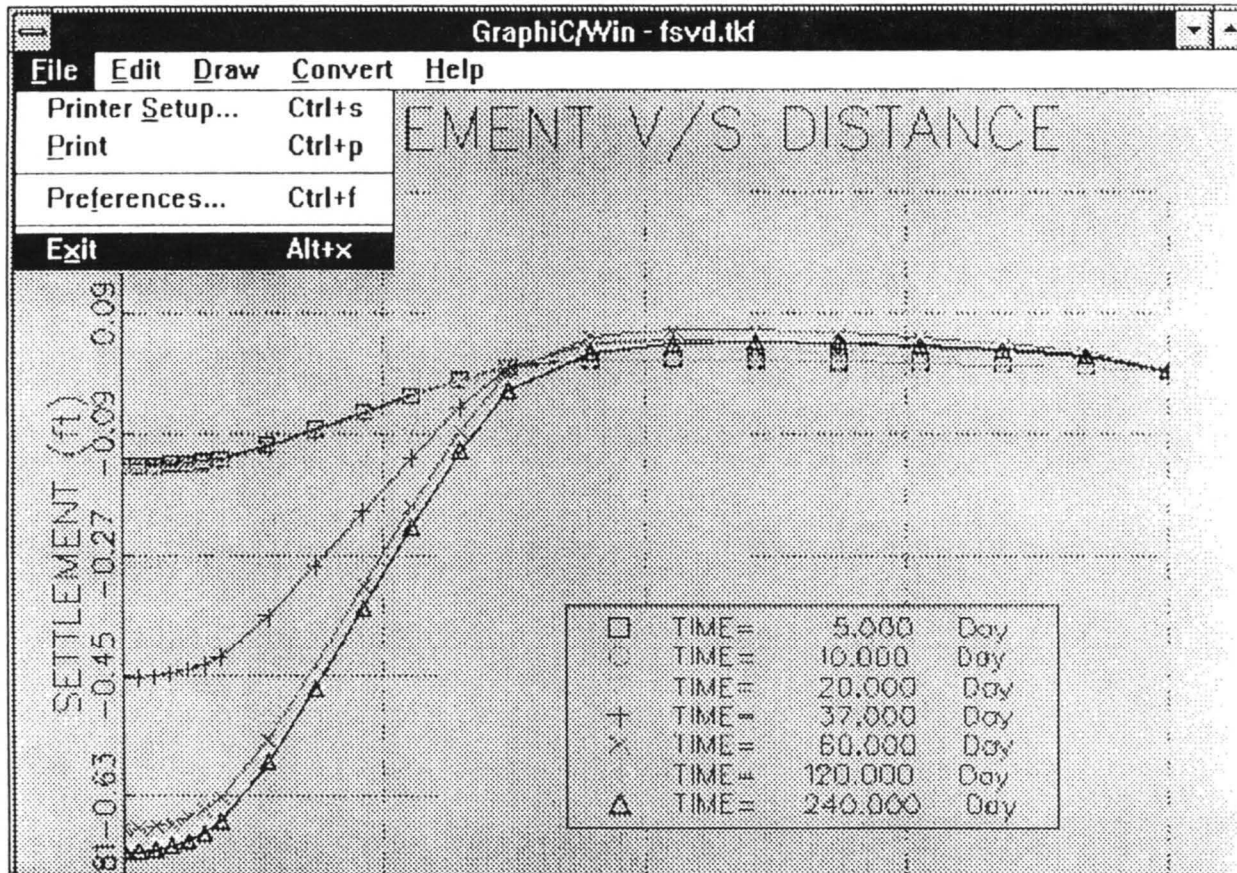


Fig. 3.31 GraphiC Window for Postprocessor



## CHAPTER 4

### APPLICATION EXAMPLES, RESULTS AND COMPARISONS

#### 4.1 Site Description

The Captain Creek Bridge (Bridge no. 41-38x1250) is located on State Highway SH 102 in Lincoln County, Oklahoma near the town of Wellston (see Fig. 4.1). The bridge is about 10 years old, 183 ft. in length, 32 ft. in width, and serves an average traffic of about 500 vehicles per day. The north bridge approach is 30 ft. in length and the south approach is 40 ft. long. Both approaches consist of flexible pavements. Maintenance at this site has been performed frequently in the past to correct the settlements within tolerable limits. The embankment consists mainly of reddish brown silty sands and silty clay soils of low to medium plasticity. The observed cumulative approach settlement is approximately 7 inches.

The foundation soils in the Captain Creek Bridge site are Port and Pulaski loams, which belong to the alluvial great soil group, and are reddish brown clayey sand and sandy clays of low to medium plasticity arranged in stratified layers. The top 5 ft. is clayey sand, followed by 20 ft. of sandy clay, below which there is a 10 ft. layer of clayey sand (Fig. 4.4 and Fig. 4.5).

Groundwater table data recorded in nearby well-points, as shown in the United States Geological Survey (USGS) map, indicates the water table at an annual average

depth of 21 ft. below ground surface. In the finite element analysis, the depth of water table is idealized as 23 ft. below the ground surface so that the top of the water table coincides with the top of one of the foundation layers.

A general description of the site is given in a concise manner in Table 4.1.

## **4.2 Soil Sampling**

Soil exploration and sampling was performed at this site in December 1989 with the assistance of Oklahoma Department of Transportation (ODOT) drilling crew. Two methods of soil exploration were employed. At first, an electric Cone Penetration Test (CPT) was performed on the foundation soil, followed by a Standard Penetration Test (SPT) in a "continuous flight auger" boring designated as BH #1. It was decided to sample continuously using a split-spoon sampler and push tubes.

A second boring designated as BH #2 was drilled through the highway pavement on the north embankment next to the approach slab. Standard Penetration Test (SPT) as well as split-spoon and pushtube sampling were conducted at this hole. The boring penetrated the embankment fully and continued to a depth of about 40 ft. below the ground surface. Locations of the boreholes and some of relevant samples are shown in Fig. 4.2 and Fig. 4.3.

As part of the field investigation, a level survey was conducted to determine the borehole location and elevations. The survey data provided an accurate measurement of the embankment height.

### **4.3 Discussion of Laboratory Test Results**

Gradation and Atterberg limit tests were performed on composite samples obtained from the split-spoon sampler and on individual samples obtained from push tubes for the purpose of soil classification. Consolidation and unconsolidated undrained triaxial tests were performed on most of the push tube samples to obtain the strength and permeability parameters of the soil samples. Harvard miniature tests were performed on the push tube samples to determine the maximum dry density and optimum moisture content.

The composite samples were created by combining samples on the soil profile that exhibited textural and visual similarities. The soil profiles obtained from the test results are shown in Fig. 4.4 and Fig. 4.5. Specifically, for BH #1 gradation analysis and Atterberg limits tests were performed on 4 composite samples and 2 push tube samples. The soils encountered were AASHTO designation A-4 clayey sands and A-6 sandy clays of low to medium plasticity ( $PI = 8-18$ ). The moisture content of the soils ranged between 17% and 28%. The SPT blowcount  $N$ , ranged between 0 and 13 indicating that the soil compactness is loose to very loose. The clay layer from 4.5 ft. to 25 ft. (depth)

had blowcounts of 0-9 suggesting that it can undergo extensive compression. The CPT tip resistance values ranged between 12-20 ton/ft<sup>2</sup> down to a depth of 47 ft. where a well consolidated soil layer of 110 ton/ft<sup>2</sup> capacity was encountered (see Fig. 4.4 and correlations by Hunt, 1986). In case of the BH #2, there were 5 pushtube samples and 6 composite samples tested. The laboratory tests indicated that the embankment consisted of a 4 ft. thick A-4 non-plastic silty sand layer, followed by a 2 ft. thick A-6 silty clay with a plasticity index of 23, followed by a non-plastic silty sand. The foundation under the embankment consisted of stratified layers of A-2-4 silty sand and A-6 silty clay of medium plasticity (PI = 10-21). Only SPT tests were conducted for borehole 7-2 in the field. The N values obtained, ranged between 4 and 24 indicating loose to medium dense compactness (see Fig. 4.5). Based on the field and the laboratory investigation the foundation was discretized as three soil layers and the embankment was discretized as one soil layer plus the pavement, as shown in Fig. 4.14.

#### **4.4 Possible Causes for Approach Slab Settlement**

The soil profiles (Fig. 4.4 and Fig. 4.5) depict the presence of a loose clayey sand layer on the embankment suggesting that possibly the embankment material was not compacted properly during construction. The low SPT blowcount and the CPT data clearly underscore the potential for compression of the layer under traffic load. In addition, the erosion of the embankment slope is indicative of possible improper construction practice. The use of A-6 soil as embankment

material (2 ft out of 8 ft) is a source of potential problem. Due to the low height of the embankment and the silty sand layers in the foundation, the potential for consolidation settlement of the silty clay layers is low. Nevertheless, the FEM-based computer program was employed to investigate the consolidation settlement potential. The results are presented in the following section.

#### **4.5 Analysis of Consolidation Settlement Using the FEM**

From the soil profile obtained, the soil medium was idealized as three layers as shown in Fig. 4.14. The soil properties presented were determined through laboratory testing and/or were estimated from SPT and CPT field data using empirical correlations (Hunt, 1986).

The idealized model of the foundation soil was discretized into a number of elements as shown in Fig. 4.15 and Fig. 4.16. Due to the symmetric geometry and applied loads, only one-half of the embankment was analyzed. The extended soil medium was modeled using infinite elements that extended 110 ft. from the roadway centerline. This distance equals approximately 2.5 times the base width of the embankment. Extending the element mesh to 2.5 times the base width is considered adequate for analysis. Previous studies, performed with different mesh types, have indicated that satisfactory results may be obtained with a minimum of 2:1 ratio of mesh width over base width (Zaman et al., 1991).

The embankment construction history was approximated in a manner, depicted in Fig. 4.17. The soil profile was based on the field and the laboratory test data. The properties of soil

used for the embankment analysis are shown in Table 4.5. Soil properties are obtained from a number of laboratory tests. The specific values of various soil properties used in this analysis are given in Tables 4.2-4.4. Some of the important laboratory test results are also shown in Fig. 4.6 through Fig. 4.13. Traffic loading is as shown in Fig. 4.18.

## **4.6 Interpretation of the FEM Results**

The results from the FE main program provide a lot of information. It is laborious to interpret these results. In order to avoid this difficulty the post-processor was developed. Information regarding settlement, excess pore pressure, and the maximum stress are stored in separate output files in the FE main program. The post-processor uses these files for plotting the results.

### ***4.6.1 Foundation Analysis***

#### ***a. Settlement versus Horizontal Distance***

Fig. 4.19 shows the settlement versus distance plot for the Captain Creek bridge site. The horizontal distance from the center line of the foundation is plotted along the X-axis and the settlement is plotted along the Y-axis. This plot helps in studying the consolidation settlement history with age.

For the problem selected, it was observed that the foundation settlement occurs within 44 ft. from the centerline, with the maximum settlement (0.23 ft. or 2.76 in.) occurring under the

centerline of the embankment. The observed settlement of the approach is 7 in. Therefore, the computed settlement is about 40% of the field settlement. The following points explain this difference in results.

- a) The soil properties used in this analysis are based on the laboratory tests performed on soil samples collected from already consolidated site, not the original site. In fact, the soil properties obtained from the original site before the construction of the embankment requires to be input in the FE program. The soil which has already consolidated is likely to settle less with the application of same amount of embankment load in comparison with the original soil at the site. This is why, the computed settlement is less than the reported field settlement.
- b) The field settlement value was not recorded by using any systematic and instrumented facility - it was merely estimated by an approximate manner based on overlays added to the pavement from time to time, etc. The real settlement of the site may be less than the value reported (7 inches).

***b. Depth versus Excess Pore Pressure***

Excess pore pressure distribution with respect to time, in days, for the Captain Creek Bridge Site is shown in Fig. 4.20. The analysis indicates that the maximum pore pressure was generated near the impervious boundary as expected. During the first twenty days the amount of excess pore water pressure dissipated was less than the newly developed excess pore water pressure due to the additional height of the embankment

completed at the particular stage. As such, the excess pore water pressure is found to be increasing at this stage. After this period, no more embankment load was added on the foundation, and hence, the excess pore water pressure started dissipating. Most of the excess pore water pressure dissipation took place during the first 150 days. The plot indicates that the excess pore pressure for the sandy soil layer is zero which is obvious because the layers are above the water table.

### *c. Maximum Normal Stress Contours*

Fig. 4.21 shows the normal stress contours. A close examination of the contours shows that the stresses are maximum at the center line of the cross section and gradually reduce with distance away from the center line. The contours show the stresses in the cross section at the end of 250 days. The data file contains information on stresses at the end of different time steps. In order to plot these contours at different time steps, the user needs to edit the output file containing information about this.

## **4.6.2 Embankment Analysis**

### *a. Surface Settlement versus Distance*

Fig. 4.22 shows the variation of settlement along the surface of the embankment. Horizontal distance is plotted along the X-axis and the corresponding settlements are plotted along the Y-axis. In this example, the embankment is analyzed due to the effects of the wheel loads only (Fig. 4.18) with the wheels placed at a distance of 2 ft and 8 ft



from the center line. The self-weight of the embankment materials is not considered in this example for simplicity. The maximum settlement is found to occur at the center line of the roadway and it gradually decreases at a distance away from the center line.

#### ***b. Settlement versus Depth***

Fig. 4.23 shows the variation of settlement along the depth of the cross-section for the Captain Creek bridge site. The pavement is extremely stiff compared to the embankment soil. As such, the pavement shows almost a rigid body movement of 0.125 ft. The bottom of the embankment was assumed to be fixed. Therefore, the settlement observed at the bottom of the embankment was zero.

#### ***c. Maximum Normal Stress Plot***

Maximum normal stress contours along with the embankment cross section of the Captain Creek Bridge Site is shown in Fig. 4.24. This plot gives the condition of normal stresses within the embankment. The study of stress contours helps in the design of embankment in terms of selection of embankment material, degree of compaction required, and side slope of the embankment.

### **4.8 Verification of the Results**

For validation of a numerical algorithm, such as the software package developed in this study, it is important to verify the accuracy of the results by comparing them with results obtained from other sources. The previous studies (Gopalasingam, 1989, Zaman et al, 1990) conducted using the similar finite element (FE) algorithm, indicated that the results (for some simplified cases where closed form solutions are available) obtained for

the degree of consolidation and the excess pore pressure at different times show a good agreement between the FE results and Terzaghi's closed form solutions. Further more the stresses in the embankment cross-section, predicted by the software were compared by Vavarapis (1991) with the results from a commercial software, SAP90 developed at the University of California, Berkeley. Good agreement was observed both in terms of the magnitude of stresses as well as their distribution across the cross-section. Also, the embankment settlements obtained from the software were compared by Vavarapis (1991) with those obtained from NON-SAP, and the variation was found to be less than 10% in most locations.

In addition, the finite element results have been compared with the results obtained by analyzing the problem using Terzaghi's classical theory of one-dimensional consolidation. The idealized site condition for this analysis is shown in Fig. 4.25. Here,

$q'$  = Average effective pressure at the mid-point of the clay layer before the construction of the embankment

$$= 12 (130) + 11 (132) + (22/2) (135 - 62.4) \text{ psf}$$

$$= 3811 \text{ psf}$$

$Q$  = maximum intensity of the embankment load

$$= 10 (141.5) \text{ psf}$$

$$= 1415 \text{ psf}$$

$$\frac{1}{2}q' = (Q/\pi) [(a+b)(\alpha_1 + \alpha_2)/a - b\alpha_2/a]$$

$$= (1415/3.14) [(20+16)/20 * \tan^{-1}(36/34) - 16/20 * \tan^{-1}(16/34)] \text{ psf}$$

$$= 1415 (0.354) \text{ psf}$$

$\Delta q$  = increase in effective pressure at the mid-point of the clay layer after the construction of the embankment

$$= 1415 (0.7087) \text{ psf}$$

$$= 1003 \text{ psf}$$

$\Delta H_t$  = overall consolidation settlement of the clay layer

$$= C_c / (1 + e_0) * H_t * \log [(q' + \Delta q) / q']$$

$$= 0.1 / (1 + 1.045) * (22) * \log [(3811 + 1003) / 3811]$$

$$= 0.109 \text{ ft.}$$

Also, the software package developed in this study was used to analyze the same problem with one-dimensional idealization. To achieve this objective, the lateral (horizontal) displacement was restrained to simulate the one-dimensional consolidation situation (see Fig. 4.26) and the input data files were changed accordingly. The results obtained from all these analyses are compared in Fig. 4.25 and Fig. 4.26. It is found that all the results match very well. It is also found that the two dimensional finite element analysis produces a higher settlement value than the one-dimensional FEM analysis. This is due to the lateral movement of soil in the former analysis. It is also found that Terzaghi's solution produces much higher settlement in comparison with the 2-D FEM analysis.

**Table 4.1: General site description**

Description		Comments
Location	Captain Creek, Lincoln County	
Highway	SH 102	
Bridge	41-38x1250	
Year of construction of bridge	1985	
Length of bridge (ft)	183	
Width of bridge (ft)	32	
Traffic volume over the bridge (vehicles per day)	450	
Thickness of pavement (ft)	1	
Height of embankment excluding pavement (ft)	9	
Top width of embankment (ft)	32	Embankment is assumed to be symmetric
Bottom width of embankment (ft)	72	
Annual average depth of water table below the ground level (GL) (ft)	21  23	(see note-2 below)  idealized for this analysis

**Note-1:** The information contained in the table above are compiled after Zaman, et al. (1993).

**Note-2:** The depth of water table is 21 ft according to the USGS report. But in this analysis the water table must coincide with the top of one of the foundation layers. To satisfy this criterion, the depth of water table is taken to be 23 ft. Alternatively, one could assume one more layer of saturated silty sand extending from 21 ft to 23 ft.

**Table 4.2: Soil layers**

Sample no.	Depth below ground level, ft	Soil type
A to C	0 to 4.5	SC
1E	6 to 7.5	CL
1D to 1I	4.5 to 14	CL
2G to 2J	0.5 to 6.5	CL
2K to 2M	6.5 to 11.5	CL-ML
<b>Layer 1</b>	<b>0 to 12</b>	<b>"Clay"</b>
1J to 1P	14.5 to 25	CL
2N	11.5 to 13.5	SM
2T	21 to 23	SM
<b>Layer 2</b>	<b>12 to 23</b>	<b>"Silt"</b>
1Q to 1U	25 to 34.5	CL
1U	32 to 34.5	SC
2U to 2AA	23 to 33.5	CL
2BB	33.5 to 35.5	CL
2CC to 2EE	35.5 to 40	CL
<b>Layer 3</b>	<b>23 to 45</b>	<b>"Clay"</b>

**Note:** The information contained in the table above are compiled after Zaman, et al. (1993).

**Table 4.3: Strength Parameters from Triaxial Compression Tests**

Sample no.	Depth (ft)	Cohesion, c; psi (psf)	Angle of Internal Friction, $\phi$ (deg)	Young's Modulus, E; psi ( $10^6$ psf)	Slope of Critical State Line, M
2K	17.5	3.5 (504)	15.8	10500 (1.512)	0.286
2T	22	4.3 (620)	12.1	8300 (1.195)	0.444
2BB	34	7.0 (1008)	5.9	8000 (1.152)	0.1
1U	33.25	13.25 (1908)	12.7	16700 (2.405)	0.303

**Note:** The information contained in the table above are compiled after Zaman, et al (1994).

**Table 4.4 Consolidation test results**

Properties	Sample 1U	Sample 2K	Sample 2T	Sample 2BB
1. Depth of sample (ft)	33.25	7.5	22.0	34.5
2. Effective overburden pressure, $P'_0$ , (tsf)	1.89	1.136	2.09	2.58
3. Initial void ratio, $e_0$			0.49	1.045
4. Coefficient of consolidation, $C_v$ (ft <sup>2</sup> /day)	0.179	0.231	0.481	0.165
5. Compression index, $C_c$	0.1	0.074	0.026	0.115
6. Swelling index, $C_s$	0.024	0.017	0.004	0.025
7. Preconsolidation pressure, $P_c$ (tsf)	0.97	1.6	1.7	1.1
8. Overconsolidation ratio, OCR	0.52	1.41	0.81	0.43
9. Coefficient of permeability, $k$ (ft/day)				$0.5 \times 10^{-5}$
10. Comments	Below WT	Above WT	Above WT	Below WT

**Note:** The information contained in the table above are compiled after Zaman, et al (1994).

**Table 4.5: Input soil properties for the example problem**

Properties	Embkt. Layer 1	Embkt. Layer 2	Fdn. Layer 1	Fdn. Layer 2	Fdn. Layer 3
1. Unit Weight, $\gamma$ (pcf)	<b>141.5</b>	<b>141.5</b>	<b>130</b>	<b>132</b>	<b>135</b>
2. Young's Modulus, E (ksf)	<b>40,000</b>	<b>200</b>	<b>239</b>	<b>250</b>	<b>173</b>
3. Angle of Internal Friction, $\phi$ ( $^\circ$ )	30	9.5	<b>15.8</b>	<b>12.1</b>	<b>9.3</b>
4. Cohesion, c (psf)	0	432	504	619	1440
5. Poisson's Ratio, $\nu$	<b>0.3</b>	<b>0.3</b>	<b>0.4</b>	<b>0.3</b>	<b>0.4</b>
6. Coefficient of Permeability, k (ft/day)	0.001	0.001	$1.05 \times 10^{-4}$	$1.0 \times 10^{-4}$	$5 \times 10^{-6}$
7. Critical State Line Slope, M	NA	.169	0.286	NA	<b>0.1</b>
8. Compression Index, $C_c$	NA	0.082	0.78	NA	<b>0.1</b>
9. Swelling Index, $C_s$	NA	0.021	0.015	NA	<b>0.042</b>
10. Initial Void Ratio, $e_0$	NA	0.88	0.731	NA	<b>1.045</b>

**Note:** Only the values typed in bold in the above table have actually been used by the finite element program. However, the values presented in the above constitute the complete input data for the problem.



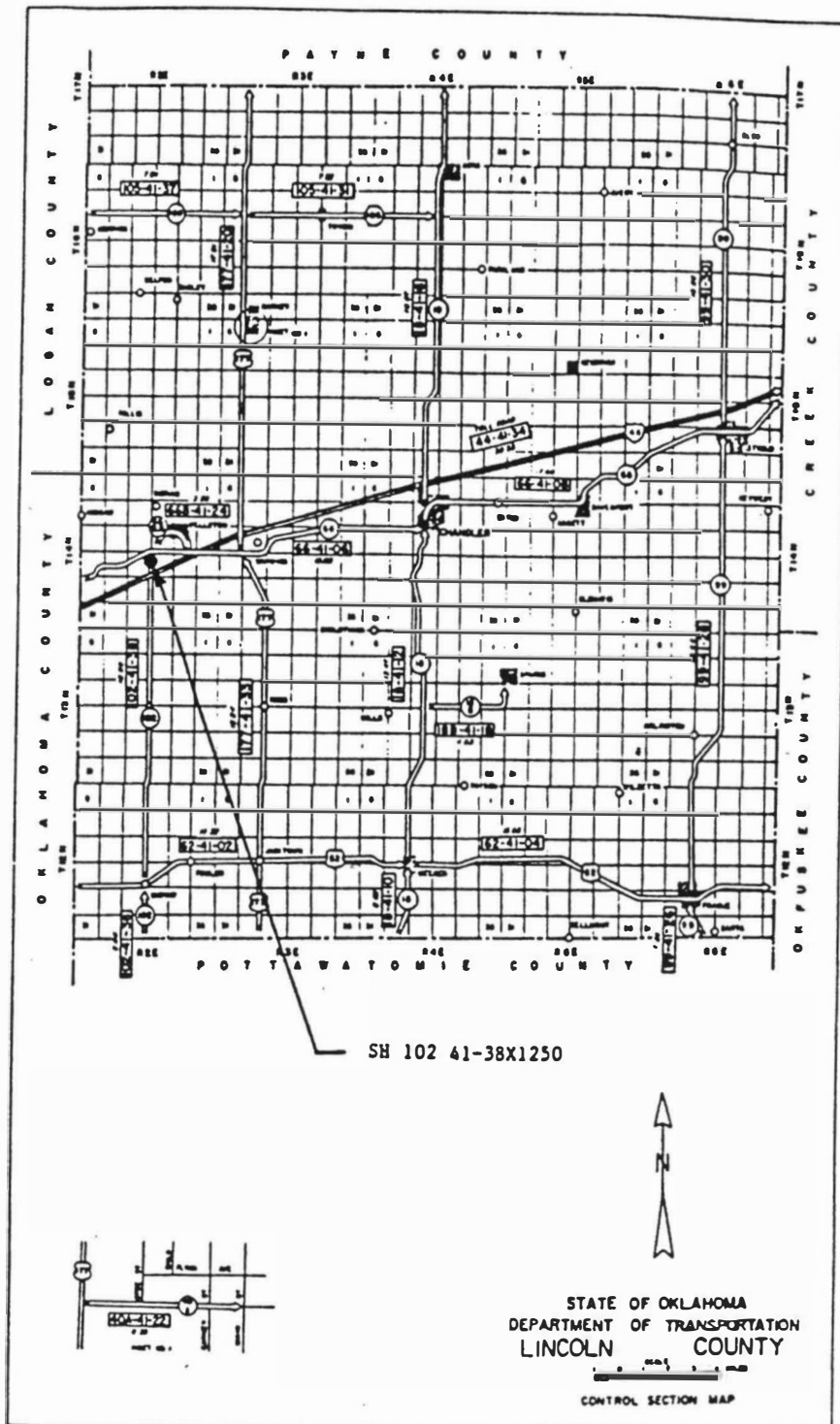


Fig. 4.1 Location of Captain Creek Bridge Site

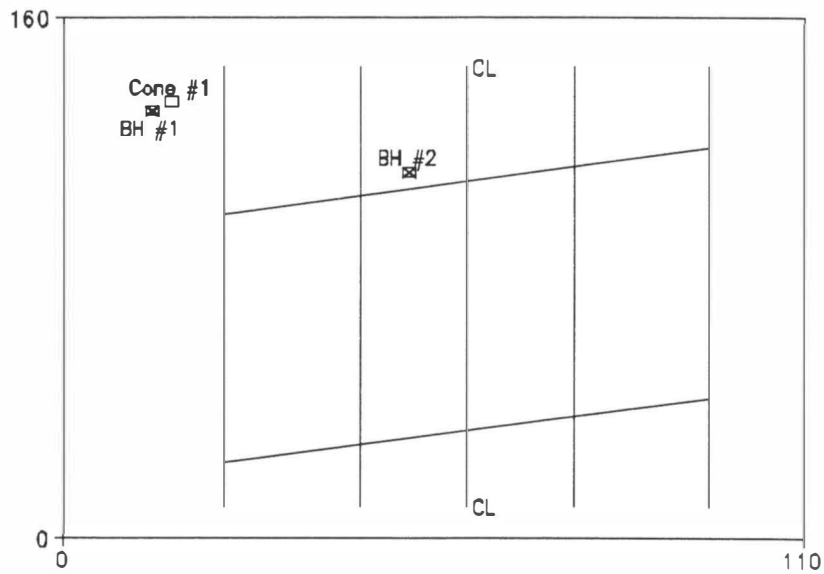


Fig. 4.2 Bore Hole Locations

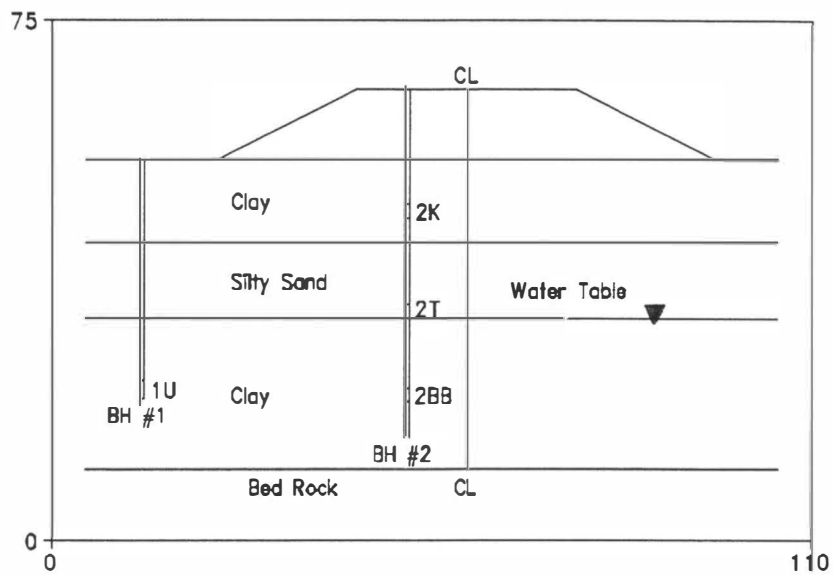


Fig. 4.3 Elevation Showing Bore Holes and Selected Samples

SITE : #7  
 DIVISION : 4                      COUNTY : LINCOLN  
 BRIDGE NO : SH 102, 41-38x1250  
 BOREHOLE HOLE : #1

DEPTH (ft)	SOIL PROFILE	SOIL CLASSIFICATION				WATER CONTENT %	ATTERBERG LIMITS		STANDARD PEN. TEST, N	CORE PENET. TEST			FIELD / MAX DENSITY (pcf)	U <sub>c</sub> Test	Cohesion C <sub>v</sub> (pcf)	Friction Angle φ
		SAND %	SILT %	CLAY %	ORGANIC		LL	PI		TIP RESIST. (tons/ft <sup>2</sup> )	LOCAL FN (ton/ft <sup>2</sup> )	FRICT. RATIO %				
						20.3			9							
		60	23	17	SC	19.4			7		20.3	0.28	1.4			
						20.0			1							
						24.9	22	8	7							
						26.7			0							
		29	51	20	CL		29	18			16.8	0.48	2.8			
						17.1			9							
		33	43	24	CL	19.1	28	14	11							
						24.4			3							
						27.7			0							
						26.9			0							
						20.8			5							
						19.3			8							
						18.3			9		12.3	0.29	2.3			
		22	55	23	CL	21.0	27	14	2							
						23.7			2							
						24.7			0							
						22.9			1							
		48	34	18	SC	23.0	20	9	1							
						21.7			7							
		18	52	30	CL	25.9	27	16	13							
													130.9			
											17.1	0.73	4.3			
											LAYER THICKNESS TO 43.5 FT					

Fig. 4.4 Soil Profile for Borehole #1 at Captain Creek Bridge Site

SITE : 07  
 DIVISION : 4 COUNTY : LINCOLN  
 BRIDGE NO : SH 102, 41-38x1250  
 BOREHOLE NO : #2 (ON THE EMBANKMENT)

PAGE 1 OF 2

DEPTH (ft)	SOIL PROFILE	SOIL CLASSIFICATION				WATER CONTENT %	ATTERBERG LIMITS		STANDARD PER. TEST, D	CORE PERT. TEST			FIELD MOE DENSITY, (pcf)	P <sub>v</sub> Test	Cohesion C, (pcf)	Friction Angle
		SAND %	SILT %	CLAY %	UNIFIED		LL	PI		TIP RESIST. (tonf/ft <sup>2</sup> )	LOCAL FR. (tonf/ft <sup>2</sup> )	FRIC. RATIO %				
	Asph. Pav.					11.2			16							
		56	29	15	SH	17.4			5							
5		7	63	30	CL	18.3	38	23		N/A		141.5		3.0	9.5	
						13.6			18							
		73	16	11	SH	14.9			24							
10						17.7			19							
						15.1			12							
						14.1			4							
15		29	47	24	CL	18.2	23	10	13							
		16	56	28	CL	18.0	33	21				130		3.5	15.8	
						16.1			8	N/A						
20		29	52	19	ML CL	19.3	20	6	12							
						21.5						132.2				
25						23.8			4							
						21.1			3							
						20.1			8							
						19.2			10							
30						18.9			17							
		45	37	18	SH	18.6	21	4		N/A		131.9		4.3	12.1	
						16.9			17							
35						22.0			18							
						18.6			11							
						17.2			14							
		29	44	27	CL	20.3	28	16	16							

Fig. 4.5 Soil Profile for Borehole #2 at Captain Creek Bridge Site

SITE : 07  
 DIVISION : 4 COUNTY : LINCOLN  
 BRIDGE NO : SH 102, 41-38x1250  
 BORING HOLE : #2 (ON THE EMBANKMENT)

PAGE 2 OF 2

DEPTH (ft)	SOIL PROFILE	SOIL CLASSIFICATION				WATER CONTENT %	ATTERBERG LIMITS		STANDARD PEN. TEST, N	COKE PENETR. TEST			FIELD / MAX DENSITY, (pcf)	$\phi_c$ , %	Cohesion C, (pcf)	Friction Angle $\phi$
		SAND %	SILT %	CLAY %	UNITED		LL	PI		TIP RESIST. (tonf/ft <sup>2</sup> )	LOCAL FR. (tonf/ft <sup>2</sup> )	FRICT. RATIO %				
	45 50					20.6			21							
						23.0			20							
		13	49	38	CL	22.4	30	17		N/A		134.5		7.0	5.9	
						21.0			18							
		15	45	40	CL	25.3	35	18	21							
					24.3			15								

Fig. 4.5: (Continued)

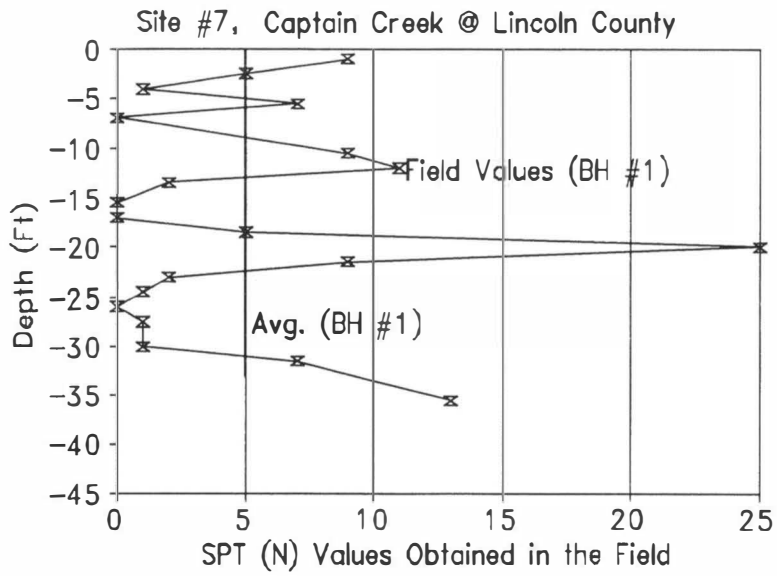


Fig. 4.6 SPT Values Obtained in the Field in Bore Hole 1

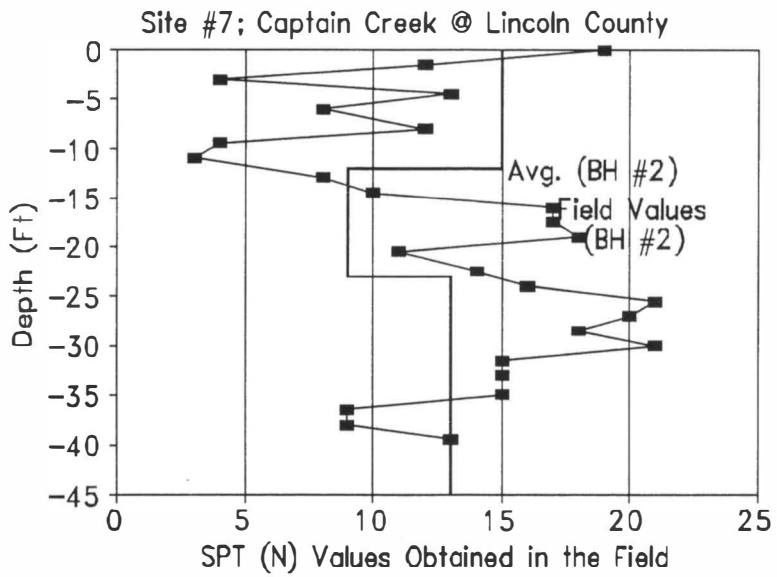


Fig. 4.7 SPT Values Obtained in the Field in Bore Hole 2

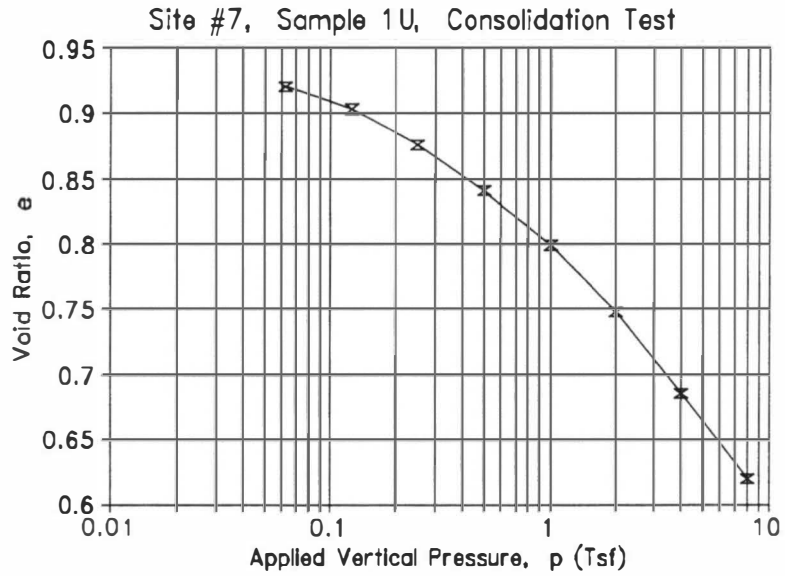


Fig. 4.8  $e$  vs  $\log(p)$  Curve for Sample 1U

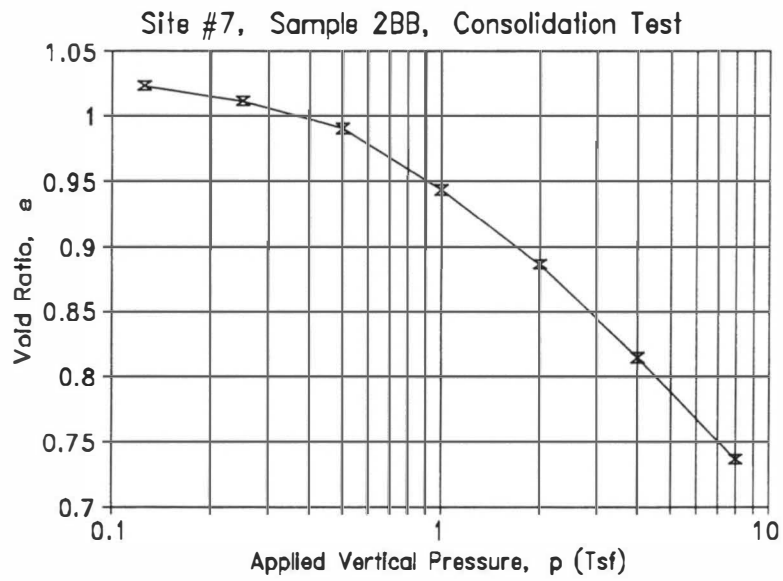


Fig. 4.9  $e$  vs  $\log(p)$  Curve for Sample 2BB

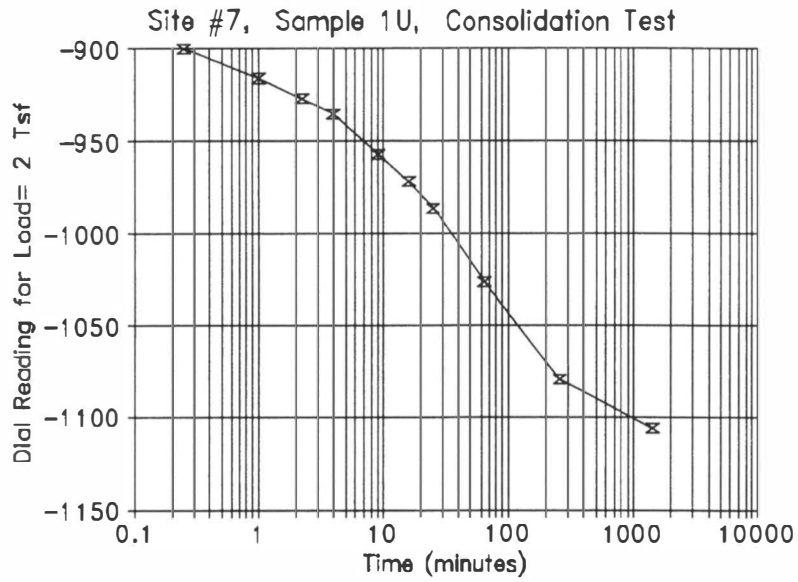


Fig. 4.10 Determination of  $C_v$  for Sample 1U

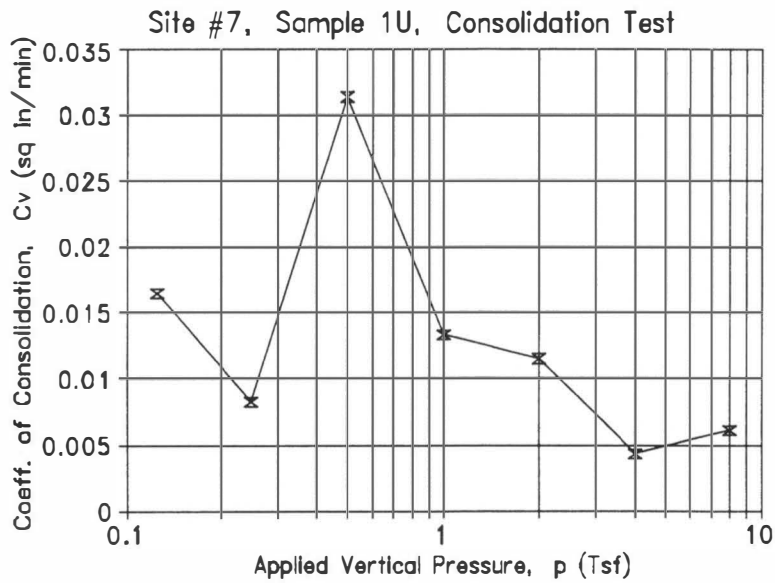


Fig. 4.11 Variation of  $C_v$  with Applied Pressure for Sample 1U



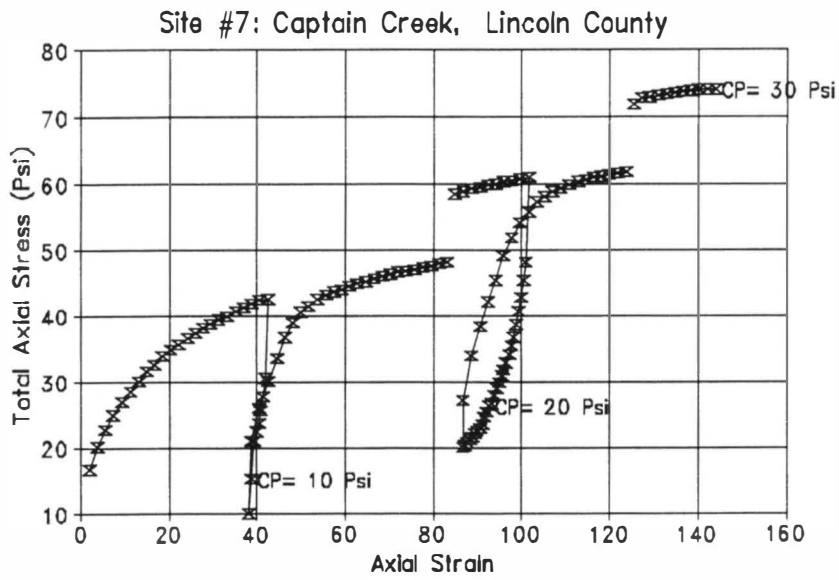


Fig. 4.12 Stress-strain Variation from Triaxial Compression Test of Sample 1U

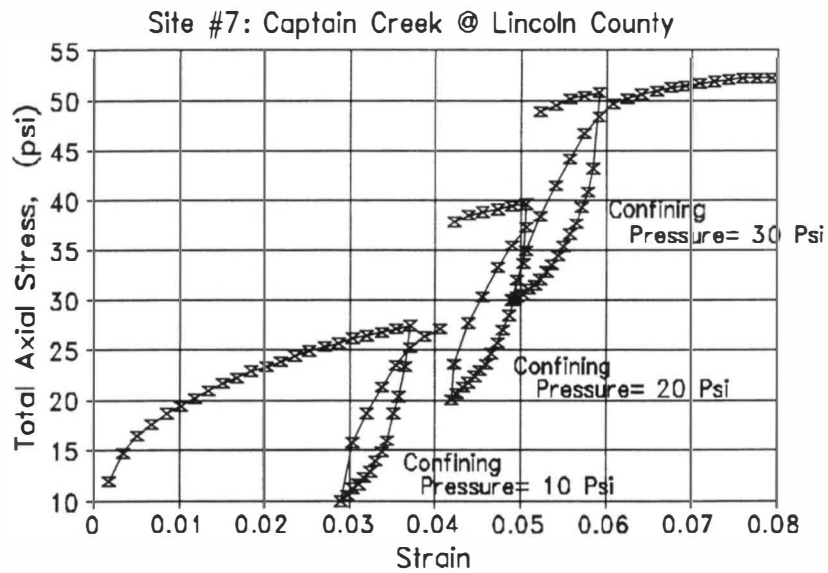


Fig. 4.13 Stress-strain Variation from Triaxial Test of Sample 2BB

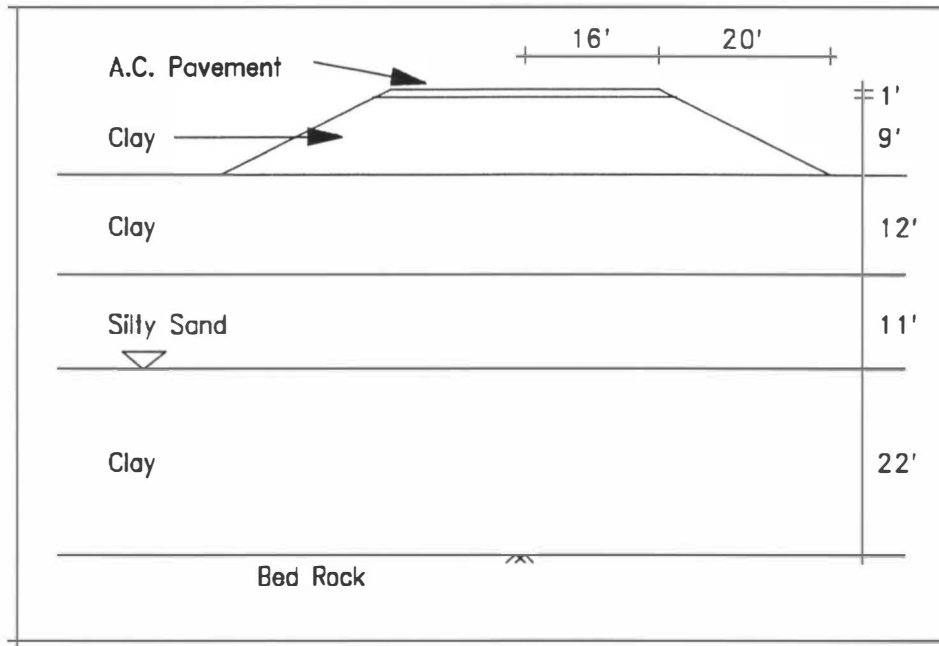


Fig. 4.14 Idealized Geometry of the Example Problem (Captain Creek Site)

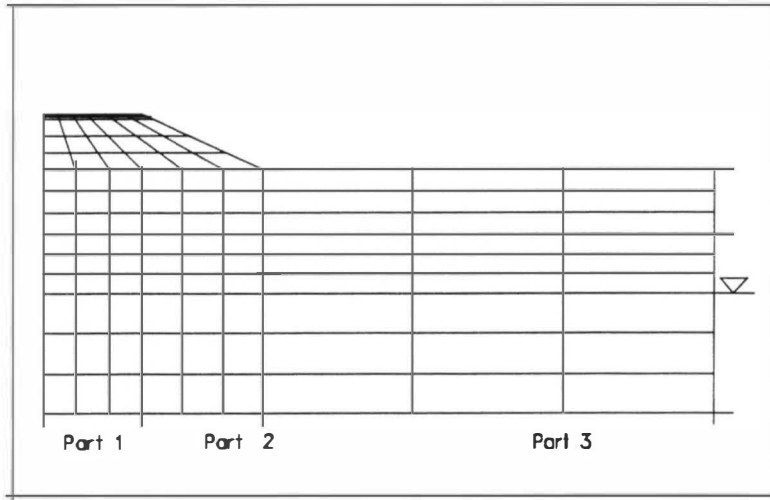


Fig. 4.15 Default Mesh for the Example Problem

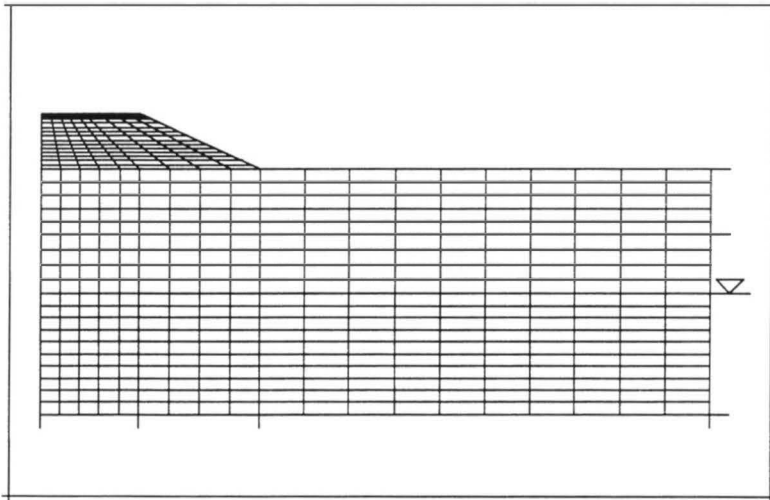


Fig. 4.16 Custom Mesh for the Example Problem

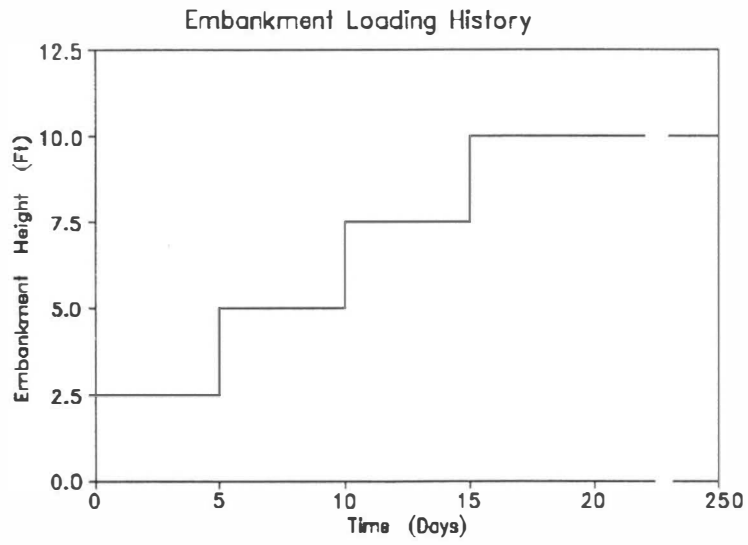


Fig. 4.17 Embankment Loading History

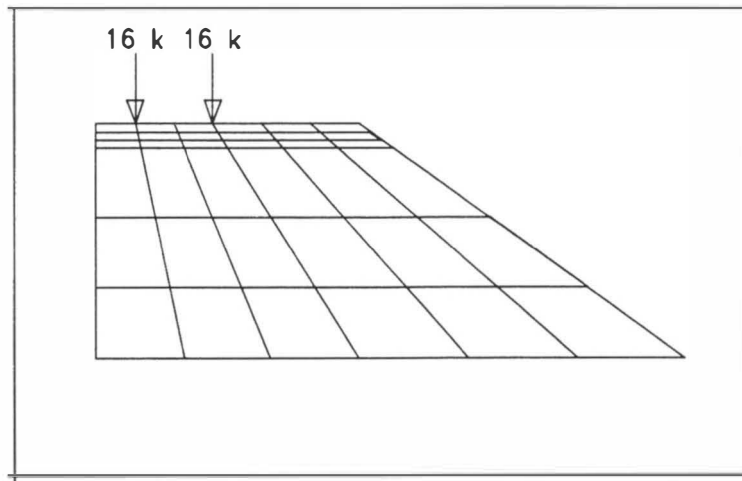


Fig. 4.18 Traffic Load Acting on the Embankment

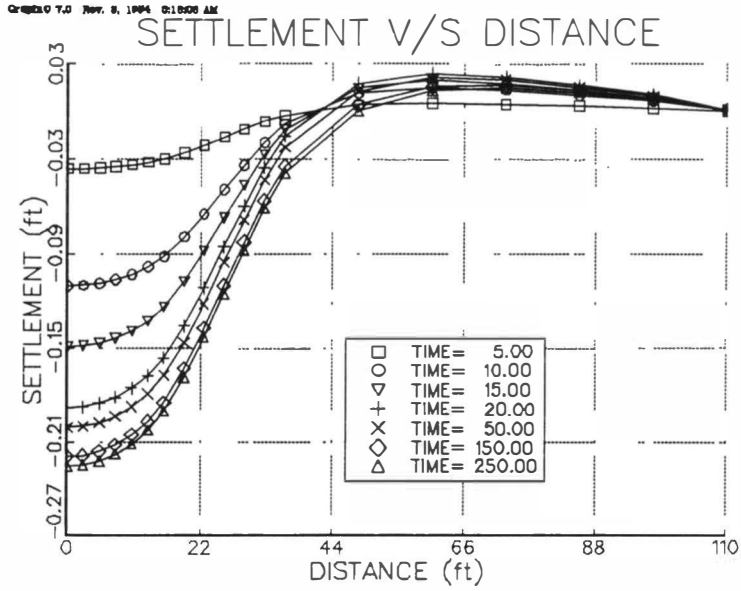


Fig. 4.19 Foundation Surface Settlement

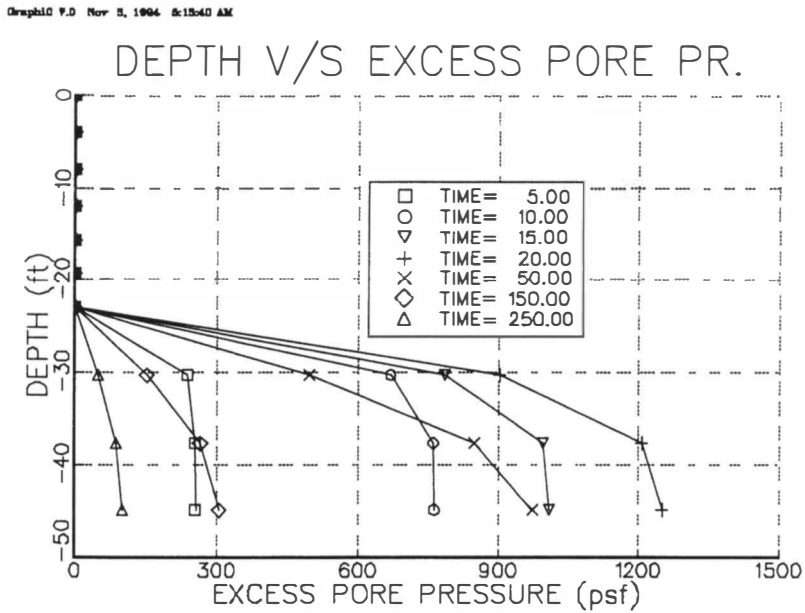


Fig. 4.20 Pore Pressure in Foundation

### MAX NOR STRESS CONTOURS (psf)

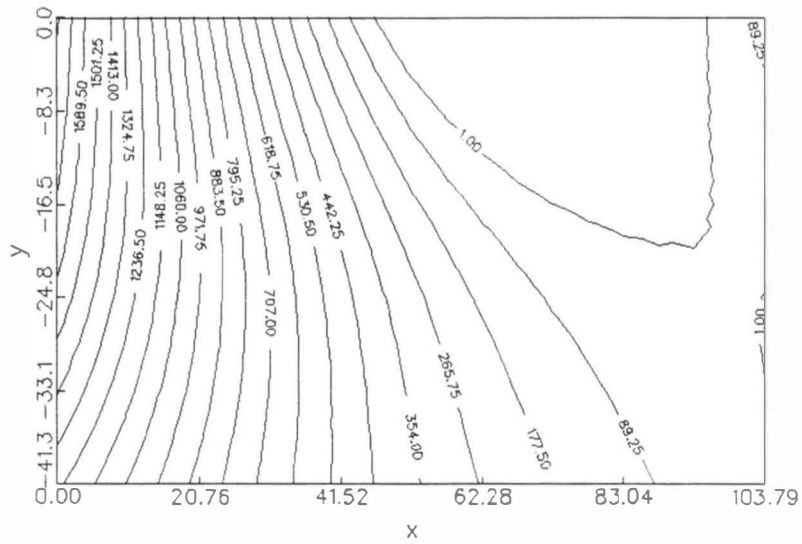


Fig. 4.21: Normal Stress Contours in Foundation at 250 Days

### SURFACE SETTLEMENT V/S DIST.

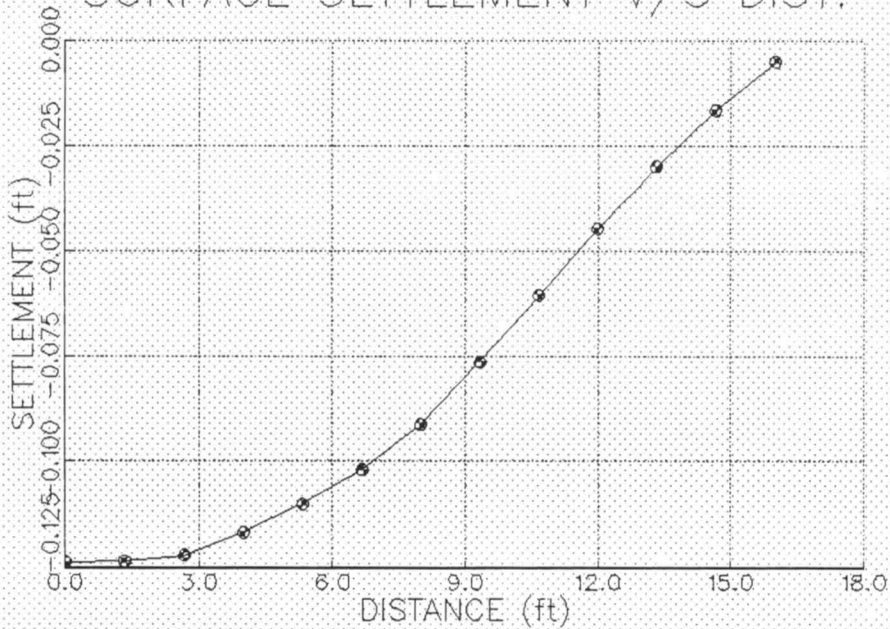


Fig. 4.22: Embankment Surface Settlement

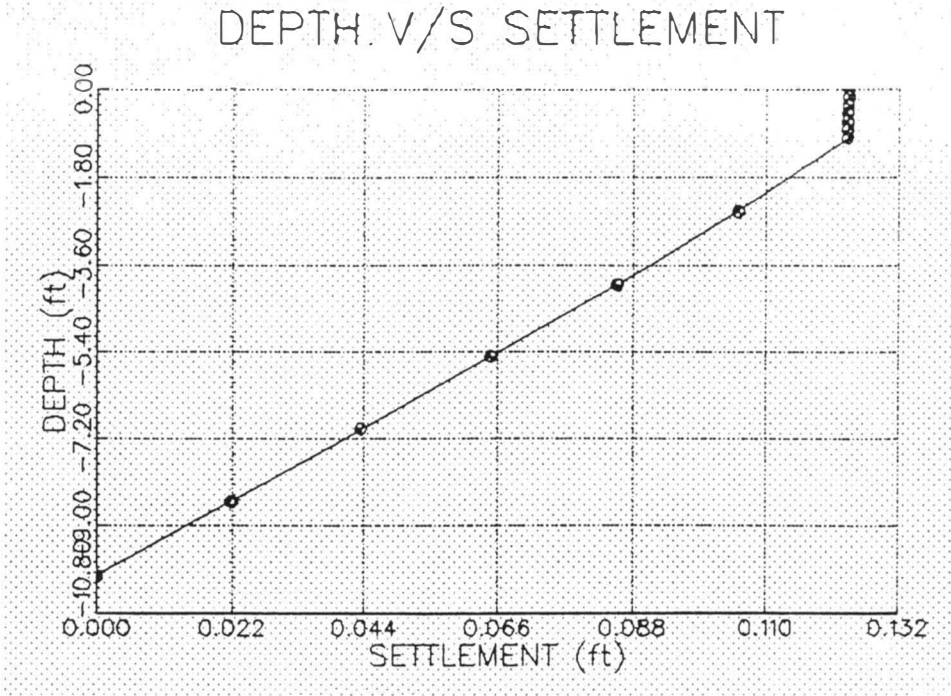


Fig. 4.23 Settlement at Various Depths of Embankment

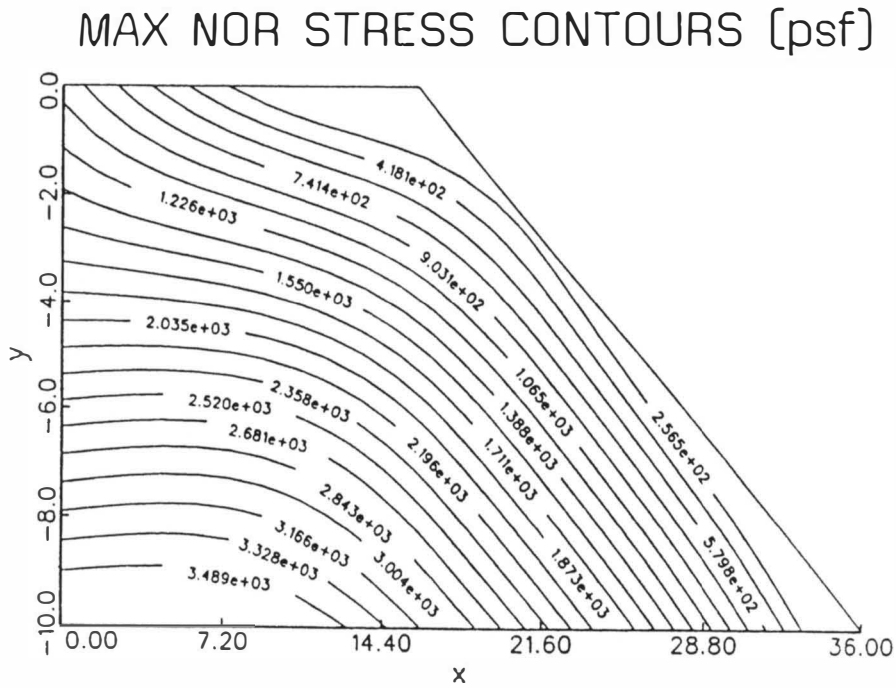


Fig. 4.24 Embankment Maximum Normal Stress Contours

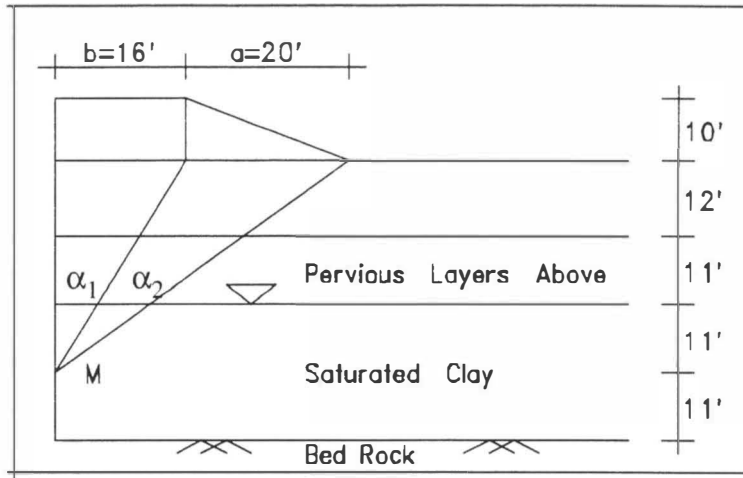


Fig. 4.25 Idealized site condition for analysis using Terzaghi's theory of 1-D consolidation

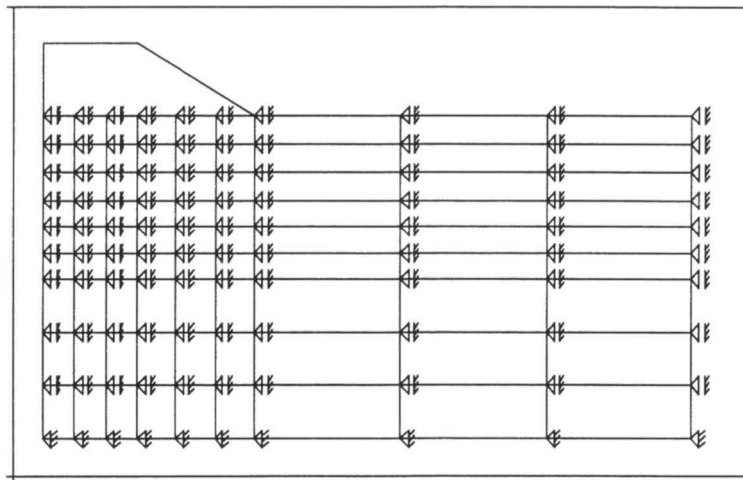


Fig. 4.26 One dimensional idealization using the finite element method



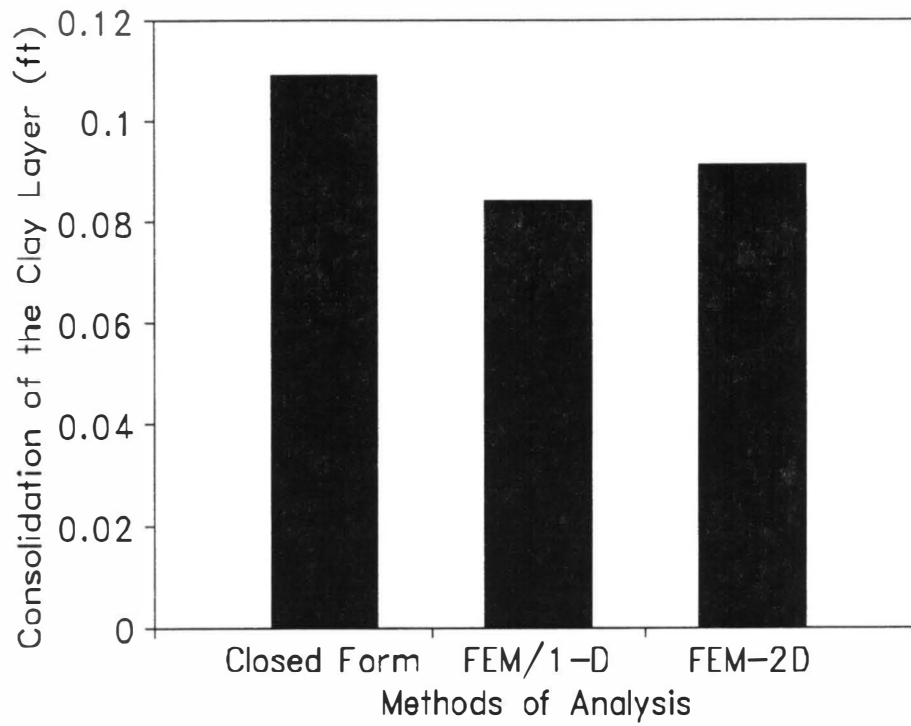


Fig. 4.27 Comparison of Total Settlement of 22'-Clay Layer as Found by Different Methods

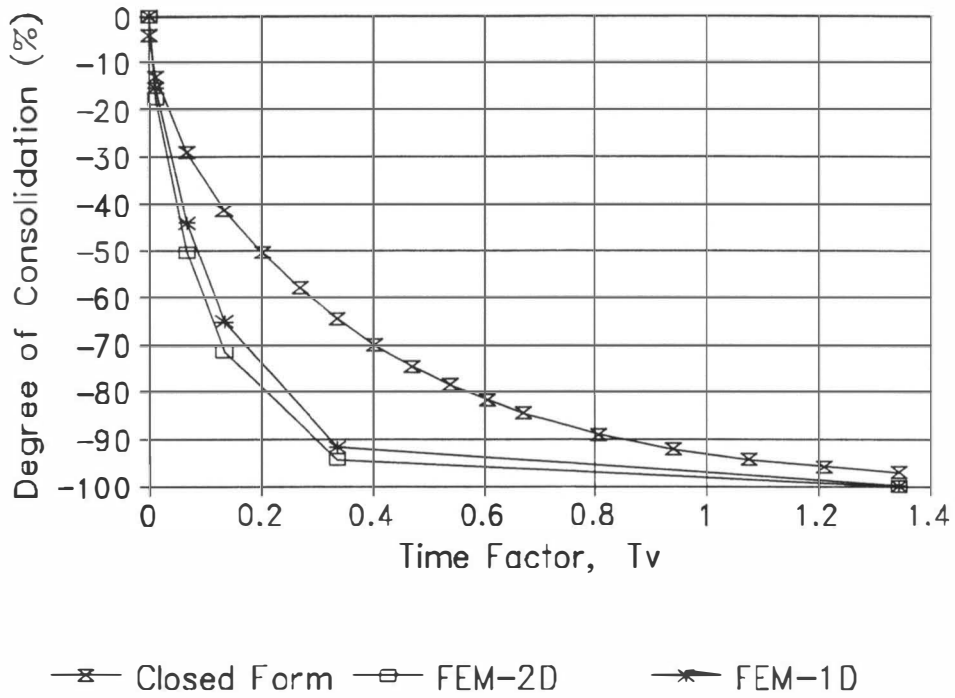


Fig. 4.28 Comparison of Degree of Consolidation as Found by Different Methods

## CHAPTER 5

### CONCLUSIONS AND RECOMMENDATIONS

#### 5.1 Conclusions

The software package developed in the course of this study is a very effective tool for analyzing the consolidation settlement of bridge approach foundation due to construction of the approach embankment. It is capable of evaluating the settlement of approach embankment itself due to its self weight and vehicular traffic load. Some of the important features of the software package are:

1. The nonlinear finite element technique, including soil grain-pore fluid interaction and two-dimensional idealization, is used to compute the consolidation settlements. This method is much more accurate and versatile compared with the Terzaghi one-dimensional consolidation theory which is commonly used in practice.
2. The infinite element concept employed represents the actual field boundary conditions in a realistic manner because it accounts for the semi-infinite nature of the soil medium in lateral directions.
3. The nonlinear behavior of foundation soil is idealized by an elasto-plastic (Modified Cam-Clay) model.
4. To enhance user-friendliness, the total software package is divided into several

components: *Preprocessor*, *Data Converter*, *FE Main Program*, and *Postprocessor*. The entire package can be run in Windows environment.

5. The interactive nature of the *Preprocessor* makes the software very user-friendly and facilitates the analysis of bridge approach settlement without an in-depth knowledge of the finite element method.
6. The graphical capabilities incorporated in the interactive *Preprocessor* help check any error in input data and provide a way for visual observation of the problem being analyzed.
7. The graphical capabilities incorporated in the *Postprocessor* are an effective tool for a graphical display of results. This attribute is expected to help in the interpretation of results.

The software package can be used to predict the potential for bridge approach settlement at a prospective site. Specifically, the software package can be used to determine the amount of expected settlements contributed by the foundation soil and the amount contributed by the approach embankment itself, for various design scenarios including preloading, embankment height, construction rate, and site improvement (e.g., wick drains). Both the best and the worst design scenarios can be analyzed to examine if approach settlement problems are likely to occur at a site. The total settlements and their time rates can be examined.

The software package can also be used to assess the future settlement potential

at an existing bridge site so as to plan the maintenance measures accordingly.

Although the software package does not provide information on any remedial measures directly, it is expected to be very useful in making important design and maintenance decisions in term of site modification/improvement, backfill material selection and alternate designs, among others.

## **5.2 Recommendations for Future Study**

For future enhancements, the following features may be included in the software:

1. Extend the software for unsymmetric embankments and uneven ground surfaces.
2. Batch processing option: the user will have an option to input data to the *Preprocessor* from a data file instead of interactive mode.
3. Include other elasto-plastic constitutive model such as the Drucker-Prager model to represent nonlinear behavior of sandy soils.
4. Consider dynamic nature of traffic loading on settlement.
5. Include secondary compression and drainage effects.
6. Account for large deformation in the finite element formulation.
7. Account for time-dependent deformation (e.g. creep, secondary compression) within the embankment.
8. Study various remedial measures to control bridge approach settlements including field performance study for different design scenarios ( Snethen, 1995).

## REFERENCES

1. American Society of Testing and Materials (ASTM), *Book of ASTM Standards, Part 10*, 1973.
2. Ardani, A., Bridge Approach Settlement, Colorado Department of Highway, *Report No. CDOH-DTP-R-87-6*, Colorado, 1987.
3. Biot, M.A., General Theory of Three Dimensional Consolidation, *J. Applied Physics*, vol. 12, 1941, pp. 155 - 164.
4. Booker, J.R., and Small, J.C., An Investigation of Stability of Numerical Solutions of Biot's Equations of Consolidation, *Int. J. Solids and Structures*, 1975, pp. 151 - 172.
5. Desai, C.S., and Abel, J.F., *Introduction to Finite Element Method*, Van Nostrand Reinhold Company, New York, 1972.
6. Desai, C.S., and Siriwardane, H.J., Subsidence due to Consolidation Including Nonlinear Behavior, *Int. Conf. on Pred. of Subsidence* (Ed. Saxena, S.K.), Pensacola, Florida, 1978, pp. 501-515.
7. Desai, C.S., and Siriwardane, H.J., *Constitutive Laws for Engineering Materials*, Prentice-Hall, Inc., Englewood, NJ, 1984.
8. Desai, C.S., Personal Communication, University of Arizona, Tucson, Arizona.
9. Erdelyi, A., Asymptotic Representations of Fourier Integrals and the Method of Stationary Phase, *J. Soc. Indust. Appl. Math.* Vol. 3, No. 1, 1955, pp.17-27.
10. Hopkins, T.C., Long Term Movements of Highway Bridge Approach Embankments and Pavements, *Report UKTRP-85-12, Kentucky Transportation Research Program*, Lexington, Kentucky, 1985.
11. Gopalasingam, A., *Analysis of Consolidation Settlement of Bridge Approach Foundation by Nonlinear Finite Element Method Including Infinite Elements*, M. S. Thesis, The University of Oklahoma, OK, 1989.
12. Hunt, R.E., *Geotechnical Engineering Analysis and Evaluation*, McGraw-Hill Inc., New York, 1986.

13. Laguros, J.G., Zaman, M.M., and Mahmood, I.U., Evaluation of Excessive Settlements of Pavements Behind Bridge Abutments and Their Remedies - Phase I, *Progress Report*, The University of Oklahoma, OK, 1986.
14. Laguros, J.G., Zaman, M.M., and Mahmood, I.U., Evaluation of Excessive Settlements of Pavements Behind Bridge Abutments and Their Remedies - Phase II, *Progress Report*, The University of Oklahoma, OK, 1990.
15. Laguros, J.G., Zaman, M.M., Alvappillai, A., Vavarapis, K.E., Evaluation of Causes of Excessive Settlements of Pavements Behind Bridge Abutments and Their Remedies - Phase III, *Progress Report*, The University of Oklahoma, OK, 1991.
16. Mahmood, I.U., Evaluation of Causes of Bridge Approach Settlement and Development of Settlement Prediction Models, *Ph.D. dissertation*, The University of Oklahoma, OK, 1990.
17. McNamee, J., and Gibson, R.E., Plane Strain and Axially Symmetric Problems of the Consolidation of a Semi-Infinite Clay Stratum, *Q. J. of Mech. and App. Maths.*, Vol.13, 1960, pp. 210 - 227.
18. McNamee, J., and Gibson, R.E., Displacement Functions and Linear Transforms Applied to Diffusion Through Porous Elastic Media, *Q. J. Mech. Appl. Math.*, Vol. 13, 1960, pp. 98 - 111.
19. Rajapakse, R.K.N.D., and Karasudhi, P., Elastostatic Infinite Elements for Layered Half Spaces, *J. of Eng. Mech.*, ASCE, Vol 111, 1985, pp. 1144 - 1158.
20. Roscoe, K.H., and Burland, J. B., On the Generalized Stress Strain Behavior of Wet Clay, *Engineering Plasticity*, Cambridge University Press, pp. 535 - 609.
21. Roscoe, K.H., Schofield, A. N., and Thurairaja, A., Yielding of Clays in States Wetter than Critical, *Geotechnique*, Vol. 13, No. 3, 1963, pp. 211 - 240.
22. Sandhu, R.S., and Wilson, E. L., Finite Element Analysis of Flow of Saturated Porous Elastic Media, *J. Eng. Mech. Div.*, ASCE, Vol. 95, No. EM3, 1969, pp. 641 - 652.
23. Schapery, R.A., Approximate Methods of Transform Inversion for Viscoelastic Stress Analysis, *Proc. 4th US National Cong. Appl. Mech.*, 1962, pp.364 - 398.

24. Schiffman, R.L., Chen, A.T. and Jordan, J. C., An Analysis of Consolidation Theories, *J. Soil Mech. Found. Div., ASCE*, Vol.95, 1969, pp. 285 - 312.
25. Schofield, A.N., and Wroth, C.P., *Critical State Soil Mechanics*, McGraw-Hill Book Co., London, 1968.
26. Snethen, D., Personal Communication, Oklahoma State University, Stillwater, OK.
27. Stewart, C.F., Highway Structure Approaches, *Report No. FWHA/CA/SD-85-05*, California Department of Transportation, Sacramento, California, 1985.
28. Tadros, M.K. and Benak, J.V., Bridge Abutment and Approach Slab Settlement, Phase I, *Final Report*, University of Nebraska-Lincoln, 1989.
29. Terzaghi, K., and Peck, R.E., *Soil Mechanics in Engineering Practice*, John Wiley, New York, 1948.
30. Vavarapis, K.E., *Factors Influencing Bridge Approach Settlement*, Unpublished M.S. Thesis, The University of Oklahoma, OK, 1991.
31. Zaman, M.M., Gopalasingam, A., and Laguros, J.G., Consolidation Settlement of Bridge Approach Foundation, *J. of Geotechnical Engr.*, ASCE, Vol. 117, No. 2, 1991, pp. 219-240.
32. Zaman, M.M., Laguros, J.G., Jar, R.K., Statistical Models for Identification of Problematic Bridge Sites and Estimation of Approach Settlements - Phase IV, *Progress Report*, The University of Oklahoma, OK, 1993.
33. Zaman, M.M., Laguros, J.G., Pandey, K.K., Bhat, D., Evaluation of Causes of Excessive Settlements of Pavements Behind Bridge Abutments and Their Remedies - Phase IV, *Draft Report*, The University of Oklahoma, OK, 1994.
34. Zaman, M.M., Laguros, J.G., Chen, H., Rahman, M., A User-friendly Software for Prediction of Bridge Approach Settlement, *Final Report*, The University of Oklahoma, OK, 1995.
35. Zienkiewicz, O.C., *The Finite Element Method in Engineering Science*, 3rd Ed., McGraw-Hill Publishing Co., Ltd., London, 1977.



## APPENDIX I

### SUMMARY OF DIFFERENT RESEARCH PHASES

#### I.1 Overview of ODOT Project

In order to evaluate the causes of excessive approach settlement and recommend appropriate remedial measures, the University of Oklahoma and the Department of Transportation (ODOT), in cooperation with the Federal Highway Administration (FHWA), proposed to conduct a five phase study as outlined below:

- Phase I      Literature review and survey of transportation agencies to explore the extent of approach settlement problems in Oklahoma and other states.
- Phase II     Level-one survey of selected bridge approaches in Oklahoma for qualitative assessment of causative factors.
- Phase III    Level-two survey of selected bridge approaches in Oklahoma for field testing and collecting samples for laboratory testing.
- Phase IV    Developing numerical and statistical model for prediction of approach settlement.
- Phase V     Developing guidelines for design, construction, and maintenance of bridge approaches.

The following section gives a detail description of the four phases completed so far.

#### 1. Phase I

Phase I (Laguros et al., 1986) of this research work was conducted during the

period of May 1985 - February 1986 and was mainly devoted to the collection of all pertinent information regarding the bridge approach settlement problem. In order to achieve this goal, the following tasks were identified: (1) comprehensive literature search, (2) survey of various state, federal and private agencies involved in the construction and/or maintenance of bridges, and (3) analysis of the survey responses. Extensive literature search on the referenced problem was conducted by utilizing the computer search facilities of the Highway Research Information Service (HRIS) and other data bases such as DIALOG, ORBIT and BRS available at the University of Oklahoma. Manual searches were also conducted in this process.

In connection with task (2), a questionnaire was prepared, in consultation with ODOT, and was sent to 52 state DOTs and 36 US Corps of Engineers Districts, as well as few other private agencies associated with the design, construction, and maintenance of bridges and highways. Responses were received from 61 agencies, out of which 42 agencies (approximately 70%) reported to have the approach settlement problems significant or very significant. The responses of the questionnaire also revealed that only 6 states (California, Iowa, Kentucky, Louisiana, Ohio and Texas) had undertaken some sort of research work to investigate this problem (Hopkins et al., 1969, 1985; Timmerman, 1976). However, several other states, viz. Colorado, North Carolina, Washington, Wyoming and Maryland have recently been involved in investigating certain specific aspects of the approach settlement problems (Wolde-Tinasae et al., 1987; Kramer et al., 1991).

The findings of Phase I conclusively demonstrated that the bridge approach settlement problems are quite extensive in many areas of the United States, including Oklahoma. An in-depth understanding of the settlement process and the various causative factors are essential for finding any remedial measure.

## 2. Phase II

Phase II (Laguros et al., 1990) started in February 1987 and was completed in December 1989. The major tasks for this phase of the research involved: (a) selection of bridge sites for level-one survey, (b) survey of those selected bridge sites, and (c) characterization of approach pavement settlement in the state. A total of 381 bridge sites, scattered in seventy seven counties of Oklahoma, were selected in consultation with ODOT and were later surveyed to obtain data related to the following factors: (i) bridge, abutment and approach geometry, (ii) existing conditions of the approach, abutment headwall, slope protection structure, drainage, and embankment slope, and (iii) embankment material. In addition, information related to construction and maintenance history of the selected bridges was obtained by interviewing ODOT personnel and examining ODOT records. Based on extensive analysis of survey data, the following conclusions were reported:

1. The problem of approach settlement is extensive in Oklahoma. Approximately 83% of the bridge approaches surveyed experienced settlement.
2. The problem seems to be more pronounced in absence of any drainage in the fill behind abutment.

3. The long term performance of both rigid and flexible approaches are similar, however, in terms of short term performance, rigid approaches undergo lower differential settlements.
4. Pile supported abutments are more susceptible to approach settlements than the stub type.
5. The higher embankment height might be partly responsible for larger approach settlements.
6. Skewed approaches generally undergo larger settlements than nonskewed approaches.
7. A major portion of the settlement of approaches occurs within the first twenty years of the service life of the bridge approach.

Apart from these, regression analyses on data collected from the level-one survey were conducted to develop an empirical relationship between the bridge approach settlement and the various causative factors (Mahmood, 1990). In addition, as a preliminary work for phase III, level-two survey, a detailed field and laboratory testing program was conducted at two selected bridge sites with the aim of determining their site-specific embankment and foundation soil characteristics.

As the majority of data collected from the level-one survey was based on visual inspections of the selected bridge sites, only qualitative characterization of the approach settlement problem was possible in phase II. For quantitative characterization, however, a level-two survey of the selected bridge sites were deemed necessary which

was conducted during phase III of this research work.

### 3. Phase III

Phase III (Laguros et al., 1991) was started with conducting level-two survey of some selected bridge sites in Oklahoma. The main objectives of conducting level-two survey were:

- i) To obtain comprehensive site-specific data, mainly pertaining to embankment and foundation soil characteristics, that can be used for a quantitative characterization of causes and mechanisms of approach settlements at these sites.
- ii) To acquire data for validation of the numerical model for the prediction of approach pavement settlement.
- iii) To build a data-base which can be used for assessment and/or estimate of approach settlement at similar sites.

The site-specific properties related to compaction, creep, consolidation and drainage, among many others, were considered to be necessary for the quantitative characterization of approach settlement. In order to achieve the objectives of phase III, the following tasks were identified:

1. Selection of bridge approaches for level-two survey.
2. Collection of soil samples from the selected sites and laboratory testing.
3. Instrumentation and monitoring of selected sites.
4. Quantitative characterization of approach settlement causes and mechanisms based on survey data.

As a part of level-two survey, it was proposed to include field instrumentation and monitoring of approach settlements at selected sites (Task 3) so as to evaluate the significance of creep movements of alluvium soil deposits in the overall settlement problem. This task was not pursued due to financial constraint, but is presently being pursued by ODOT in cooperation with the Oklahoma State University (OSU) (Snethen, 1995). The quantitative characterization of approach settlement defined in task 4 involved comparison and correlation of data collected from the field and laboratory tests. It was originally planned to conduct statistical analysis to obtain the desired correlations. It was estimated that the test results from at least 20 bridge sites would be required to obtain meaningful correlations from the statistical analysis. Subsequently, the plan was modified and samples were collected from 29 different bridge sites. Statistical analysis has been conducted to obtain bridge approach settlement from the field data. Field and laboratory test results for each site were analyzed in detail to identify the site specific causative factors of the approach settlements. The contribution of settlement from consolidation settlement of the approach foundation and the embankment settlement due to traffic loads necessitated the development of a user-friendly computer code and the salient features of this are presented in this thesis.

Apart from the aforementioned tasks, an additional task of finding an appropriate definition for the terms "excessive settlement" or "bump" at the ends of a bridge was undertaken as a part of phase III; and the findings of this task were reported separately to ODOT (Laguros et al., 1990). The report concluded that the approach settlement

of 2 inches or more can be considered as an "excessive settlement" or "bump". Approach settlement of such amounts was considered hazardous to traffic safety and needed immediate maintenance. An approach settlement of 0 to 0.5 inch was considered as minor, while settlement of 0.5 to 1 inch was considered as moderate.

#### 4. Phase IV

Phase IV (Zaman et al., 1993) involved two major tasks: (a) Developing the numerical model for predicting the bridge approach settlement; (b) Developing the statistical model for predicting the bridge approach settlement.

The User-friendly software presented in this report is the main tool used to achieve the task of developing a numerical model for prediction of approach settlement. The complete software package consists of four different programs: *Preprocessor*, *Data Converter*, *FE Main Program*, and *Postprocessor*. The *preprocessor* program is developed in a Windows environment using the programming features available in Actor 4.0, including graphical capabilities. This makes the *preprocessor* much more easy to use. The *data converter* was developed in FORTRAN77 language. It takes the data from the *preprocessor* and separates it into two compatible data files, one for analyzing the foundation and the other for analyzing the embankment. The *FE Main Program*, written in FORTRAN77, was originally developed by Dr. C.S. Desai, and his co-workers at the University of Arizona, Tucson (Desai, 1987). It was modified and extended substantially by Gopalasingam (Gopalasingam, 1989) to incorporate the isoparametric quadrilateral and infinite elements. The FEM algorithm developed in the

above is based on the Biot's theory of coupled three-dimensional consolidation (Biot's 1941) as proposed by Sandhu and Wilson (Sandhu et al., 1969). Further details of the FEM algorithm are given in Chapter 2. The *postprocessor* helps in presenting the results from the *FE Main Program* in the form of graphical plots which are much easier to understand and more convenient to interpret. The graphic software package, called Graphic/Win developed by the Scientific Endeavors Corporation, was employed to develop the *postprocessor*. A detailed view of this user-friendly software package is presented in Chapter 3.

A statistical model was developed based on the field tests of 29 selected bridge sites in Oklahoma ( Zaman et al., 1993). The majority of the data was obtained from the field tests (e.g. CPT and SPT tests) which were conducted as a part of level-two survey of these sites. However, some of the data such as age and skewness of the approach, traffic count (ADT) and height of the embankment was obtained from the level-one survey and/or from the records at the Bridge Division, ODOT. The selection of the sites was done in such a way that the selected sites encompass a wide range of variation with respect to the total settlement and the various causative factors such as: age of the approach, traffic count, skewness of the approach, height of the embankment, thickness of the foundation soil underlying the embankment, and the embankment and the foundation soil characteristics. The site-specific SPT and CPT results are used for a quantitative representation of the embankment and foundation soil characteristics. Extensive statistical analyses were performed using a statistical package



program, called SAS. The following SAS procedures were opted: REG, RSQUARE, STEPWISE and MODEL. Both linear and nonlinear multiple regression models were developed to predict the approach settlements. The multiple regression analyses were restricted to the use of quantitative variables only. The validity of the variables/parameters in the models is judged based on their level of significance, partial  $R^2$  (square of coefficient of correlation), t- and F- statistics; while the best models are decided on the basis of their overall  $R^2_{(adjusted)}$ , Mallows'  $C_p$ -statistic, mean square error ( $MS_E$ ), and their goodness of fit. The goodness of fit of the models is assessed based on their predictive capabilities and the analysis of the residuals of the predicted values.

The statistical models developed in this study can be used to evaluate approach settlements at predominantly clayey sites. However, it is expected that it may be applicable to sandy sites. Based on the estimate of settlements given by these models, a problematic bridge site can be identified. The special "Field Test Model" was also developed with the aim of identifying the problematic bridge sites before the construction of the bridge structure, so that appropriate precautionary and remedial measures such as ground improvement, preconsolidation (preloading) of the foundation, etc. can be implemented before or during the construction phase of the bridge. Moreover, the variables used in the field test model can be easily obtained from the Standard Penetration and Electric Cone Penetration tests.

Based on the data obtained and the model correlations made during the course

of the extensive statistical analyses, the following conclusions were made:

1. The factors which significantly affect the approach settlement are : age of the approach, height of the embankment, traffic count (ADT), foundation soil thickness, and the embankment and the foundation soil characteristics.
2. There is no strong correlation between the bridge approach settlement and a single individual causative factor (variable), indicating that bridge approach settlement is a complex problem and several factors need to be considered in order to fully explain the phenomenon.
3. The site-specific SPT value, thickness of the foundation soil, and cone resistance  $q_c$  are more significant variables as compared to the other variables (e.g. age of the approach, height of the embankment and traffic count); indicating that the site-specific embankment and the foundation soil characteristics are the most influential causative factor responsible for the approach settlement problem.
4. SPT value (N-value), tip resistance and friction ratio are found to be effective in representing the site-specific embankment and the foundation soil characteristics. However, the SPT value gives better correlation with the approach settlement as compared to the tip resistance ( $q_c$ ).
5. Skewness of the approach embankment SKEW is found to have negligible effect on the approach settlement.
6. The linear multiple regression model developed herein seems to fit the data set under consideration very well ( $R^2_{\text{adjusted}}=0.9361$ ). The prediction obtained by

this model is fairly accurate, and therefore this model can be used to predict approach settlement to a reasonable level of accuracy.

7. The nonlinear regression analyses indicate that the best nonlinear model is the one which tends to behave like a linear and/or close-to-linear model. Also, there seems to be absence of any specific nonlinear relationship between the approach settlement and the individual causative factors. Therefore, for the data set under consideration, the linear approach seems to be more reasonable.
8. The predictive ability of the nonlinear regression model, taking into account the number of parameters in the model, is quite comparable with that of the linear model.
9. The "field test" model developed primarily with the aim of identifying the problematic bridge sites before the construction of the bridge structure, seems to be ineffective. This is because of the fact that this model does not take into account the effect of embankment on the approach settlement. However, this leads to an important conclusion that the settlement within the embankment itself is a potential cause of the bridge approach settlement.

**APPENDIX II**  
**DETAILS OF THE CONSTITUTIVE MODEL**

**II-A. Nomenclature**

$[B]$	Strain-displacement transformation matrix
$C_{ijkl}^{ep}$	Components of elastic or plastic material property tensor
$e$	Void ratio at $p = p_0$
$e_c$	Void ratio at $p=1$
$e_o$	Initial void ratio
$F_i$	Body force vector component
$J_{2D}$	Second invariant of deviatoric stress tensor
$k_{ij}$	Components of permeability stress tensor
$M$	Slope of the failure Line in q-p plane
$n_j$	Unit normal vector
$p$	Pore water pressure
$p_o$	Current diameter of ellipse in P-direction
$q_i$	Components of pore fluid flow vector

$\bar{Q}$  Prescribed fluid flow

$[Q_o]$  Load term which represents the contribution of initial plastic strain

$\{Q_o^P\}_n$  Contribution of residual load due to plastic strain during a given load increment

$S_{ij}$  Deviatoric stress tensor

$S_{i(i=1,2,3,4)}$  Surfaces of the Boundary

$T_i$  Prescribed surface traction vector

$U_i$  Cartesian components ( $u,v,w$ ) of the displacement vector in ( $x,y,z$ ) directions,  
respectively

$dV$  Total volumetric strain

$\delta_{ij}$  Kronecker's delta used in tensor notation

$=1$  for  $i=j$  and  $=0$  for  $i \neq j$

$\epsilon_{kt}$  Strain tensor components

$\{\Delta \epsilon^P\}_n$  Incremental plastic strain at given load increment

$\rho$  Mass density of soil

$\rho_w$  Mass density of pore fluid

$\sigma'$  Effective stress

## II-B. Governing Equations and Boundary Conditions

Biot's theory of 3-D consolidation as proposed by Sandhu & Wilson (Sandhu et al., 1969) modified for plain strain idealization has been adopted. The behavior of soil skeleton deformation coupled with pore pressure effects is incorporated in the expression:

$$\sigma_{ijj} + p_j \delta_{ij} + \rho F_i = 0 \quad (\text{II.1})$$

Flow equilibrium can be written in the form:

$$[K_{ij}(p_j + \rho_w F_i) + \dot{u}_{i,i}] = 0 \quad (\text{II.2})$$

The generalized Darcy's law for the flow behavior is given by:

$$q_i = k_{ij}(p_j + \rho_w F_j) \quad (\text{II.3})$$

Refer Fig. 2.2 for schematic representation of consolidating soil mass.

The following boundary conditions are possible:

$$\text{Displacements: } u_i = \bar{u}_i \text{ on } S_1 \quad (\text{II.4})$$

$$\text{Pore pressure: } p = \bar{p} \text{ on } S_2 \quad (\text{II.5})$$

$$\text{Applied pressure: } T_i = (\bar{\sigma}_{ij} + \delta_{ij} p) n_j \text{ on } S_3 \quad (\text{II.6})$$

$$\text{Applied flow: } \bar{Q} = q_i n_i \text{ on } S_4 \quad (\text{II.7})$$

The overbar represents that the quantity is prescribed.

## **II-C. Modified Cam-Clay Model**

The modified Cam-clay model is used here to represent the nonlinear elasto-plastic behavior of soil (clay). This model is based on the concept of a critical state line, in conjunction with a strain-dependent yield surface (see Fig. II-1). If there is no change in void ratio as well as effective stress components during the continuous deformation of the soil, then the soil is said to have reached the critical state. According to the critical state models, a soil undergoing shear deformation can pass from one yield point to another without collapse and continue to deform until the critical state line or surface is reached. At this point ideal plasticity conditions exist. Starting from two alternative assumptions regarding the dissipation of energy during plastic yielding, Rosco, Schofield, Thurairajah and Worth (Roscoe et al., 1963; Schofield et al., 1968) proposed the "Cam-Clay" model. Rosco and Burland (Roscoe et al., 1968) extended this model and called it the "Modified Cam-Clay model."

The modified Cam-Clay model fits the experimental data for clayey soils satisfactorily. Yield surface is assumed to be an ellipse in the  $q$ - $p$  plane. Fig. II-2 represents strain hardening experienced by the soil between stages 1 and 2. Associative flow rule is assumed in the model and the principle of normality is applied to the yield surface. Direction of plastic strain is uniquely defined for every point on the surface. At the intersection of the critical state line and the ellipse, the normal to yield surface is vertical. Hence, at this point no component of plastic volumetric strain exists and all the plastic strain is distortional, meaning the soil can deform at constant volume.

The constitutive law for the soil skeleton can be written in an incremental form as (Desai et al., 1985)

$$\Delta \sigma_{ij} = C_{ijkl}^{ep} \Delta \epsilon_{kl} \quad (\text{II.8})$$

The yield surface is given by (Roscoe et al., 1968)

$$f_c = p^2 - p_o p + \frac{q^2}{M^2} = 0 \quad (\text{II.9})$$

where,

$$q = \sqrt{3J_{2D}} \quad (\text{II.9a})$$

$$p = (\sigma'_{11} + \sigma'_{22} + \sigma'_{33})/3 \quad (\text{II.9b})$$

$$J_{2D} = \frac{1}{2} S_{ij} S_{ij} \quad (\text{II.9c})$$

A schematic representation of the Modified Cam-Clay model is represented in Fig. II-3.

#### II-D. Derivation of Constitutive Relation

Consolidation parameter  $\lambda$ , which is the slope of the void ratio vs  $\ln(p)$  plot during virgin loading and  $\kappa$ , which is the initial slope during rebound, are shown in Fig. II-4. The equation of consolidation curve in  $e - \ln(p)$  can be written as

$$e - e_c = -\lambda \ln p_o \quad (\text{II.10})$$

and the equation of swelling curve is

$$e - e_c = -\kappa \ln p_o \quad (\text{II.11})$$

Differentiating Eqs. II.10 and II.11 and separating the variables, the following



expressions can be obtained:

$$-de = \lambda \frac{dp_o}{p_o} \quad (\text{II.12})$$

$$-de^e = \kappa \frac{dp_o}{p_o} \quad (\text{II.13})$$

Superscript e denotes elastic quantity. Volumetric strain is defined as

$$dv = - \frac{de}{(1 - e_o)} \quad (\text{II.14})$$

$$dv^e = \frac{k}{(1 + e_o)} \frac{dp_o}{p_o} \quad (\text{II.15a})$$

$$dv = \frac{\lambda}{(1 + e_o)} \frac{dp_o}{p_o} \quad (\text{II.15b})$$

$$dv^p = dv - dv^e = \frac{(\lambda - k)}{(1 + e_o)} \frac{dp_o}{p_o} \quad (\text{II.15c})$$

The equation of the modified Cam-Clay model (Eq. II.9) can now be expressed

as

$$F = \eta^2 - M^2 \left[ \frac{p_o}{p} - 1 \right] \quad (\text{II.16a})$$

where,

$$\eta = q/p \quad (\text{II.16b})$$

q is defined as

$$\begin{aligned} q &= \frac{3}{\sqrt{2}} \tau_{oct} \\ &= \frac{1}{\sqrt{2}} [(\sigma_x - \sigma_y)^2 + (\sigma_y - \sigma_z)^2 + (\sigma_z - \sigma_x)^2 \\ &\quad + 6\tau_{xy}^2 + 6\tau_{xz}^2 + 6\tau_{zx}^2]^{1/2} \end{aligned} \quad (\text{II.17})$$

and p is defined as

$$p = \frac{1}{3}(\sigma'_x + \sigma'_y + \sigma'_z) \quad (\text{II.18})$$

where the prime denotes effective stress components.

Substituting for  $\eta$  in Eq. II.16, the equation for yield surface can be obtained as

$$F_{(p,q,v^p)} = q^2 - M^2 p_o p + M^2 p^2 \quad (\text{II.19})$$

and

$$dF = \frac{\partial F}{\partial p} dp + \frac{\partial F}{\partial q} dq + \frac{\partial F}{\partial v^p} dv^p = 0 \quad (\text{II.20})$$

The flow rule for plastic flow can be written as

$$d\varepsilon_{ij}^p = \bar{\lambda} A_{ij} \quad (\text{II.21})$$

where,

$$A_{ij} = \frac{\partial Q}{\partial p} \frac{\partial p}{\partial \sigma_{ij}} + \frac{\partial Q}{\partial q} \frac{\partial q}{\partial \sigma_{ij}} \quad (\text{II.22})$$

The gradient of the yield function F is given by the expression,

$$B_{ij} = \frac{\partial F}{\partial p} \frac{\partial p}{\partial \sigma_{ij}} + \frac{\partial F}{\partial q} \frac{\partial q}{\partial \sigma_{ij}} \quad (\text{II.23})$$

Eq. II.20 can be expressed in terms of  $B_{ij}$  i.e.,

$$dF = B_{ij} d\sigma_{ij} + \frac{\partial F}{\partial v^p} dv^p = 0 \quad (\text{II.24})$$

$$d\varepsilon_{ij}^e = d\varepsilon_{ij} - d\varepsilon_{ij}^p \quad (\text{II.25})$$

$$d\sigma_{ij} = C_{ijkl}(d\varepsilon_{kl} - d\varepsilon_{kl}^p) \quad (\text{II.26})$$

Substituting Eq. II.26 in Eq. II.24,

$$\begin{aligned}
dF &= B_{ij} C_{ijkl} (d\epsilon_{kl} - d\epsilon_{kl}^p) + \frac{\partial F}{\partial v^p} \cdot dv^p \\
&= B_{ij} C_{ijkl} (d\epsilon_{kl} - \bar{\lambda} A_{kl}) + \frac{\partial F}{\partial v^p} \cdot \bar{\lambda} \frac{\partial F}{\partial p} = 0
\end{aligned} \tag{II.27}$$

$$(B_{ij} C_{ijkl} - \frac{\partial F}{\partial v^p} \cdot \frac{\partial F}{\partial p}) \bar{\lambda} = B_{ij} C_{ijkl} A_{kl} d\epsilon_{kl}$$

and

$$\bar{\lambda} = \frac{B_{ij} C_{ijkl} d\epsilon_{kl}}{(B_{ij} C_{ijkl} A_{kl} - \frac{\partial F}{\partial v^p} \cdot \frac{\partial F}{\partial p})} \tag{II.28}$$

From Eqs. II.22, II.23 and II.28

$$d\sigma_{ij} = \left[ C_{ijrs} - \frac{C_{ijkl} A_{kl} B_{mn} C_{mnr}}{B_{mn} C_{mnr} A_{rs} - \frac{\partial F}{\partial v^p} \frac{\partial F}{\partial p}} \right] \tag{II.29}$$

For associative plasticity,  $Q = F$  and  $A_{ij} = B_{ij}$ . From Eq. II.17.

$$\frac{dp_o}{dv^p} = p_o \frac{(1 + e_o)}{(\lambda - k)} \tag{II.30}$$

$$\frac{\partial F}{\partial v^p} = \frac{\partial F}{\partial p_o} \frac{\partial p_o}{\partial v^p} = \frac{\partial F}{\partial p_o} p_o \frac{(1 + e_o)}{(\lambda - k)} \tag{II.31}$$

So, the Eq. II.27 can be rewritten as,

$$\bar{\lambda} = \frac{A_{ij} C_{ijkl} d\epsilon_{kl}}{A_{ij} C_{ijkl} A_{kl} - \gamma A_{ii}} \tag{II.32a}$$

where,

$$\gamma = \frac{\partial F}{\partial p_o} p_o \frac{(1 + e_o)}{(\lambda - k)} \quad (\text{II.32b})$$

$$A_{ij} = \frac{\partial F}{\partial p} \quad (\text{II.32c})$$

### II-e Nonlinear Behavior: Initial Strain Method

The elastic constitutive relation can be expressed as

$$[\sigma] = [C][\epsilon^e] = [C]([\epsilon] - [\epsilon^p]) \quad (\text{II.33})$$

Stress and strains contribute only to the strain energy part of the total potential functional. Therefore, the strain energy of the functional needs to be considered. This term can be rewritten as

$$\begin{aligned} U = & \frac{1}{2} \iiint_V [\epsilon]^T [C] [\epsilon] dV - \iiint_V [\epsilon]^T [C] [\epsilon^p] dV \\ & + \frac{1}{2} \iiint_V [\epsilon^p]^T [C] [\epsilon^p] dV \end{aligned} \quad (\text{II.34})$$

The net effect on resulting equilibrium equations for finite element is the addition of the load term  $[Q_o]$ , which represents the contribution of the initial plastic strain

$$[K]\{q\} = \{Q\} + \{Q_o\} \quad (\text{II.35})$$

where,

$$\{Q_o\} = \iiint_V [B]^T [C] [\epsilon^p] dV \quad (\text{II.36})$$

The term  $\{Q\}$  permits the inclusion of the effects of all initial plastic strains in the formulation.

During consolidation, the initial tangent slope (i.e., stiffness) is kept constant and the plastic behavior is taken into account by the addition of a residual load. The residual load vector is computed by adding the contribution of plastic strains at various time steps after application of an external increment.

$$\{Q_o^P\}_n = \{Q_o^P\}_{n-1} + \int_V [B]^T [C^e] \{\Delta \epsilon^P\}_n dV \quad (\text{II.37})$$

The calculated equivalent load vector is averaged over the element as:

$$(\Delta \bar{Q}_o^P)_x = \frac{\sum_{i=1}^8 [\{\Delta Q_o^P\}]_{x_i} \cdot \Delta U_{x_i}}{\sum_{i=1}^8 \Delta U_{x_i}} \quad (\text{II.38a})$$

and

$$(\Delta \bar{Q}_o^P)_y = \frac{\sum_{i=1}^8 [\{\Delta Q_o^P\}]_{y_i} \cdot \Delta U_{y_i}}{\sum_{i=1}^8 \Delta U_{y_i}} \quad (\text{II.38b})$$

Where,  $(\{\Delta Q_o^P\}_{x_i})$  and  $(\{\Delta Q_o^P\}_{y_i})$  are x and y components, respectively, of  $(\{\Delta Q_o^P\}_n)$  and

$$\{\Delta U_x\} = \{U_x\}_n - \{U_x\}_{n-1} \quad (\text{II.38c})$$

$$\{\Delta U_y\} = \{U_y\}_n - \{U_y\}_{n-1} \quad (\text{II.38d})$$

At any given stage of the consolidation process, the average load given by Eq.

II.38 is applied to all 8 nodes of the quadrilateral element and are grouped as in Eq. II.37. The approach is assumed to yield better results due to the fact that strains and stresses due to residual load are smoothed over the element.

Using the above nonlinear approach and an integration scheme, the governing differential equation (Eq. I.11) can be modified to account for plastic behavior as

$$\begin{bmatrix} [K_1] & [K_3] \\ [K_3]^T & -\alpha \Delta t [K_2] \end{bmatrix} \begin{Bmatrix} \Delta r_q(t_n) \\ \Delta r_p(t_n) \end{Bmatrix} = \begin{Bmatrix} \Delta R_Q(t_n) + Q_{on}^p \\ \Delta R_p(t_n) \end{Bmatrix} \quad (\text{II.39})$$

where,

$$\begin{aligned} \langle \Delta R_Q(t_n) \rangle &= -\langle \Delta M_1(t_n) \rangle + \langle \Delta M_2(t_n) \rangle - \langle \Delta P_1(t_n) \rangle \\ \langle \Delta R_p(t_n) \rangle &= -[K_3]^T(\Delta t_q(t_{n-1})) + \Delta r(1 - \alpha)[K_2]\langle \Delta r_p(t_{n-1}) \rangle \\ &\quad + \alpha \Delta t \langle \Delta M_3(t_n) \rangle + \Delta t(1 - \alpha)\langle \Delta M_3(t_{n-1}) \rangle \\ &\quad + \alpha \Delta t \langle \Delta P_2(t_n) \rangle - \Delta t(1 - \alpha)\langle \Delta P_2(t_{n-1}) \rangle \end{aligned} \quad (\text{II.40})$$

A more detailed description of the finite element formulation, including the Cam-Caly model, is given by Gopalasingam (Gopalasingam, 1989).

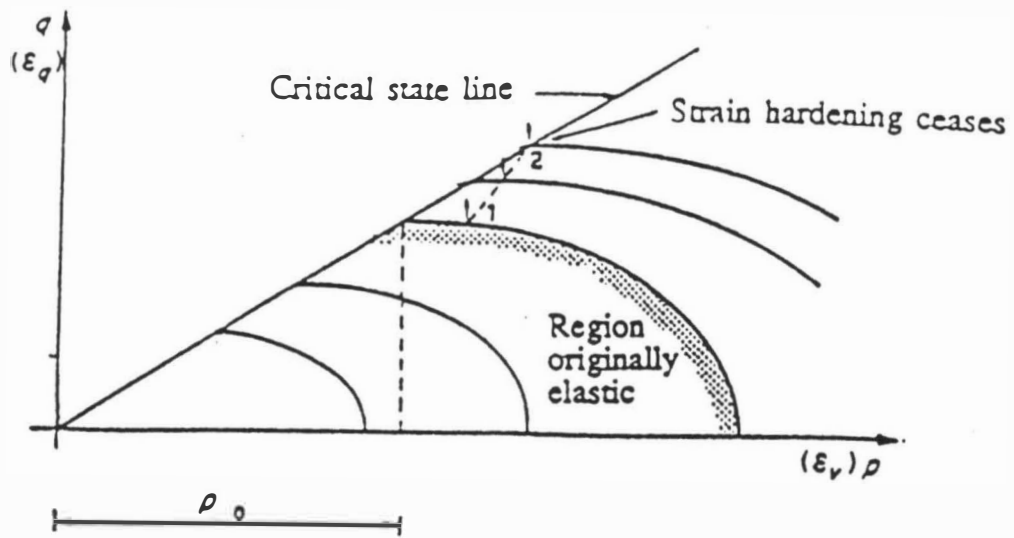


Fig. II-1 Modified Cam-Clay Model on the q-p Plane

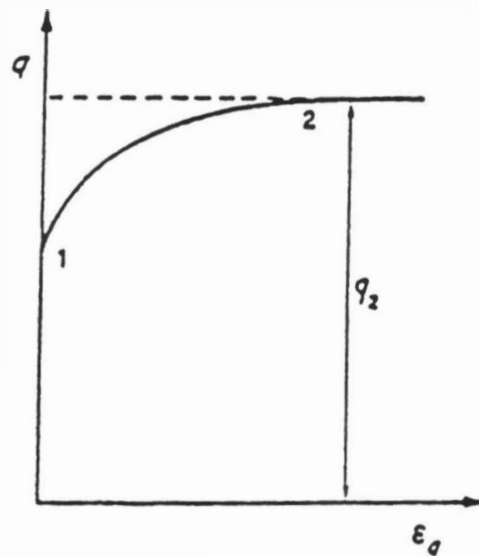


Fig. II-2 Strain Hardening Behavior

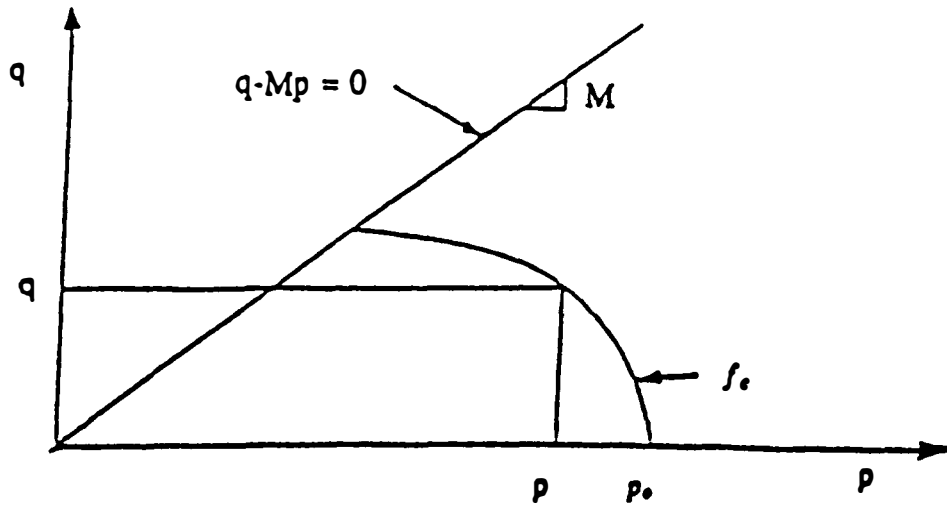


Fig. II-3 Modified Cam-Clay Model

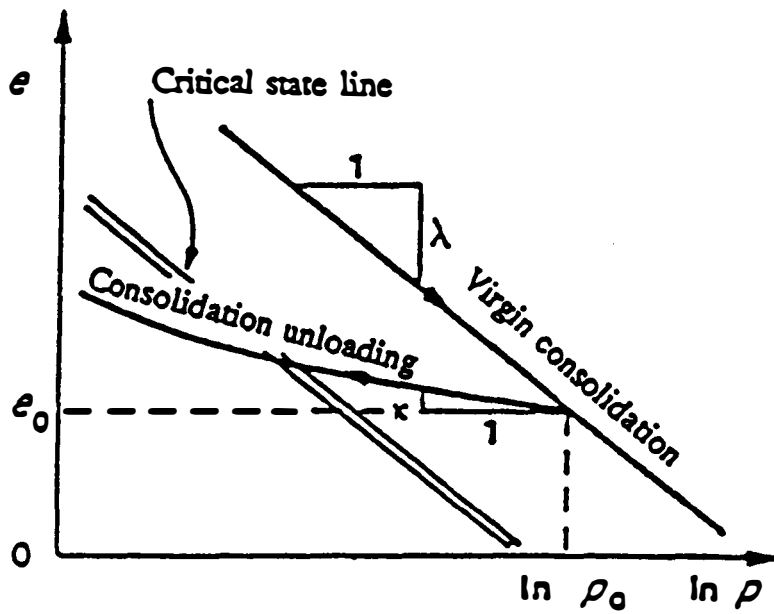


Fig. II-4 Typical  $e-\ln p$  Curve



## APPENDIX III

### NOTES ON INPUT FOR THE FE MAIN PROGRAM

This section provides details of the format and arrangement to be followed for input of the variables for the FE Main program. The Captain Creek bridge site, analyzed in Chapter 4, has been selected as an example site. Even though the preprocessor generates the data for the FE Main program, this part of the user's manual helps in checking the output from the data converter. Table III.1 contains the variable name, type, corresponding format and number of lines required to enter that variable. Table III.2 identifies the input variables presented in Table III.1. Figure III.2-III.5 contain excerpts from an actual input data file (Capdmf.dat) and shows the way the input variables are stored in the file.

**Table III.1 Format and order of the input variables for the FE main Program**

Item No.	Variables	Type	Format	No. of Lines
1.	Title	Character*70	5X, A	1
2.	Msym	Integer	Free	1

3.	Munit, Ulen, Uforce, Utime	Integer Character*2 Character*2 Character*5	I7, 1X, A2, 2X, A2, 2X, A5	1
4. (a)	Mcontr	Integer		1
(b)	Xsett	Real		1
(c)	Height, Top, Bottom	Real Real Real	Free	1
5. (a)	Numnp	Integer		
(b)	Numel	Integer		
(c)	Nummat	Integer		
(d)	Ro	Real		
(e)	Timend	Real	Free	1 line each
(f)	Acelz	Real		
(g)	Numpc	Integer		
(h)	Nflbc	Integer		

6. (a)	E (1, m), E (2, m), E (3, m), E (4, m)	Real Real Real Real	Free	(1 + 1)*Nummat (see note 4 below)
(b)	EA (1, m), EA (2, m), EA (3, m), ISO (m)	Real Real Real Integer		
7.	Xfact, Yfact	Real Real	Free	1

8. (a)	n, Kode (n), Kt (n)	Integer Integer Integer		
8. (b)	X (n), Y (n), Ux (n), Uy (n), F (n), Sig (n, 1), Sig (n, 2), Sig (n, 3)	Real Real Real Real Real Real Real Real	Free	(1+1)*Numnp (see note 5 below)
9.	m, Ix (m, 1), Ix (m, 2), ..., Ix (m, 11)	Integer	Free	(1)*Numel (see note 6 below)

10.	Em (i), Alam (i), Ak (i), Strx (i), Stry (i), Void (i)	Real	Free	See note 7 below
11. (a)	Dt,	Real	Free	1 (see note 8 below)
	Ndt,	Integer		
	Inter,	Integer		
	Jemb	Integer		
(b)	Ibc (l),	Integer	Free	Numpc (see note 8 below)
	Jbc (l),	Integer		
	Kbc (l),	Integer		
	Pr (l, 1),	Real		
	Pr (l, 2)	Real		
(c)	Ifbc (l),	Integer	Free	Nflbc (see note 8 below)
	Jfbc (l),	Integer		
	Fbc (l)	Real		

**Note 1:** In item no. 1 the character variable *Title* can contain a maximum of 70 alphanumeric characters.

**Note 2:** In item no. 3 the value of the integer variable *Munit* can be typed anywhere between columns 1 and 7.

**Note 3:** Skip item no. 4(b) if the value of *Mcontr* in item no. 4(a) is equal to 2 and skip item no. 4(c) if the value of *Mcontr* in item no. 4(a) is equal to 1.

**Note 4:** There are two data cards for each type of material in item no. 6 - one for properties in X direction (item no. 6(a)) and the other for properties in Y direction (item no. 6(b)). These two data cards are to be repeated as many times as the number of materials (*Nummat*) present in the domain under consideration. As such the total no. of lines is equal to  $2 * \text{Nummat}$  for this item.

**Note 5:** There are two data cards for each node in item no. 8 - the first one for the boundary conditions and the second one for the prescribed quantities. These two data cards are to be repeated as many times as the number of nodes (*Numnp*) present in the domain under consideration. Therefore, the total no. of lines is equal to  $2 * \text{Numnp}$  for this item.

**Note 6:** The only data card in item no. 9 is to be repeated as many times as the number of elements (*Numel*) present in the domain under consideration. Hence, the total no. of lines is equal to  $1 * \text{Numel}$  for this item.

**Note 7:** The data for critical state model in item no. 10 are to be input for each element

of clay type material. Each data card contains information about one such element. As a result, the total number of data cards for this item is equal to the total no. of elements of clay type material present in the mesh.

**Note 8:** The item no. 11 is to be repeated for as many times as the number of time levels at which analysis is desired. For the current study, the item no. 11(c) (information regarding nodes with prescribed flow and the quantity of flow prescribed at those nodes) is not expected to appear because of the idealizations made do not call for these terms.

**Table III.2 Identification of the input variables for the FE main Program**

Item No.	Variables	Identification
1.	Title	A description for the problem identification purpose.
2.	Msym	A control variable: = 0 if the embankment is symmetric and = 1 if the embankment is not symmetric.
3.	Munit	Munit is a control variable. Munit = 0 indicates FPS and Munit = 1 indicates SI system of units.
	Ulen	Unit of length. It has a size of two characters.
	Uforce	Unit of force. It has a size of two characters.
	Utime	Unit of time. It has a size of five characters.

4. (a)	Mcontr	Mcontr is a control variable. It has a value of 1 for foundation analysis and 2 for embankment analysis.
(b)	Xsett	Xsett is the distance at which pore pressure values are to be written in during the foundation analysis. These values are latter used to generate pore pressure plots. The value of Xsett is usually taken as 0 meaning that the pore pressures along the center line of the foundation are to be plotted.
(c)	Height	Height of the embankment.
	Top	Top half width of the embankment.
	Bottom	Bottom half width of the embankment.
5. (a)	Numnp	Number of nodal points in the mesh.
(b)	Numel	Number of elements in the mesh.
(c)	Nummat	Number of layers in the mesh.
(d)	Ro	Unit weight of pore water (62.4 pounds/cubic foot or 9810 Newton/cubic meter).
(e)	Timend	The time limit at which the analysis must stop.
(f)	Acelz	Vertical downward acceleration of pore water.
(g)	Numpc	Number of elements with prescribed displacement.
(h)	Nflbc	Number of elements with prescribed flow.



6. (a)	E (1, m)	Young's modulus for the m'th layer in X direction.	
	E (2, m)	Poisson's ratio for the m'th layer in X direction.	
	E (3, m)	Permeability for the m'th layer in X direction.	
	E (4, m)	Unit weight of soil for the m'th layer.	
	(b)	Ea (1, m)	Young's modulus for the m'th layer in Y direction.
		Ea (2, m)	Permeability for the m'th layer in Y direction.
		Ea (3, m)	Poisson's ratio for the m'th layer in Y direction.
	Iso (m)	Iso = 0 for isotropic soil layers and Iso = 1 for anisotropic soil layers.	
7.	Xfact	= 1.0 (control variable).	
	Yfact	= 1.0 (control variable).	
8. (a)	Kode (n)	Boundary condition specifier.	
	Kt (n)	Kt = 1 for corner nodes and Kt = 0 for intermediate nodes.	
	(b)	X (n)	X coordinate of the n'th node.
		Y (n)	Y coordinate of the n'th node.
		Ux (n)	Prescribed displacement of the n'th node in X direction.
		Uy (n)	Prescribed displacement of the n'th node in Y direction.
		F (n)	Prescribed flow at the n'th node.
Sig (n, 1) through Sig (n, 3)	Control variables, each of them are to be initialized as 0.0.		

9.	Ix (m, 1) through Ix (m, 8)	Nodal indices of the m'th element. See note 1 below.
	Ix (m, 9)	Layer index for the m'th element.
	Ix (m, 10)	Ix (m, 10) = 0 for sand; = 1 for clay.
	Ix (m, 11)	Ix (m, 11) = 0 for finite element; = 1 for infinite element.
10.	Em (i)	Critical state line slope for the soil material corresponding to the i'th element.
	Alam (i)	Consolidation curve slope (compression) from the e vs. ln p curve for the soil material corresponding to the i'th element.
	Ak (i)	Consolidation curve slope (swelling) from the e vs. ln p curve for the soil material corresponding to the i'th element.
	Strx (i)	In-situ stress in x-direction at the c.g. of the i'th element.
	Stry (i)	In-situ stress in y-direction at the c.g. of the i'th element.
	Void (i)	Initial void ratio of the material in the i'th element.
11. (a)	Dt	Duration of each sub-increments of time comprising a complete time step sequence. (See note 2 below).
	Ndt	No. of time increments at a particular time step sequence.
	Inter	No. of time increments between two consecutive printed output in the general output file.
	Jemb	Jemb = 0 for foundation and 1 for embankment.

(b)	Ibc (l)	Index of the top left node of the l'th loaded element.
	Jbc (l)	Index of the top middle node of the l'th loaded element.
	Kbc (l)	Index of the top right node of the l'th loaded element.
	Pr (l, 1)	Load on the top left node of the l'th loaded element.
	Pr (l, 2)	Load on the top right node of the l'th loaded element.
(c)	Ifbc (l)	Index of the top left node of the l'th element with applied flow.
	Jfbc (l)	Index of the top right node of the l'th element with applied flow.
	Fbc (l)	Amount of flow on the l'th element with applied flow.

**Note 1:** The values of IX (1) through IX (8) are to be consistent with finite element formulation. For example, those values for the central element in Fig. III.1 are 16, 27, 25, 14, 21, 26, 20, 15.

**Note 2:** A certain amount of height is added to the embankment at each time step sequence. These time steps are again subdivided into a number of subincrement.  $Dt$  is the duration of one such subincrement.

The use and format of the input variables are shown in figures III.2 through III.5 in the following pages. Note that a number of annotations are added by the data

converter at the end of the original data in many cards to facilitate clear understanding of the data by the user.

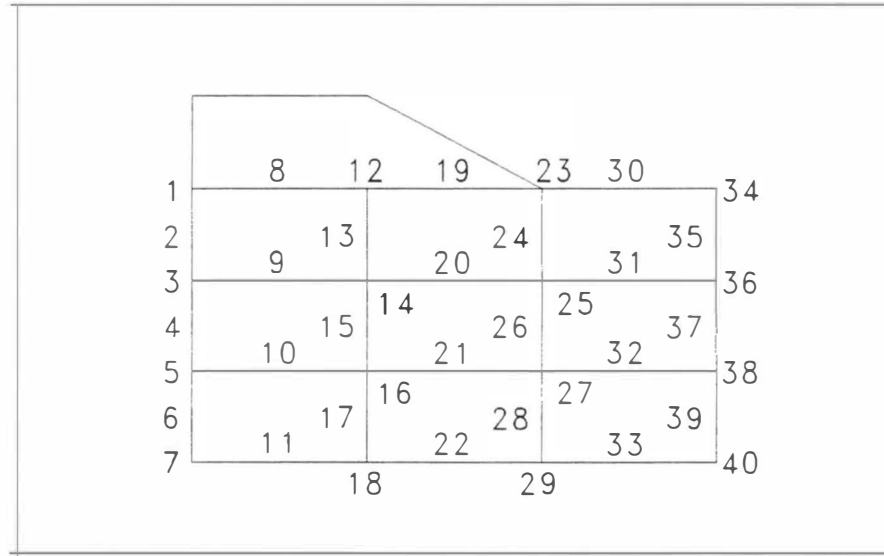


Fig. III.1 Example of Nodal Index - the Variable IX (1) through IX (8)

```

Consolidation Analysis for Foundations of Bridge Approach Embankments
0      = MSYM [= 0 : Symmetric Embankment; = 1 : Not Symm
0 Ft Lb Day mUnit (=0 : FPS); Length, Force, Time
1      = MCONTR [= 2 Case for Plotting Embankment Contours
      .000000 = XSETT (Distance At Which Pore Pressures Need To Be Written
280      [NUMNP] Total Number of Nodal Points
90      [NUMEL] Total Number of Elements
3      [NUMMAT] Total Number of Soil Layers
62.4000 [RO] Unit Weight of Pore Fluid
1000.0000 [TIMEND] Time When Execution of Program Must Stop
      .0000 [ACELZ] Vertical Acceleration
6      [NUMPC] No. of Elements with Specified Stress
0      [NFLBC] No. of Elements with Specified Flow
239000.000 .40000 .1050E-03 130.00 15.800 504.00 : Ex. Nux, kx, U_Wt, AIF, Cohesion
239000.000 .1050E-03 .40000 0 : Ey, ky, Nuy, Iso
250000.000 .30000 .1000E-03 132.00 12.100 619.00 : Ex. Nux, kx, U_Wt, AIF, Cohesion
250000.000 .1000E-03 .30000 0 : Ey, ky, Nuy, Iso
173000.000 .40000 .5000E-05 135.00 9.3000 1440.0 : Ex. Nux, kx, U_Wt, AIF, Cohesion
173000.000 .5000E-05 .40000 0 : Ey, ky, Nuy, Iso
1.000000 1.00000 XFACTOR, YFACTOR
      1 Node, KODE, KT
      .0000 1 .0000 .0000 .0000 .0000 .0000 .0000
      2 5 0
      .0000 2.0000 .0000 .0000 .0000 .0000 .0000 .0000
      3 5 1
      .0000 4.0000 .0000 .0000 .0000 .0000 .0000 .0000

```

Fig. III.2 First 26 lines of the data file Capdmf.dat showing items no. 1 through 7 completely and first six lines of item no. 8

```

      279 0 0
110.0000 41.3333 .0000 .0000 .0000 .0000 .0000 .0000
      280 3 1
110.0000 45.0000 .0000 .0000 .0000 .0000 .0000 .0000
1 3 32 30 1 21 31 20 2 1 1 0
2 5 34 32 3 22 33 21 4 1 1 0
3 7 36 34 5 23 35 22 6 1 1 0
4 9 38 36 7 24 37 23 8 2 0 0
5 11 40 38 9 25 39 24 10 2 0 0

```

Fig. III.3 Lines 577 to 585 from input data file Capdmf.dat showing last four lines of item no. 8 and first five lines of item no. 9

89	276	277	278	0	0	0	0	0	3	1	1
90	278	279	280	0	0	0	0	0	3	1	1
.286000		.078000		.015000		-189.207136		-260.000000		.7310	1
.286000		.078000		.015000		-567.621407		-780.000000		.7310	2
.286000		.078000		.015000		-946.035679		-1300.000000		.7310	3
.100000		.100000		.042000		-2940.255399		-3507.000000		1.0450	7
.100000		.100000		.042000		-3770.267616		-4497.000000		1.0450	8
.100000		.100000		.042000		-4600.279834		-5487.000000		1.0450	9
.286000		.078000		.015000		-189.207136		-260.000000		.7310	10
.286000		.078000		.015000		-567.621407		-780.000000		.7310	11

Fig. III.4 Lines 669 to 678 from input data file Capdmf.dat showing last two lines of item no. 9 and first eight lines of item no. 10

.100000		.100000		.042000		-3770.267616		-4497.000000		1.0450	89
.100000		.100000		.042000		-4600.279834		-5487.000000		1.0450	90
2.5000	2	2	0	:	DT, NDT, INTER, IIT						
1	20	30	353.75000		353.75000	:	IBCF, JBCF, KBCF, PRF1, PRF2				
30	49	59	353.75000		353.75000						
59	78	88	353.75000		353.75000						
88	107	117	353.75000		235.83333						
117	136	146	235.83333		117.91667						
146	165	175	117.91667		.00000						
2.5000	2	2	0	:	DT, NDT, INTER, IIT						
1	20	30	1061.25000		1061.25000	:	IBCF, JBCF, KBCF, PRF1, PRF2				
30	49	59	1061.25000		1061.25000						
59	78	88	1061.25000		1061.25000						
88	107	117	1061.25000		707.50000						
117	136	146	707.50000		353.75000						
146	165	175	353.75000		.00000						

Fig. III.5 Lines 729 to 744 of input data file Capdmf.dat showing last two lines of item no. 10 and two repetitions of item no. 11

## APPENDIX IV

### NOTES ON THE OUTPUT DATA OF PREPROCESSOR

It is quite possible that few values may be wrongly keyed-in while running the *Preprocessor*. Depending on the type of this value, the user can correct the mistake by moving the cursor to a corresponding field or by selecting an appropriate option or reloading the input data file (\*.inp). In a parametric study, i.e., when studying the effect of few selected parameters on the results (approach settlement, excess pore pressure), the user can select the same option to change a parameter or a set of parameters and select the Process-Save option to save the data in different output files (\*.dat). Refer to Section 3.2 for details. The other alternative would be to correct or change the data by editing the output file (\*.dat) created by *Preprocessor* directly. There are certain variables which are used for the purpose of generating the finite element mesh and boundary condition data. Such variables should not be edited. The variables which can be altered without affecting the other variables are material properties, heading, etc.. In the following section an attempt has been made to describe the variables so that it will be easier for the user to edit the data file (\*.dat). The data file "site.dat" for the East Cordell Bridge site is used to explain the result from the *Preprocessor*. Fig. 3.14 shows the input data for this site. The original output data which are listed below are italicized.



\* Units

Note: 0 for FPS system of units, 1 for SI system of units. FPS system of units has been used for this example problem. This variable cannot be altered because this will make other input data inconsistent.

0

\* Title

This card helps in identifying the problem. It can be altered.

*East Cordell Bridge Site, Nov.19, 1994*

\* Embankment Dimensions

The following information must be provided in this set of cards:

- a. Embankment height,
- b. Top half width, and
- c. Bottom half width.

22. 15. 59.

Note: None of these dimensions can be altered. Because these dimensions will affect the FE mesh generation. If the user needs to change any of these values, then the *Preprocessor* should be rerun.

\* Pore fluid density

62.4

Note: This value can be altered to reflect the actual pore fluid density in the field.

\* Number of embankment layers

2

\* Embankment layer information

- a. Thickness of the layer,
- b. Type of material,
- c. Material density.

1. 0 140.

21. 1 112.7

Note: Only the material density can be changed without affecting the other parameters.

\* Number of foundation layers

3

\* Foundation layer information

- a. Thickness of the layer,
- b. Type of material, ( 1 for clay type material, 0 for nonclay type material)
- c. Material density.

20. 1 113.

25. 1 115.

15. 1 117.

Note: In this case there are three layers in foundation. Only the density of the material can be altered without affecting the other parameters.

\* Water table depth

20.

Note: The water table depth cannot be changed. Another important point to keep in

mind is that, the water table depth should coincide with the boundary between two adjacent layers. Thus, if it is located in between a layer for the purpose of analysis, this layer should be treated as two layers - one above the water table and other below the water table.

\* Material properties

Note: In this section the following information for each of the embankment and foundation layers from top to bottom are provided.

- a.  $\nu$  for Isotropic material,
- b. Elastic modulus,
- c. Angle of internal friction,
- d. Cohesion,
- e. Poisson's ratio,
- f. Permeability coefficient,
- g. Slope of the critical state line,
- h. Compression index,
- i. Swelling index, and
- j. Void ratio.

*0 5000000. 0.3 3. 30. 0.*

*0 144000. 0.4 1.9e-004 0. 50. 1.1 8.7e-002 1.4e-002 0.66*

*0 80640. 0.4 2.4e-004 10. 50. 1.1 8.7e-002 1.4e-002 1.1*

*0 187200. 0.4 5.26e-005 10. 85. 0.73 0.232 4.4e-002 0.95*

*0 112320. 0.4 2.2e-004 10. 100. 1.15 9.4e-002 1.8e-002 1.05*

Note: There are two layers in the embankment and three layers in the foundation. So there are five sets of data. All the material properties can be changed without affecting the other data except the first data at each set (a. 0 for isotropic). If the material is anisotropic, i.e., the first data is 1, the user should furnish the following information for the layer:

- a. 1 for Anisotropic material,
- b. Elastic modulus-X,
- c. Poisson's ratio-X,
- d. Permeability coefficient-X,
- e. Angle of internal friction,
- f. Cohesion,
- g. Elastic modulus-Y,
- h. Poisson's ratio-Y,
- i. Permeability coefficient-Y
- j. Slope of critical state line,
- k. Compression index,
- l. Swelling index, and
- m. Void ratio.

Note: Any of the anisotropic material property information can be changed. The modulus of elasticity (E) value can be estimated using the triaxial test data for the push tube samples. For example, the initial slope of the stress-strain plot gives the modulus

of elasticity ( $E$ ). For anisotropic case, laboratory tests need to be conducted on samples from each direction to get the respective  $E$  values (i.e.  $E_x$ ,  $E_y$ ). These values can also be estimated using the empirical expressions based on the field Standard Penetration Test (SPT) values. The cohesion  $c$ , the angle of internal friction  $\phi$ , and the slope of the critical state line  $M$ , can also be obtained from the triaxial test data. From the results of the triaxial test plot, the failure parameters can be evaluated. The slope of this line gives the angle of internal friction  $\phi$ , and the vertical intercept on Y-axis give the cohesion  $c$ . In order to obtain the value of the slope of the critical state line  $M$ , draw the critical state line first from the triaxial test results and measure the slope of this line (see section 4.3 for details). The void ratio  $e_0$ , the compression index  $C_c$ , and the swelling index  $C_s$  can be obtained from the results of the consolidation tests on the push tube samples.

**The following data is generated by the *Preprocessor* based on the data given above.**

\* Foundation node information

Note: The data contains information about (1) foundation nodes number, (2) nodal coordinate X, (3) nodal coordinate Y, and (4) 1 for corner node, and 0 for mid-side node.

(1)	(2)	(3)	(4)				
				5	0.	10.	1
				6	0.	12.5	0
				7	0.	15.	1
				8	0.	17.5	0
				9	0.	20.	1
				10	0.	24.16666667	0
1	0.	0.	1				
2	0.	2.5	0				
3	0.	5.	1				
4	0.	7.5	0				

11	0.	28.33333333	1
12	0.	32.5	0
13	0.	36.66666667	1
14	0.	40.83333333	0
15	0.	45.	1
16	0.	48.75	0
17	0.	52.5	1
18	0.	56.25	0
19	0.	60.	1
20	2.5	0.	0
21	2.5	5.	0
22	2.5	10.	0
23	2.5	15.	0
24	2.5	20.	0
25	2.5	28.33333333	0
26	2.5	36.66666667	0
27	2.5	45.	0
28	2.5	52.5	0
29	2.5	60.	0
30	5.	0.	1
31	5.	2.5	0
32	5.	5.	1
33	5.	7.5	0
34	5.	10.	1
35	5.	12.5	0
36	5.	15.	1
37	5.	17.5	0
38	5.	20.	1
39	5.	24.16666667	0
40	5.	28.33333333	1
41	5.	32.5	0
42	5.	36.66666667	1
43	5.	40.83333333	0
44	5.	45.	1
45	5.	48.75	0
46	5.	52.5	1
47	5.	56.25	0
48	5.	60.	1
49	7.5	0.	0
50	7.5	5.	0
51	7.5	10.	0
52	7.5	15.	0
53	7.5	20.	0
54	7.5	28.33333333	0
55	7.5	36.66666667	0
56	7.5	45.	0
57	7.5	52.5	0
58	7.5	60.	0
59	10.	0.	1
60	10.	2.5	0
61	10.	5.	1
62	10.	7.5	0
63	10.	10.	1
64	10.	12.5	0
65	10.	15.	1
66	10.	17.5	0
67	10.	20.	1
68	10.	24.16666667	0
69	10.	28.33333333	1
70	10.	32.5	0
71	10.	36.66666667	1
72	10.	40.83333333	0
73	10.	45.	1
74	10.	48.75	0
75	10.	52.5	1
76	10.	56.25	0
77	10.	60.	1
78	12.5	0.	0
79	12.5	5.	0
80	12.5	10.	0
81	12.5	15.	0
82	12.5	20.	0
83	12.5	28.33333333	0
84	12.5	36.66666667	0
85	12.5	45.	0
86	12.5	52.5	0
87	12.5	60.	0
88	15.	0.	1
89	15.	2.5	0
90	15.	5.	1
91	15.	7.5	0
92	15.	10.	1
93	15.	12.5	0
94	15.	15.	1
95	15.	17.5	0
96	15.	20.	1
97	15.	24.16666667	0
98	15.	28.33333333	1
99	15.	32.5	0
100	15.	36.66666667	1
101	15.	40.83333333	0
102	15.	45.	1
103	15.	48.75	0
104	15.	52.5	1
105	15.	56.25	0
106	15.	60.	1
107	22.33333333	0.	0
108	22.33333333	5.	0
109	22.33333333	10.	0
110	22.33333333	15.	0
111	22.33333333	20.	0
112	22.33333333	28.33333333	0
113	22.33333333	36.66666667	0
114	22.33333333	45.	0

115	22.33333333	52.5	0	167	51.66666667	10.	0
116	22.33333333	60.	0	168	51.66666667	15.	0
117	29.66666667	0.	1	169	51.66666667	20.	0
118	29.66666667	2.5	0	170	51.66666667	28.33333333	0
119	29.66666667	5.	1	171	51.66666667	36.66666667	0
120	29.66666667	7.5	0	172	51.66666667	45.	0
121	29.66666667	10.	1	173	51.66666667	52.5	0
122	29.66666667	12.5	0	174	51.66666667	60.	0
123	29.66666667	15.	1	175	59.	0.	1
124	29.66666667	17.5	0	176	59.	2.5	0
125	29.66666667	20.	1	177	59.	5.	1
126	29.66666667	24.16666667	0	178	59.	7.5	0
127	29.66666667	28.33333333	1	179	59.	10.	1
128	29.66666667	32.5	0	180	59.	12.5	0
129	29.66666667	36.66666667	1	181	59.	15.	1
130	29.66666667	40.83333333	0	182	59.	17.5	0
131	29.66666667	45.	1	183	59.	20.	1
132	29.66666667	48.75	0	184	59.	24.16666667	0
133	29.66666667	52.5	1	185	59.	28.33333333	1
134	29.66666667	56.25	0	186	59.	32.5	0
135	29.66666667	60.	1	187	59.	36.66666667	1
136	37.	0.	0	188	59.	40.83333333	0
137	37.	5.	0	189	59.	45.	1
138	37.	10.	0	190	59.	48.75	0
139	37.	15.	0	191	59.	52.5	1
140	37.	20.	0	192	59.	56.25	0
141	37.	28.33333333	0	193	59.	60.	1
142	37.	36.66666667	0	194	71.625	0.	0
143	37.	45.	0	195	71.625	5.	0
144	37.	52.5	0	196	71.625	10.	0
145	37.	60.	0	197	71.625	15.	0
146	44.33333333	0.	1	198	71.625	20.	0
147	44.33333333	2.5	0	199	71.625	28.33333333	0
148	44.33333333	5.	1	200	71.625	36.66666667	0
149	44.33333333	7.5	0	201	71.625	45.	0
150	44.33333333	10.	1	202	71.625	52.5	0
151	44.33333333	12.5	0	203	71.625	60.	0
152	44.33333333	15.	1	204	84.25	0.	1
153	44.33333333	17.5	0	205	84.25	2.5	0
154	44.33333333	20.	1	206	84.25	5.	1
155	44.33333333	24.16666667	0	207	84.25	7.5	0
156	44.33333333	28.33333333	1	208	84.25	10.	1
157	44.33333333	32.5	0	209	84.25	12.5	0
158	44.33333333	36.66666667	1	210	84.25	15.	1
159	44.33333333	40.83333333	0	211	84.25	17.5	0
160	44.33333333	45.	1	212	84.25	20.	1
161	44.33333333	48.75	0	213	84.25	24.16666667	0
162	44.33333333	52.5	1	214	84.25	28.33333333	1
163	44.33333333	56.25	0	215	84.25	32.5	0
164	44.33333333	60.	1	216	84.25	36.66666667	1
165	51.66666667	0.	0	217	84.25	40.83333333	0
166	51.66666667	5.	0	218	84.25	45.	1

219	84.25	48.75	0	271	134.75	24.16666667	0
220	84.25	52.5	1	272	134.75	28.33333333	1
221	84.25	56.25	0	273	134.75	32.5	0
222	84.25	60.	1	274	134.75	36.66666667	1
223	96.875	0.	0	275	134.75	40.83333333	0
224	96.875	5.	0	276	134.75	45.	1
225	96.875	10.	0	277	134.75	48.75	0
226	96.875	15.	0	278	134.75	52.5	1
227	96.875	20.	0	279	134.75	56.25	0
228	96.875	28.33333333	0	280	134.75	60.	1
229	96.875	36.66666667	0	281	147.375	0.	0
230	96.875	45.	0	282	147.375	5.	0
231	96.875	52.5	0	283	147.375	10.	0
232	96.875	60.	0	284	147.375	15.	0
233	109.5	0.	1	285	147.375	20.	0
234	109.5	2.5	0	286	147.375	28.33333333	0
235	109.5	5.	1	287	147.375	36.66666667	0
236	109.5	7.5	0	288	147.375	45.	0
237	109.5	10.	1	289	147.375	52.5	0
238	109.5	12.5	0	290	147.375	60.	0
239	109.5	15.	1	291	160.	0.	1
240	109.5	17.5	0	292	160.	2.5	0
241	109.5	20.	1	293	160.	5.	1
242	109.5	24.16666667	0	294	160.	7.5	0
243	109.5	28.33333333	1	295	160.	10.	1
244	109.5	32.5	0	296	160.	12.5	0
245	109.5	36.66666667	1	297	160.	15.	1
246	109.5	40.83333333	0	298	160.	17.5	0
247	109.5	45.	1	299	160.	20.	1
248	109.5	48.75	0	300	160.	24.16666667	0
249	109.5	52.5	1	301	160.	28.33333333	1
250	109.5	56.25	0	302	160.	32.5	0
251	109.5	60.	1	303	160.	36.66666667	1
252	122.125	0.	0	304	160.	40.83333333	0
253	122.125	5.	0	305	160.	45.	1
254	122.125	10.	0	306	160.	48.75	0
255	122.125	15.	0	307	160.	52.5	1
256	122.125	20.	0	308	160.	56.25	0
257	122.125	28.33333333	0	309	160.	60.	1
258	122.125	36.66666667	0	-9999	0	0	0
259	122.125	45.	0				
260	122.125	52.5	0				
261	122.125	60.	0				
262	134.75	0.	1				
263	134.75	2.5	0				
264	134.75	5.	1				
265	134.75	7.5	0				
266	134.75	10.	1				
267	134.75	12.5	0				
268	134.75	15.	1				
269	134.75	17.5	0				
270	134.75	20.	1				

Note: -9999 is a control parameter for data separation. The element information calculated by the *Preprocessor* is printed. The printed information essentially consists of (1) element number, (2) eight nodes



forming that element in anti-clockwise direction, (3) layer number, and (4) type of node, 1 for corner node, 0 for mid-side node.

(1)           (2)           (3) (4)

```

1 3 32 30 1 21 31 20 2 1 1
2 5 34 32 3 22 33 21 4 1 1
3 7 36 34 5 23 35 22 6 1 1
4 9 38 36 7 24 37 23 8 1 1
5 11 40 38 9 25 39 24 10 2 1
6 13 42 40 11 26 41 25 12 2 1
7 15 44 42 13 27 43 26 14 2 1
8 17 46 44 15 28 45 27 16 3 1
9 19 48 46 17 29 47 28 18 3 1
10 32 61 59 30 50 60 49 31 1 1
11 34 63 61 32 51 62 50 33 1 1
12 36 65 63 34 52 64 51 35 1 1
13 38 67 65 36 53 66 52 37 1 1
14 40 69 67 38 54 68 53 39 2 1
15 42 71 69 40 55 70 54 41 2 1
16 44 73 71 42 56 72 55 43 2 1
17 46 75 73 44 57 74 56 45 3 1
18 48 77 75 46 58 76 57 47 3 1
19 61 90 88 59 79 89 78 60 1 1
20 63 92 90 61 80 91 79 62 1 1
21 65 94 92 63 81 93 80 64 1 1
22 67 96 94 65 82 95 81 66 1 1
23 69 98 96 67 83 97 82 68 2 1
24 71 100 98 69 84 99 83 70 2 1
25 73 102 100 71 85 101 84 72 2 1
26 75 104 102 73 86 103 85 74 3 1
27 77 106 104 75 87 105 86 76 3 1
28 90 119 117 88 108 118 107 89 1 1
29 92 121 119 90 109 120 108 91 1 1
30 94 123 121 92 110 122 109 93 1 1
31 96 125 123 94 111 124 110 95 1 1
32 98 127 125 96 112 126 111 97 2 1
33 100 129 127 98 113 128 112 99 2 1
34 102 131 129 100 114 130 113 101 2 1
35 104 133 131 102 115 132 114 103 3 1
36 106 135 133 104 116 134 115 105 3 1
37 119 148 146 117 137 147 136 118 1 1
38 121 150 148 119 138 149 137 120 1 1
39 123 152 150 121 139 151 138 122 1 1

```

```

40 125 154 152 123 140 153 139 124 1 1
41 127 156 154 125 141 155 140 126 2 1
42 129 158 156 127 142 157 141 128 2 1
43 131 160 158 129 143 159 142 130 2 1
44 133 162 160 131 144 161 143 132 3 1
45 135 164 162 133 145 163 144 134 3 1
46 148 177 175 146 166 176 165 147 1 1
47 150 179 177 148 167 178 166 149 1 1
48 152 181 179 150 168 180 167 151 1 1
49 154 183 181 152 169 182 168 153 1 1
50 156 185 183 154 170 184 169 155 2 1
51 158 187 185 156 171 186 170 157 2 1
52 160 189 187 158 172 188 171 159 2 1
53 162 191 189 160 173 190 172 161 3 1
54 164 193 191 162 174 192 173 163 3 1
55 177 206 204 175 195 205 194 176 1 1
56 179 208 206 177 196 207 195 178 1 1
57 181 210 208 179 197 209 196 180 1 1
58 183 212 210 181 198 211 197 182 1 1
59 185 214 212 183 199 213 198 184 2 1
60 187 216 214 185 200 215 199 186 2 1
61 189 218 216 187 201 217 200 188 2 1
62 191 220 218 189 202 219 201 190 3 1
63 193 222 220 191 203 221 202 192 3 1
64 206 235 233 204 224 234 223 205 1 1
65 208 237 235 206 225 236 224 207 1 1
66 210 239 237 208 226 238 225 209 1 1
67 212 241 239 210 227 240 226 211 1 1
68 214 243 241 212 228 242 227 213 2 1
69 216 245 243 214 229 244 228 215 2 1
70 218 247 245 216 230 246 229 217 2 1
71 220 249 247 218 231 248 230 219 3 1
72 222 251 249 220 232 250 231 221 3 1
73 235 264 262 233 253 263 252 234 1 1
74 237 266 264 235 254 265 253 236 1 1
75 239 268 266 237 255 267 254 238 1 1
76 241 270 268 239 256 269 255 240 1 1
77 243 272 270 241 257 271 256 242 2 1
78 245 274 272 243 258 273 257 244 2 1
79 247 276 274 245 259 275 258 246 2 1
80 249 278 276 247 260 277 259 248 3 1
81 251 280 278 249 261 279 260 250 3 1
82 264 293 291 262 282 292 281 263 1 1
83 266 295 293 264 283 294 282 265 1 1
84 268 297 295 266 284 296 283 267 1 1
85 270 299 297 268 285 298 284 269 1 1
86 272 301 299 270 286 300 285 271 2 1
87 274 303 301 272 287 302 286 273 2 1
88 276 305 303 274 288 304 287 275 2 1
89 278 307 305 276 289 306 288 277 3 1
90 280 309 307 278 290 308 289 279 3 1
-9999 0 0 0 0 0 0 0 0 0 0

```

Note: -9999 is a control parameter for separating the finite and infinite elements. In case of infinite elements each element is defined by only three nodes as compared to eight nodes for finite elements.

```

91 291 292 293 0 0 0 0 0 1 1
92 293 294 295 0 0 0 0 0 1 1
93 295 296 297 0 0 0 0 0 1 1
94 297 298 299 0 0 0 0 0 1 1
95 299 300 301 0 0 0 0 0 2 1
96 301 302 303 0 0 0 0 0 2 1
97 303 304 305 0 0 0 0 0 2 1
98 305 306 307 0 0 0 0 0 3 1
99 307 308 309 0 0 0 0 0 3 1
-9999 0 0 0 0 0 0 0 0 0 0

```

Note: After this, (1) the node number, and (2) the boundary conditions associated with that node are printed.

(1) (2)

1	5	27	0	53	0	79	0
2	5	28	0	54	0	80	0
3	5	29	3	55	0	81	0
4	5	30	4	56	0	82	0
5	5	31	0	57	0	83	0
6	5	32	4	58	3	84	0
7	5	33	0	59	4	85	0
8	5	34	4	60	0	86	0
9	5	35	0	61	4	87	3
10	1	36	4	62	0	88	4
11	1	37	0	63	4	89	0
12	1	38	4	64	0	90	4
13	1	39	0	65	4	91	0
14	1	40	0	66	0	92	4
15	1	41	0	67	4	93	0
16	1	42	0	68	0	94	4
17	1	43	0	69	0	95	0
18	1	44	0	70	0	96	4
19	3	45	0	71	0	97	0
20	0	46	0	72	0	98	0
21	0	47	0	73	0	99	0
22	0	48	3	74	0	100	0
23	0	49	0	75	0	101	0
24	0	50	0	76	0	102	0
25	0	51	0	77	3	103	0
26	0	52	0	78	0	104	0

105	0	157	0	209	0	261	3
106	3	158	0	210	4	262	4
107	0	159	0	211	0	263	0
108	0	160	0	212	4	264	4
109	0	161	0	213	0	265	0
110	0	162	0	214	0	266	4
111	0	163	0	215	0	267	0
112	0	164	3	216	0	268	4
113	0	165	0	217	0	269	0
114	0	166	0	218	0	270	4
115	0	167	0	219	0	271	0
116	3	168	0	220	0	272	0
117	4	169	0	221	0	273	0
118	0	170	0	222	3	274	0
119	4	171	0	223	0	275	0
120	0	172	0	224	0	276	0
121	4	173	0	225	0	277	0
122	0	174	3	226	0	278	0
123	4	175	4	227	0	279	0
124	0	176	0	228	0	280	3
125	4	177	4	229	0	281	0
126	0	178	0	230	0	282	0
127	0	179	4	231	0	283	0
128	0	180	0	232	3	284	0
129	0	181	4	233	4	285	0
130	0	182	0	234	0	286	0
131	0	183	4	235	4	287	0
132	0	184	0	236	0	288	0
133	0	185	0	237	4	289	0
134	0	186	0	238	0	290	3
135	3	187	0	239	4	291	4
136	0	188	0	240	0	292	0
137	0	189	0	241	4	293	4
138	0	190	0	242	0	294	0
139	0	191	0	243	0	295	4
140	0	192	0	244	0	296	0
141	0	193	3	245	0	297	4
142	0	194	0	246	0	298	0
143	0	195	0	247	0	299	4
144	0	196	0	248	0	300	0
145	3	197	0	249	0	301	0
146	4	198	0	250	0	302	0
147	0	199	0	251	3	303	0
148	4	200	0	252	0	304	0
149	0	201	0	253	0	305	0
150	4	202	0	254	0	306	0
151	0	203	3	255	0	307	0
152	4	204	4	256	0	308	0
153	0	205	0	257	0	309	3
154	4	206	4	258	0	-9999	
155	0	207	0	259	0		
156	0	208	4	260	0		

Note:-9999 is used to indicate the end of this data field.

\* Embankment node information

The following data are the embankment information which includes the (1) embankment node number, (2) coordinates X, (3) coordinates Y, and (4) node type.

(1)	(2)	(3)	(4)	(1)	(2)	(3)	(4)
1	0	0.	1	40	3.920454545	1.	0
2	0	0.5	0	41	4.517045455	4.5	0
3	0	1.	1	42	5.113636364	8.	0
4	0	2.75	0	43	5.710227273	11.5	0
5	0	4.5	1	44	6.306818182	15.	0
6	0	6.25	0	45	6.903409091	18.5	0
7	0	8.	1	46	7.5	22.	0
8	0	9.75	0	47	5.	0.	1
9	0	11.5	1	48	5.113636364	0.5	0
10	0	13.25	0	49	5.227272727	1.	1
11	0	15.	1	50	5.625	2.75	0
12	0	16.75	0	51	6.022727273	4.5	1
13	0	18.5	1	52	6.420454545	6.25	0
14	0	20.25	0	53	6.818181818	8.	1
15	0	22.	1	54	7.215909091	9.75	0
16	1.25	0.	0	55	7.613636364	11.5	1
17	1.306818182	1.	0	56	8.011363636	13.25	0
18	1.505681818	4.5	0	57	8.409090909	15.	1
19	1.704545455	8.	0	58	8.806818182	16.75	0
20	1.903409091	11.5	0	59	9.204545455	18.5	1
21	2.102272727	15.	0	60	9.602272727	20.25	0
22	2.301136364	18.5	0	61	10.	22.	1
23	2.5	22.	0	62	6.25	0.	0
24	2.5	0.	1	63	6.534090909	1.	0
25	2.556818182	0.5	0	64	7.528409091	4.5	0
26	2.613636364	1.	1	65	8.522727273	8.	0
27	2.8125	2.75	0	66	9.517045455	11.5	0
28	3.011363636	4.5	1	67	10.51136364	15.	0
29	3.210227273	6.25	0	68	11.50568182	18.5	0
30	3.409090909	8.	1	69	12.5	22.	0
31	3.607954545	9.75	0	70	7.5	0.	1
32	3.806818182	11.5	1	71	7.670454545	0.5	0
33	4.005681818	13.25	0	72	7.840909091	1.	1
34	4.204545455	15.	1	73	8.4375	2.75	0
35	4.403409091	16.75	0	74	9.034090909	4.5	1
36	4.602272727	18.5	1	75	9.630681818	6.25	0
37	4.801136364	20.25	0	76	10.22727273	8.	1
38	5.	22.	1	77	10.82386364	9.75	0
39	3.75	0.	0	78	11.42045455	11.5	1

79 12.01704545 13.25 0  
 80 12.61363636 15. 1  
 81 13.21022727 16.75 0  
 82 13.80681818 18.5 1  
 83 14.40340909 20.25 0  
 84 15. 22. 1  
 85 8.75 0. 0  
 86 9.367424242 1. 0  
 87 11.52840909 4.5 0  
 88 13.68939394 8. 0  
 89 15.85037879 11.5 0  
 90 18.01136364 15. 0  
 91 20.17234848 18.5 0  
 92 22.33333333 22. 0  
 93 10. 0. 1  
 94 10.4469697 0.5 0  
 95 10.89393939 1. 1  
 96 12.45833333 2.75 0  
 97 14.02272727 4.5 1  
 98 15.58712121 6.25 0  
 99 17.15151515 8. 1  
 100 18.71590909 9.75 0  
 101 20.28030303 11.5 1  
 102 21.84469697 13.25 0  
 103 23.40909091 15. 1  
 104 24.97348485 16.75 0  
 105 26.53787879 18.5 1  
 106 28.10227273 20.25 0  
 107 29.66666667 22. 1  
 108 11.25 0. 0  
 109 12.42045455 1. 0  
 110 16.51704545 4.5 0  
 111 20.61363636 8. 0  
 112 24.71022727 11.5 0  
 113 28.80681818 15. 0  
 114 32.90340909 18.5 0  
 115 37. 22. 0  
 116 12.5 0. 1  
 117 13.22348485 0.5 0  
 118 13.9469697 1. 1  
 119 16.47916667 2.75 0  
 120 19.01136364 4.5 1  
 121 21.54356061 6.25 0  
 122 24.07575758 8. 1  
 123 26.60795455 9.75 0  
 124 29.14015152 11.5 1  
 125 31.67234848 13.25 0  
 126 34.20454545 15. 1  
 127 36.73674242 16.75 0  
 128 39.26893939 18.5 1  
 129 41.80113636 20.25 0  
 130 44.33333333 22. 1

131 13.75 0. 0  
 132 15.47348485 1. 0  
 133 21.50568182 4.5 0  
 134 27.53787879 8. 0  
 135 33.57007576 11.5 0  
 136 39.60227273 15. 0  
 137 45.6344697 18.5 0  
 138 51.66666667 22. 0  
 139 15. 0. 1  
 140 16. 0.5 0  
 141 17. 1. 1  
 142 20.5 2.75 0  
 143 24. 4.5 1  
 144 27.5 6.25 0  
 145 31. 8. 1  
 146 34.5 9.75 0  
 147 38. 11.5 1  
 148 41.5 13.25 0  
 149 45. 15. 1  
 150 48.5 16.75 0  
 151 52. 18.5 1  
 152 55.5 20.25 0  
 153 59. 22. 1  
 -9999 0 0 0

-9999 indicte the end of the data set.

The next data set essentially consists of (1) element number, (2) eight nodes forming that element in anti-clockwise direction, (3) layer number, and (4) type of node, 1 for corner node, 0 for mid-side node.

(1)	(2)	(3)	(4)
1	3 26 24 1 17 25	16	2 1 0
2	5 28 26 3 18 27	17	4 2 1
3	7 30 28 5 19 29	18	6 2 1
4	9 32 30 7 20 31	19	8 2 1
5	11 34 32 9 21 33	20	10 2 1
6	13 36 34 11 22 35	21	12 2 1
7	15 38 36 13 23 37	22	14 2 1
8	26 49 47 24 40 48	39	25 1 0
9	28 51 49 26 41 50	40	27 2 1
10	30 53 51 28 42 52	41	29 2 1
11	32 55 53 30 43 54	42	31 2 1
12	34 57 55 32 44 56	43	33 2 1
13	36 59 57 34 45 58	44	35 2 1
14	38 61 59 36 46 60	45	37 2 1
15	49 72 70 47 63 71	62	48 1 0
16	51 74 72 49 64 73	63	50 2 1
17	53 76 74 51 65 75	64	52 2 1
18	55 78 76 53 66 77	65	54 2 1
19	57 80 78 55 67 79	66	56 2 1
20	59 82 80 57 68 81	67	58 2 1
21	61 84 82 59 69 83	68	60 2 1
22	72 95 93 70 86 94	85	71 1 0
23	74 97 95 72 87 96	86	73 2 1
24	76 99 97 74 88 98	87	75 2 1
25	78 101 99 76 89 100	88	77 2 1
26	80 103 101 78 90 102	89	79 2 1
27	82 105 103 80 91 104	90	81 2 1
28	84 107 105 82 92 106	91	83 2 1
29	95 118 116 93 109 117	108	94 1 0
30	97 120 118 95 110 119	109	96 2 1
31	99 122 120 97 111 121	110	98 2 1
32	101 124 122 99 112 123	111	100 2 1
33	103 126 124 101 113 125	112	102 2 1
34	105 128 126 103 114 127	113	104 2 1
35	107 130 128 105 115 129	114	106 2 1
36	118 141 139 116 132 140	131	117 1 0
37	120 143 141 118 133 142	132	119 2 1
38	122 145 143 120 134 144	133	121 2 1
39	124 147 145 122 135 146	134	123 2 1
40	126 149 147 124 136 148	135	125 2 1
41	128 151 149 126 137 150	136	127 2 1
42	130 153 151 128 138 152	137	129 2 1
-9999	0 0 0 0 0 0	0 0 0 0	0 0

Note: -9999 indicte the end of this data set. The following data set contains the embankment nodal information (1) node number, and (2) nodal boundary condition.

(1)	(2)	46	2	93	4	140	0
		47	4	94	0	141	4
		48	0	95	4	142	0
1	5	49	4	96	0	143	4
2	5	50	0	97	4	144	0
3	5	51	4	98	0	145	4
4	5	52	0	99	4	146	0
5	5	53	4	100	0	147	4
6	5	54	0	101	4	148	0
7	5	55	4	102	0	149	4
8	5	56	0	103	4	150	0
9	5	57	4	104	0	151	4
10	5	58	0	105	4	152	0
11	5	59	4	106	0	153	6
12	5	60	0	107	6	-9999	
13	5	61	6	108	0		
14	5	62	0	109	0		
15	7	63	0	110	0		
16	0	64	0	111	0		
17	0	65	0	112	0		
18	0	66	0	113	0		
19	0	67	0	114	0		
20	0	68	0	115	2		
21	0	69	2	116	4		
22	0	70	4	117	0		
23	2	71	0	118	4		
24	4	72	4	119	0		
25	0	73	0	120	4		
26	4	74	4	121	0		
27	0	75	0	122	4		
28	4	76	4	123	0		
29	0	77	0	124	4		
30	4	78	4	125	0		
31	0	79	0	126	4		
32	4	80	4	127	0		
33	0	81	0	128	4		
34	4	82	4	129	0		
35	0	83	0	130	6		
36	4	84	6	131	0		
37	0	85	0	132	0		
38	6	86	0	133	0		
39	0	87	0	134	0		
40	0	88	0	135	0		
41	0	89	0	136	0		
42	0	90	0	137	0		
43	0	91	0	138	2		
44	0	92	2	139	4		
45	0						

Note : The following are the data for time-step analysis. The first data 6 indicates that there are six time steps for analysis in all. So, there are six sets of data listed below. For each set data, it contains (1) time interval, (2) # of time steps, (3) # of steps between output, (4) loaded element number, (5) loaded nodes number, and (6) the corresponding embankment height for loaded nodes.

```

6
(1) (2) (3)
1. 10 5
6
(4) (5) (6)
1 20 30 5. 5.
30 49 59 5. 5.
59 78 88 5. 5.
88 107 117 5. 3.333333333
117 136 146 3.333333333 1.666666667
146 165 175 1.666666667 0.
1. 10 10
6
1 20 30 10. 10.
30 49 59 10. 10.
59 78 88 10. 10.
88 107 117 10. 6.666666667
117 136 146 6.666666667 3.333333333
146 165 175 3.333333333 0.
1. 17 17
6
1 20 30 15. 15.
30 49 59 15. 15.
59 78 88 15. 15.
88 107 117 15. 10.
117 136 146 10. 5.
146 165 175 5. 0.
1. 23 23
6
1 20 30 22. 22.
30 49 59 22. 22.
59 78 88 22. 22.
88 107 117 22. 14.666666667
117 136 146 14.666666667 7.333333333
146 165 175 7.333333333 0.

```

```

1. 60 60
6
1 20 30 22. 22.
30 49 59 22. 22.
59 78 88 22. 22.
88 107 117 22. 14.666666667
117 136 146 14.666666667 7.333333333
146 165 175 7.333333333 0.
1. 120 120
6
1 20 30 22. 22.
30 49 59 22. 22.
59 78 88 22. 22.
88 107 117 22. 14.666666667
117 136 146 14.666666667 7.333333333
146 165 175 7.333333333 0.
-9999

```

Note: 300 is days for ending the analysis.

```

300.
-9999

```

Note: The following data set is for applied traffic loads. 1 is for one lane, 24 and 70 are the loaded nodal points, and 16 is the magnitude of loading.

```

1
24 70
16.
End of the output file.

```